SIMULTANEOUS HUMAN ACTIVITY RECOGNITION, MAPPING, AND INDOOR LOCALIZATION FOR AMBIENT ASSISTED LIVING SCENARIOS

JESÚS DAVID CERÓN BRAVO

Doctoral Thesis in Telematics Engineering

Thesis Supervisors:

Diego Mauricio López Gutiérrez
PhD. in Biomedical Sciences
University of Cauca

Björn Eskofier
PhD. in Computer Sciences
University of Erlangen-Nürnberg

University of Cauca
Faculty of Electronics and Telecommunications Engineering
Department of Telematics
Research Line in e-health
Popayán, Colombia, March 2022

JESÚS DAVID CERÓN BRAVO

SIMULTANEOUS HUMAN ACTIVITY RECOGNITION, MAPPING, AND INDOOR LOCALIZATION FOR AMBIENT ASSISTED LIVING SCENARIOS

A thesis submitted to the faculty of electronic and telecommunications engineering of the University of Cauca for the degree of

Ph.D. in:
Telematics Engineering

Thesis Supervisors:

Diego Mauricio López Gutiérrez
PhD. in Biomedical Sciences

Professor University of Cauca, Colombia

Björn Eskofier
PhD. in Computer Sciences
Professor University of Erlangen-Nürnberg, Germany

Popayán, 2022

Acknowledgments

I want to start by thanking the Ministry of Science, Technology and Innovation of Colombia because the completion of my doctorate was possible thanks to the scholarship I received through its call for national doctorates 727-2015.

It would not have been possible to complete this work without several people's guidance, accompaniment, and help. First, I would like to thank my supervisor, Professor Diego López, who has accompanied me in my academic training since my undergraduate stage. His professionalism and impeccable humanity have been an example for me to follow. Second, I also thank Professor Bjoern Eskofier, my supervisor at the University of Erlangen Nuremberg, for being interested in my project, for all his valuable guidance, and for allowing me to be part of his wonderful team, the Machine Learning and Data Analytics Lab. Third, I would like to acknowledge my supervisors for achieving the signing of the co-supervision agreement between the University of Cauca and the University of Erlangen Nuremberg. Undoubtedly, this agreement contributed to the quality of my thesis and allowed me to get to know a bit of German culture. Finally, I also thank all my professors in my doctoral studies, especially the doctorate program coordinator Alvaro Rendón, who always willing to answer any questions.

Last but not least, I thank my family. To my parents and sisters for their unconditional support all my life. To my wife and daughter for their love, patience, and companionship throughout these years.

Simultaneous Human Activity Recognition, mapping, and indoor localization for ambient assisted living scenarios

Structured Abstract

Background: The location of a person in an indoor environment and the recognition of their activity are valuable pieces of information to provide context-based assistance. This information is especially relevant for systems that assist older adults who need support in carrying out their daily living activities. However, most studies have addressed Indoor Localization (IL) and Human Activity Recognition (HAR) as isolated topics. As a result, the relationship between the place where the person is located and the activity carried out has not been completely explored. Moreover, protecting patient privacy and non-intrusiveness are fundamental aspects in Ambient-Assisted Living (AAL) scenarios.

Objectives: To propose a dynamic system for simultaneous HAR, mapping, and indoor localization for AAL scenarios.

Methods: A system that fuses data from an inertial measurement unit placed at the height of the person's ankle and proximity and human activity-related data captured with Bluetooth beacons deployed in the indoor environment has been proposed. This is done through an adaptation made to the Simultaneous Location and Mapping (SLAM) framework. The Human Activity Recognition component uses the K-Nearest Neighbor (KNN) data stream algorithm. The Pedestrian Dead-Reckoning (PDR) algorithm is the foundation of the indoor location component.

Results: The final evaluation of the system was carried out with 22 people, of whom 11 were older adults. As a result, it was obtained that the system can locate older adults with an average error of 1.02 ± 0.24 m and adults with an error of 0.98 ± 0.36 m. Activities of daily living were recognized with an F1 of 88% for older adults and an F1 of 88.02% for adults. There were no significant differences in activity recognition and indoor localization results.

Conclusions: This research introduce a system that takes advantage of the relationship between location and human activity to simultaneously and non-invasively perform the location, mapping, and recognition of human activity in indoor environments. This is the first study that uses beacon's movement as an input variable in SLAM to classify human activities. From this information, it is possible to obtain a map of the area in which the person is moving and adjust its location based on that map. The HAR was performed with a KNN data flow algorithm, which can be run on any wearable device due to low memory consumption. The proposed system is the backbone of future projects to develop flexible systems for monitoring IL and HAR based on two non-intrusive components: an Inertial Measurement Unit (IMU) and Bluetooth beacons.

Keywords: Simultaneous location and mapping, human activity recognition, pedestrian dead-reckoning, ambient assisted living, older adults, inertial measurement unit, Bluetooth beacons, particle filter, Kalman filter.

Simultane Indoor-Lokalisierung, Mapping und Erkennung menschlicher Aktivitäten für AAL-Szenarien.

Struktur abstrakt

Hintergrund: Die Lokalisierung einer Person in einer Person im Innenbereich und das Erkennen ihrer Tätigkeit sind wertvolle Informationsquellen zur kontext-basierten Unterstützung. Diese Informationen sind insbesondere für Assistenzsysteme für alltägliche Tätigkeiten älterer Menschen wichtig. Die meisten Studien haben bisher die Lokalisierung im Innenbereich (IL) und die Tätigkeitserkennung (HAR) als isolierte Disziplinen behandelt. Folglich wurde der Zusammenhang zwischen dem Aufenthaltsort einer Person und deren Aktivität noch nicht vollständig ausgenutzt. Darüber hinaus sind Privatsphäre und Unaufdringlichkeit grundlegende Aspekte bei Ambient-Assisted-Living (AAL) Szenarien.

Ziele: Implementierung eines dynamischen Systems für simultane Positionsbestimmung, Kartierung un HAR für AAL Szenarien.

Methoden: Es wurde ein System aufgebaut, das Daten von Trägheitssensoren auf Höhe der Fußgelenke einer Person mit Lage- und Aktivitäts-bezogenen Daten von im Raum verteilten Bluetooth-Beacons verbindet. Dies wird durch Anpassung des Frameworks zur gleichzeitigen Lokalisierung und Mapping. Die Aktivitäts-Erkennungs-Komponente verwendet einen K-Nearest-Neighbor (KNN) Daten-Strom-Algorithmus. Der Pedestrian-Dead-Reckoning (PDR) Algorithmus bildet die Grundlage der Innenraum-Lokalisations-Komponente.

Resultate: Das System wurde an 22 Personen evaluiert, von denen 11 ältere Erwachsene waren. Als Ergebnis wurde erreicht, dass das System ältere Personen mit einem durchschnittlichen Fehler von 1.02+-0.24m und Erwachsene mit einem Fehler von

lokalisieren kann 0.98 ± 0.36 m. Die Aktivitäten des täglichen Lebens wurden erkannt mit einem F1 von 88% für ältere Erwachsene, und einem F1 von 88,02% für Erwachsene erkannt. Es gab keine signifikanten Unterschiede bei der Aktivität-Erkennung und Innenraum-Lokalisierung.

Schlussfolgerung: In dieser Arbeit wurde ein System entwickelt, das Nutzen aus der Beziehung zwischen Ort und menschlicher Aktivität zieht, um simultane und nicht-invasiv zu lokalisieren, zu kartieren, und die menschliche Aktivität im Innenbereich zu erkennen. Dies ist die erste Studie, die Bewerbung von Beacons als Eingangsvariablen verwendet, um menschliche Aktivitäten später als Landmarken in SLAM zu klassifizieren. Mit Hilfe dieser Informationen ist es möglich, den Aufenthaltsbereich einer Person zu kartieren und den Ort basierend auf der Karte abzugleichen. Der HAR wurde mit einem KNN Datenfluss-Algorithmus realisiert, welcher wegen des geringen Speicherbedarfs auf jedem wearable lauffähig ist. Das vorgeschlagene System ist die Grundlage für künftige Projekte, um flexible Systeme zur Überwachung von IL und HAR, basierend auf zwei nicht-intrusiven Komponenten zu entwickeln: einem Inertial Measurement Unit (IMU) und Bluetooth beacons.

Stichwort: Simultane Positionsbestimmung und Kartierung, Erkennung menschlicher Aktivitäten, pedestrian dead-reckoning, ambient assisted living, älteren Erwachsenen, Trägheitsmesseinheit, Bluetooth beacons, particle filter, Kalman filter.

Reconocimiento de actividad humana, mapeo y localización en entornos cerrados simultáneos para escenarios AAL

Resumen Estructurado

Antecedentes: La localización de personas en entornos cerrados y el reconocimiento de su actividad son fuentes valiosas de información para proveer asistencia basada en el entorno. Esta información es especialmente relevante para sistemas que brindan asistencia a adultos mayores que necesitan algún tipo de ayuda en la ejecución de sus actividades de la vida diaria. Sin embargo, la mayoría de los estudios han abordado la localización en entornos cerrados (IL) y el reconocimiento de actividad humana (HAR) como temas aislados, es decir, la relación entre el lugar donde la persona se encuentra y la actividad que realiza no se ha aprovechado al máximo. Más aún, la protección de la privacidad de las personas y la no intrusión son aspectos fundamentales por considerar en este tipo de ambientes.

Objetivos: Proponer un sistema dinámico para el reconocimiento de actividades, localización y mapeo en escenarios de la vida asistida por el entorno.

Métodos: Se propone un sistema que fusiona datos de una unidad de medición inercial puesta a la altura del tobillo de la persona y datos de proximidad y relacionados con actividad humana capturados con Bluetooth beacons desplegados en el entorno cerrado. Lo anterior se hace por medio de una adaptación realizada al framework Simultaneous Location and Mapping (SLAM). El componente para el reconocimiento de actividad humana utiliza el algoritmo de data stream K-Nearest Neighbor (KNN). El algoritmo Pedestrian Dead-Reckoning (PDR) es la base del componente de localización en entornos cerrados.

Resultados: La evaluación final del sistema se realizó con 22 personas de las cuales 11 fueron adultos mayores. Como resultado se obtuvo que el sistema es capaz de localizar a los adultos mayores con un error promedio de 1.02 ± 0.24 m y a los adultos con un error de 0.98 ± 0.36 m. Las actividades de la vida diaria fueron reconocidas con una F1 de 88% para los adultos mayores y con una F1 de 88.02% para los adultos. No hubo diferencias significativas en los resultados de localización y reconocimiento de actividad entre los grupos.

Conclusiones: Se obtuvo un sistema que aprovecha la relación entre la ubicación y la actividad humana para realizar de forma simultánea y no invasiva la localización, el mapeo y el reconocimiento de la actividad humana en entornos cerrados. Este es el primer estudio que utiliza el movimiento de balizas como variable de entrada para clasificar actividades que luego se utilizan como landmarks en SLAM. A partir de esa información, es posible obtener un mapa del área por la que se mueve la persona y ajustar su localización basado en dicho mapa. El HAR se realizó con un algoritmo de flujo de datos KNN, que se puede ejecutar en cualquier wearable debido a su escaso consumo de memoria. El marco propuesto es la columna vertebral de futuros proyectos para desarrollar sistemas flexibles para monitorear IL y HAR basados en dos componentes no intrusivos: una IMU y balizas Bluetooth.

Palabras Clave: Localización y mapeo simultáneos, reconocimiento de actividad humana, navegación por estima de peatones (pedestrian dead-reckoning), vida asistida por el entorno, adultos mayores, unidades de medición inercial, balizas Bluetooth, filtro de partículas, filtro de Kalman.

Contents

List of figures

List of Tables

List of Equations

Glossary

Chapter 1

Introduction

1.1 Problem Statement

According to the United Nations and the World Health Organization, in 2010, there were 524 million people over 65 years old, representing 8% of the world's population. By 2050 that population will triple, representing 16% of the world's population [1]. The increase of the older population has social and economic repercussions since there will be more people affected by chronic and neurodegenerative diseases, and there will be more health emergencies, dramatically increasing the costs related to the provision of health services. As a consequence, more medical personnel, caregivers, and infrastructure will be needed [2,3]. Colombia is not immune to this problem. In 2013, there were 4,962,491 people over 60 years old in the country, representing 10.53% of its total population, and it is estimated that this population will grow 3.76% by the year 2020 [4]. The Colombian Ministry of Health and Social Protection has recognized that: "the progressive increase of the Colombian population, especially the group of older adults, represents a challenge for policies and resources regarding development, quality of life, compliance of rights and social inclusion "[5]. To address this problem, some countries, companies, and non-profit organizations began to promote a new paradigm: "Ambient Assisted Living (AAL)". AAL covers all the solutions supported in the Information and Communications Technologies (ICT) that seek to extend the time that older adults can live independently in their homes. In 2007, the AAL Joint Association was founded by the European Union, and with it, the AAL program was created, aimed at promoting and financing research in this area [6]. AAL is supported in different fields, those being Human Activity Recognition (HAR), the control of vital signs, and position tracking, the three areas of most interest in the AAL in recent years [7].

Regarding HAR, some authors categorize them into five types of activities: simple, complex, Activities of Daily Living (ADLs), work, and health [8]. The simple activities are standing, sitting, lying down, walking, or running. Complex activities are related to shopping, taking a bus, or driving a car. ADLs refer to any daily activity, especially those carried out at home, such as watching television, reading, brushing teeth, eating, bathing, etc. Work activities occur in a work context, such as attending a meeting, working on the computer, printing, or taking a break. Finally, activities related to health include performing exercise routines, rehabilitation activities, and detection of falls. In AAL, in addition to the importance of recognizing simple activities, the recognition of ADLs is relevant since it allows the physician to monitor the health status of the person and anticipate the risks associated with aging [7]. On the other hand, position tracking in AAL environments refers to recognizing the physical environments or usual scenarios in which older adults move, for example, indoor environments such as houses. Position tracking in this type of scenario cannot be performed with Global Navigation Satellite Systems (GNSS) due to their low accuracy, mainly due to their signals' attenuation in indoor environments. As a result, different types of Indoor Positioning Systems (IPS) have been developed to obtain a person's Indoor Localization (IL). Still, none of them has been widely accepted as a de facto IPS, as happened with the GPS for outdoor positioning tracking.

It is evident that knowing where a person is located contributes to recognizing the activity that the person may be developing and vice versa; since there is a direct relationship between what we do and where we do it [9]. Although several studies have been aimed at HAR and IL, these two topics have usually been addressed separately, and supported by different technologies and techniques. In the systematic review presented in the following section, studies related to HAR based on IL and vice versa were searched. As a result, 41 studies were found [10–50]. Of these 41 studies, 16 were focused on HAR [10]–[25], that is, they used location data to perform HAR. There are 13 studies that used HAR data to propose IL solutions [26–38]. The remaining 12 studies [39–50] present solutions focused on both HAR and IL (Figure 1.1). This last group of studies (HAR + IL) is very interesting since it contains solutions that support HAR in IL data and vice versa.

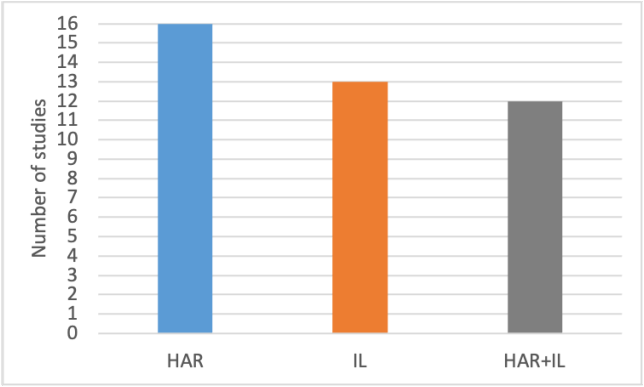

Figure 1.1 Approach of studies.

The year 2010 marks the beginning of the studies that have taken advantage of the relationship between HAR and IL. In 2015 the first study of the HAR + IL group emerged. Of the twelve studies that comprise this group, none of them were specifically focused on AAL. This means that the characteristics and restrictions of this type of environment have not been considered. A fundamental requirement for a HAR and IL solution to be usable in an AAL environment is that it be minimally obtrusive. Obtrusiveness can be viewed from two perspectives. The first is from the point of view of the number of devices that the older adult must wear for the system to work. The second is about privacy. There are many privacy concerns when a system must use cameras to perform HAR or IL, and there are also questions about what type of data the system collects and where that data is sent and saved.

Additionally, as the HAR + IL group studies have not been intended for AAL, they have not been developed or evaluated with data from older adults in real AAL settings. Therefore, developing a low-intrusive solution specifically targeted for AAL environments is currently a challenge.

There are several techniques for both HAR and IL. As a result of the state-of-the-art analysis presented in Chapter 2, the Pedestrian Dead-Reckoning (PDR) and Simultaneous Localization and Mapping (SLAM) techniques seem to be promising to develop a low-intrusive solution to perform HAR and IL in AAL environments.

PDR is a technique that mainly uses the acceleration and direction of the person to infer their position. It seems to be a good option to face the challenge presented above, especially because PDR does not require deploying infrastructure (sensors or antennas) in the user's environment. Unfortunately, it is a technique that is critically affected by drift since the sensors used (usually accelerometer, gyroscope, and magnetometer) introduce noise, which affects the precision of the person’s (wearer’s) location [51].

SLAM is one technique whose backbone can be PDR. This technique, born in the field of robotics, uses context references called landmarks to reduce the error introduced by drift caused by the use of Inertial Measurement Units (IMUs). As an additional characteristic, SLAM generates a map of the environment in which the user moves and uses it to reduce possible localization errors [39,44]. Using SLAM to address the localization of people in indoor environments is an emerging area, where the type and quantity of landmarks used, directly affect its performance. In a previous work by the author of this project, Bluetooth Low Energy (BLE) beacons were used to obtain a symbolic location of a person within an indoor environment [19]. Considering this, it is possible to use BLE beacons as landmarks in SLAM. Some BLE beacons have a built-in accelerometer. This can help to recognize actions or activities of daily living (ADL) that are related to the movement of specific objects. Beacons can also be used as indicators of proximity to strategic places of the indoor environment. No works have been found that use IMUs an BLE beacons as described above.

Last but not least, it is necessary to recognize the dynamic nature of AAL environments, that is, a system that evolves or changes over time. Consequently, modeling AAL environments needs to be approached from a dynamic perspective, it may be done with machine learning

techniques that easily update the models. There are two reasons to consider AAL environments as dynamic: the first is from the point of view of the HAR, describing how an older person executes activities whose patterns change over time. For example, the frequency of movements in older adults' change, either due to natural aging or as a result of some disease such as dementia, Parkinson's, or Alzheimer's. The second reason is from the point of view of IL, where the location of the furniture or utensils, in general, could change at any time, thus changing the possible trajectories of the person. According to the state of the art described in chapter 2, no study has considered the dynamic nature of AAL environments.

1.2 Research Question

Considering the above, the research question addressed in this doctoral thesis is the following:

How to simultaneously perform the Human Activity Recognition, mapping, and Indoor Localization for Ambient Assisted Living scenarios?

1.3 Research Objectives

The main objective of this research is to propose a dynamic system for simultaneous HAR, mapping, and indoor localization for AAL scenarios. This was achieved through the following specific objectives:

1. To develop and evaluate a system for indoor localization in AAL scenarios based on Pedestrian Dead-Reckoning and Bluetooth Low Energy beacons.

2. To propose a framework in which HAR is performed using an evolving system or incremental learning techniques. The data belonging to the HAR is fused

3. with the data made available by the system developed in the previous objective.

4. To evaluate the proposed framework regarding accuracy in the recognition of human activities and the location of the person in an AAL scenario.

1.4 Contributions

The main contributions of this doctoral thesis are mentioned below, which were obtained from the previously mentioned objectives.

1. Two datasets were used to evaluate indoor localization:

    a. One dataset publicly available and other collected by the author to evaluate indoor localization of walking, jogging, and running strides using PDR and multi-subsequence dynamic time warping

b. Dataset collected by the author to evaluate indoor localization and HAR in adults and older adults

2. A framework for indoor localization, mapping, and human activity recognition composed for:

   a. A modified PDR method to get stride length and orientation measurements from accelerometer and gyroscope data.

   b. A method for HAR based on data streaming.

   c. A method to fuse PDR with proximity and human activity-related data, based on the SLAM framework.

   d. A comprehensive evaluation of the proposed framework using real data collected from adults and older adults.

1.5 Outline

This research is comprised of the following seven chapters:

- **Chapter 1.** Introduction.

  An overview of the related work, identification of gaps, and research objectives are presented in this chapter.

- **Chapter 2.** State of the Art.

  This chapter presents the results of the systematic review carried out to obtain a state of the current knowledge about IL supported in HAR and vice versa.

- **Chapter 3.** Indoor Localization strategy.

  The decisions for the configuration of the indoor positioning system to be used are explained in this chapter, as well as the methods that comprise it.

- **Chapter 4.** Framework for Simultaneous Indoor Localization, Mapping, and Human Activity Recognition.

  Each of the components of the proposed framework for Simultaneous Indoor Localization, Mapping, and Human Activity Recognition is explained in detail. The strategy for Human Activity Recognition based on BLE beacons is presented. The first evaluation of the proposed framework is performed.

- **Chapter 5.** Framework evaluation.

  The final evaluation of the proposed framework is carried out in a real AAL environment with adults and older adults. The strategy for Human Activity Recognition is updated by using an online learning approach.

- **Chapter 6.** Conclusions and Future Work.

  Analysis of results highlighting the main contributions of the research. In addition, relevant recommendations for the development of future work are presented.

1.6 Publications

- J. D. Ceron, D. M. López, F. Kluge, and B. M. Eskofier, "Framework for non-intrusive indoor localization, mapping, and human activity recognition in ambient assisted living scenarios", Sensors (Switzerland), vol. 22, no. 9, 2022, DOI: 10.3390/s22093364 . (JCR Q1)

- J. D. Ceron, F. Kluge, A. Küderle, B. M. Eskofier, and D. M. López, "Simultaneous indoor pedestrian localization and house mapping based on inertial measurement unit and Bluetooth low-energy beacon data," Sensors (Switzerland), vol. 20, no. 17, 2020, DOI: 10.3390/s20174742. (JCR Q1)

- J. D. Ceron, C. F. Martindale, D. M. López, F. Kluge, and B. M. Eskofier, "Indoor trajectory reconstruction of walking, jogging, and running activities based on a foot-mounted inertial pedestrian dead-reckoning system," Sensors (Switzerland), 2020, DOI: 10.3390/s20030651. (JCR Q1)

- J. D. Cerón, D. M. López, and B. M. Eskofier, "Human Activity Recognition Using Binary Sensors, BLE Beacons, an Intelligent Floor, and Acceleration Data: A Machine Learning Approach," Proceedings, vol. 2, no. 19, p. 1265, 2018, DOI: 10.3390/proceedings2191265.

- J. D. Ceron and D. M. Lopez, "Human activity recognition supported on indoor localization: A systematic review," 2018. DOI: 10.3233/978-1-61499-868-6-93. (JCR Q3)

- J. D. Ceron, D. M. Lopez, and G. A. Ramirez, "A mobile system for sedentary behaviors classification based on accelerometer and location data," Computers in Industry, vol. 92–93, pp. 25–31, 2017, DOI: 10.1016/j.compind.2017.06.005. (JCR Q1)

- W. Possos, R. Cruz, J. D. Cerón, D. M. López, and C. H. Sierra-Torres, "Open dataset for the automatic recognition of sedentary behaviors," 2017. DOI: 10.3233/978-1-61499-761-0-107. (JCR Q2)

- J. D. Ceron, D. M. Lopez, and C. Hofmann, "A Two-Layer Method for Sedentary Behaviors Classification Using Smartphone and Bluetooth Beacons.," Studies in health technology and informatics, vol. 237, pp. 115–122, 2017. (JCR Q2)

- J. D. Ceron and D. M. Lopez, "Towards a Personal Health Record System for the Assessment and Monitoring of Sedentary Behavior in Indoor Locations.," Studies in health technology and informatics, vol. 228, pp. 804–806, 2016, DOI: 10.3233/978-1-61499-678-1-804. (JCR Q2)

Chapter 2

State of the art

A doctoral thesis usually begins with an in-depth analysis of the current state of the art in the research topic. This state of the art serves not only to justify the problem posed, but also to know recent and future work that led to possible hypotheses. It also allows the identification of potential conferences and scientific journals where to publish the Ph.D. results. For these reasons, a systematic review of the literature was carried out following the guidelines suggested by Kitchenham and collaborators [52], which consists of three phases: planning, execution, and documentation. Next, each of the phases is described.

2.1 Planning

This phase aims to pose the research questions that will be answered with the systematic review and plans the search of papers based on a defined protocol.

2.1.1 Research questions of the systematic review

The following research questions were considered:

RQ 1: How has the interest in taking advantage of the relationship between HAR and IL evolved over time?

RQ 2: How many and which human activities have been recognized, considering the location where they occur?

RQ 3: How many and what kind of wearable and mobile devices have been used to perform HAR and/or IL?

RQ 4: What types of Indoor Positioning Systems (IPS) have been used, and what has been their reported accuracy?

RQ 5: What machine learning techniques have been used for HAR, and what has been their accuracy?

RQ 6: Have incremental learning or evolving system techniques been used for HAR?

RQ 7: Have methods been used for fusing traditional HAR data with data from an IPS? Which ones?

RQ 8: What level of accuracy regarding the recognition of activities has been reported when applying data fusion techniques?

2.1.2 Search protocol

Based on the research questions, the following search string was structured:

("Indoor location" OR "indoor localization" OR "indoor positioning" OR "indoor navigation" OR "indoor inertial navigation" OR "SLAM" OR "simultaneous localization and mapping" OR "real-time location" OR "location data" OR "indoor tracking" OR "ambient assisted living") AND ("human activity recognition" OR "activity recognition" OR "physical activity classification" OR "physical activity recognition" OR "activity recognition and tracking" OR "activities of daily living" OR "ADLs" OR "ADL")

Then, the following libraries were consulted with that string: ACM, IEEE XPLORE, Pubmed, ScienceDirect, and Springer. The title and the summary of each resulting study were read, and their inclusion was analyzed according to these criteria: (1) The studies should describe solutions aimed at HAR based on IL or vice versa (2) Studies must be in English or Spanish.

2.2 Execution of the review, presentation, and analysis of results

After eliminating duplicate studies, 1,987 studies were selected for analysis. The title and abstract of each paper were revised. When necessary, the full paper was reviewed to decide to include or exclude the paper. After applying the inclusion criteria, 41 studies were selected. These studies allowed the researcher to respond to each one of the research questions of the systematic review:

RQ 1: How has the interest in taking advantage of the relationship between HAR and IL evolved over time?

Figure 2.1 shows the number of studies published per year. The year 2010 marks the beginning of the resulting publications, three years after the AAL Joint Association (AAL EUPORE 2007). The number of studies increased from 2010 until 2017. 2017 was the year in which more studies were published; since then, the number of studies has remained stable.

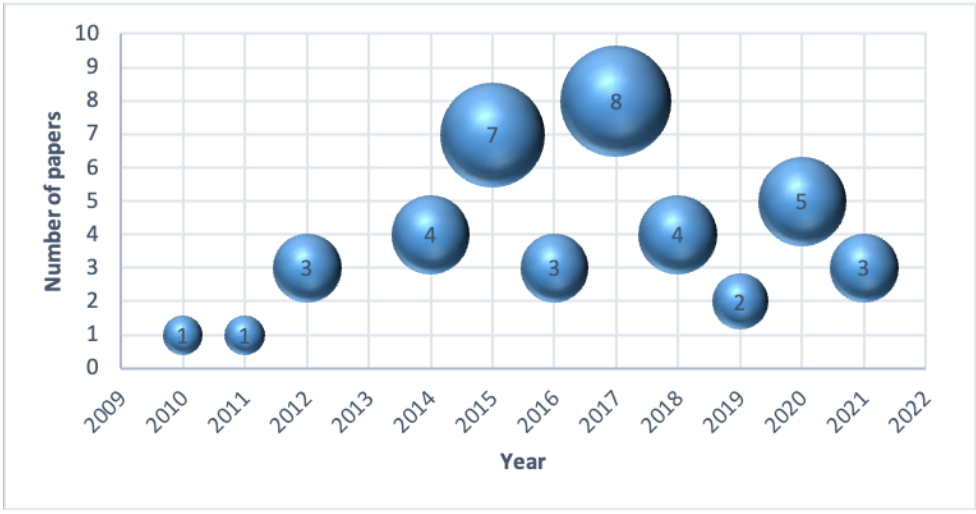

Figure 2.1 Number of papers published per year.

The 41 studies can be categorized into three groups according to the interest of the authors: Fifteen were focused on HAR (HAR group) [10–25], thirteen were focused on IL (IL group) [26–38] and twelve were focused on both HAR and IL (HAR+IL group) [39–50]. It is important to notice that since 2015 there have been publications that belong to the HAR+IL group, making evident the current interest of the scientific community regarding the topic addressed in this research. Figure 2.2 shows the paper categorization: HAR group: studies that used IL data to propose a HAR solution. IL group: Studies that used HAR data to perform IL. HAR+IL group: Studies that used HAR and IL to propose solutions aimed at both HAR and IL.

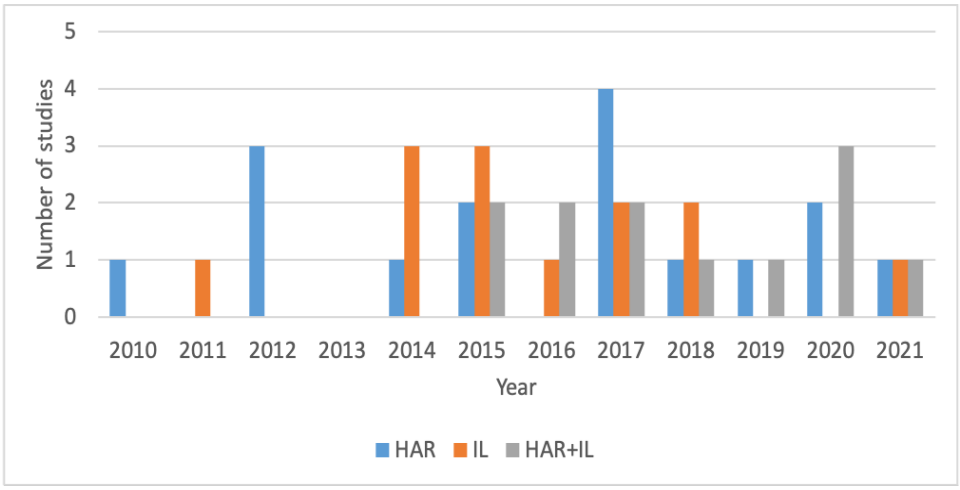

Figure 2.2 Papers per year and paper categorization.

RQ 2: How many and which human activities have been recognized, considering the location where they occur?

The response to this question is based on Figure 2.3 and Table 2.1. Based on the classification of activities of Xing Su et al [8]. Figure 2.3 shows that 16 of the studies have been addressed

specifically to the recognition of simple activities [12,13,21–23,28–31,34,35,42–44,48,49], five to simple activities and health (these five studies recognized simple activities and falls) [14,24,40,46,50], thirteen to simple and ADLs [10,11,17,20,25–27,32,33,37,38,41,47], five to ADLs only [15,16,18,19,45] and one to ADLs and work activities [39].

Regarding the number of activities that are recognized in the studies, the number is not very high. Of the five studies addressed to the recognition of ADLs, one study of our authorship recognizes a total of 23 activities [19], followed by two studies with nine [15,18], one with 8 [16], and another one with 6 [45]. Only one work recognized simple, ADLs and work activities [39]. That work recognized 23 activities in total. Thus, it can be inferred that the studies have been addressed mostly to the recognition of simple activities supported in the person's indoor location, with a clear trend towards recognizing ADLs. No studies focused on complex activities were found. According to the classification of activities of Xing Su, a possible reason is that those types of activities rarely occur in indoor environments.

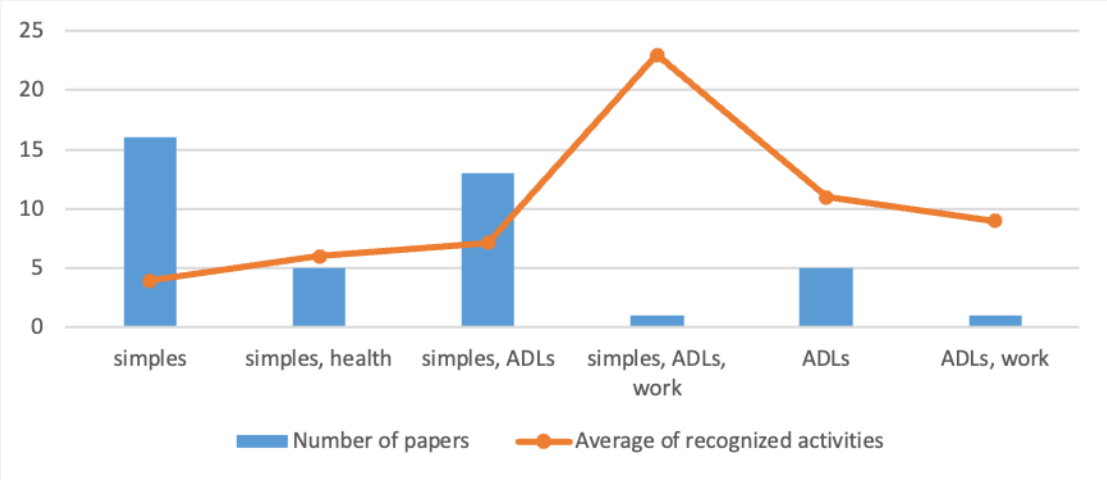

Figure 2.3 Number of studies categorized by activity type and average of recognized activities.

Several ADLs are recognized in the studies. The most common ADL is to use appliances followed by cooking and eating. Table 2.1 contains a list of all the ADLs recognized in the studies.

ADL	Number of studies	ADL	Number of studies
Using appliances	7	Watering plants	3
Cooking	5	Taking a shower	2
Eating	5	Reading	2
Open, close doors	4	Opening, closing drawers	2
Dishwashing	4	Opening, closing windows	1
Using the bathroom	3	Reclining	1
Cleaning dust	3	Using switches	1
Laying down	3	Taking an elevator	2
Using water taps	3	Climbing/descending stairs	2
Drinking	3	Climbing/descending ramp	1

Table 2.1 ADLs recognized and the number of studies in which they were recognized.

RQ 3: How many and what kind of wearable and mobile devices have been used by the person to perform HAR and/or IL?

The number of devices that the person must wear to recognize their activities and/or the tracking of their location is presented in Figure 2.4. It is important to note that in eight studies the person did not need to wear any device [18,22,32,36,41,44,45,48]. These solutions, known as device-free, take advantage of the sensors deployed in the environment by processing their data collected while the person executes activities around the house. Device-free methods usually use wireless technologies like WIFI, Infrared, ultra-wideband (UWB), and Bluetooth, among others. On the other hand, in most studies, the person must wear a device, which is usually a smartphone or a wearable

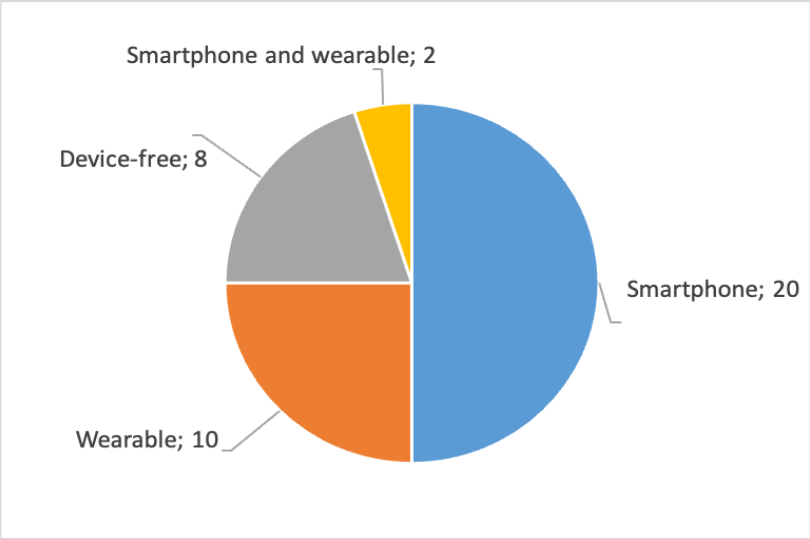

Figure 2.4 Type of device used by the person.

As described above, the two studies that recognize more activities are the one proposed in [39] and one of our authorships [19]. In [39] 23 activities are recognized among simple, ADLs and work. [19] focused on the recognition of 23 sedentary behaviors. The person had to carry only the smartphone to recognize the sedentary behaviors. However, the smartphone data is not enough to classify all those sedentary behaviors. The inclusion of indoor location data was proposed as a strategy to enhance both the precision and the number of classified sedentary behaviors. For that reason, Bluetooth Low Energy Beacons were used to obtain the symbolic location of the person at home. In [39], the person had to wear 4 IMUs for the system to recognize the 23 ADLs. (Figure 2.5).

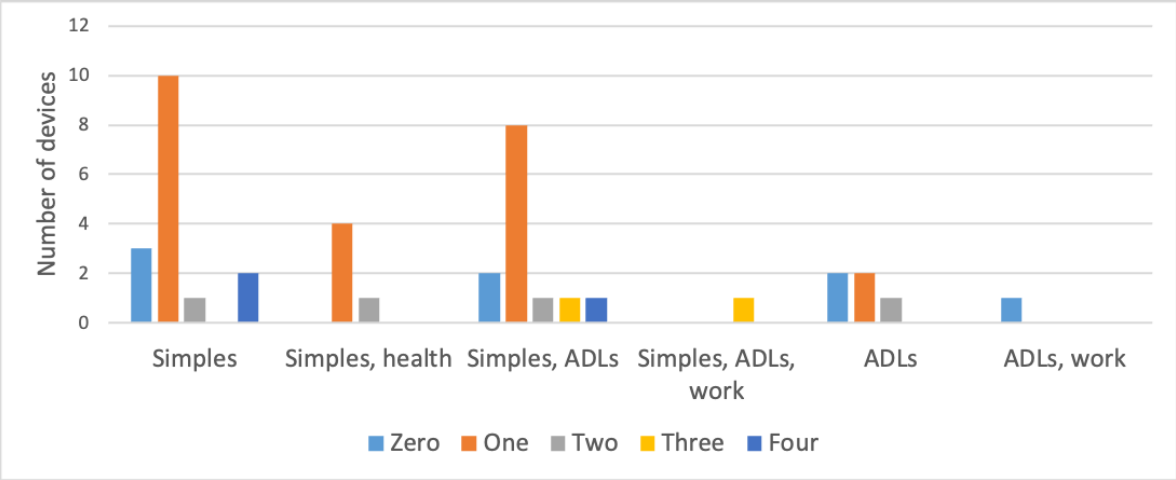

Figure 2.5 Number of devices worn by a person.

RQ 4: What types of Indoor Positioning Systems (IPS) have been used, and what has been their reported accuracy?

PDR, WIFI fingerprinting, and WIFI RSSI have been the most frequently used techniques for implementing IPSs. (Table 2.2). The most common techniques are the ones based on Wireless technologies. However, it is evident that PDR has attracted the researcher's attention.

IPS	Number of studies
PDR	7
WIFI fingerprinting	7
WIFI RSSI	7
Bluetooth	5
IR	4
Camera	4
UWB	3
Electric system + ultrasound	1

Table 2.2 IPS used (categorization based on Mautz et. al [39]).

Table 3 shows the different configurations used when implementing PDR, including the respective error declared by each study. As can be seen, the indoor location error ranges from 0.5 m to 7 m. The worst results were obtained when the data was collected on the hip.

	Number of studies	error
IMU on hip and EMG on leg	1 [28]	1.2m
IMU on foot	2 [16,39]	1.2m
smartphone on hip	2 [31,34]	3m,7m
smartphone on hand	2 [12,27]	0.5m

Table 2.3 Location of devices and error of IL using PDR.

RQ 5: What machine learning techniques have been used for HAR, and what has been their accuracy?

Table 2.4 is used to answer RQ 5 to RQ 8. Regarding RQ 5, traditional machine learning techniques have been used to perform the HAR. Among them, there are decision trees, neural networks, and deep learning. Two studies based their recognition of activities on the use of previously defined thresholds [29,35]. The precision of HAR reported in the studies can be seen in the last column of Table 2.4. Their values are related to the number of recognized activities and whether they used data fusion methods or not.

RQ 6: Have incremental learning or evolving system techniques been used for HAR?

The answer to RQ 6 is no. No study mentions having used any incremental learning or evolving system technique, which would give a dynamic capacity to their proposed systems. However, almost all studies use traditional supervised machine learning techniques at some point in their process for HAR or IL (Table 2.4).

RQ 7: Have methods been used for fusing traditional HAR data with data from an IPS? Which ones?

Twenty-seven studies (66% of the 41 studies) employed some data fusion technique (penultimate column of Table 2.4) to improve the precision of the indoor location or the recognition of activities (Figure 2.6). Two fusion methods have been used: methods based on probabilistic reasoning, especially the Bayes theory (32%), and fusion methods based on machine learning (34%).

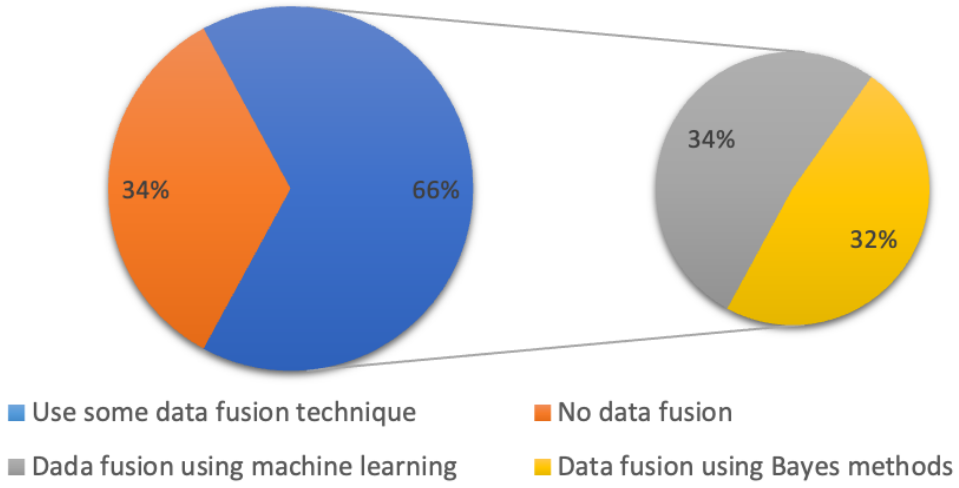

Figure 2.6 Data fusion techniques.

RQ 8: What level of accuracy regarding the recognition of activities has been reported when applying data fusion techniques?

Finally, Table 2.4 shows the studies that used a data fusion method and reported their accuracy. It is impossible to directly compare the accuracy achieved by the different studies since they used different methods, technologies and recognized different activities. For that reason, the table lists the number of recognized activities, the HAR method, their type (supervised or unsupervised), and the data fusion method involved. It is important to note that our work [19] was focused on the recognition of sedentary behaviors, so the 23 recognized activities result from combining three body postures: lying down, reclining, and sitting, the use of three devices (smartphone, PC, and TV) and the symbolic location of the person: sofa, bed or desk. On the other hand, the study proposed by Hardegger et al. [10] achieves 68% accuracy in recognizing 23 activities. It is presumed that this accuracy difference may be associated with the fact that PDR is used in this previous study, which makes it susceptible to more errors. However, they try to reduce its location error, including landmarks related to opening or closing doors and windows. Possibly the inclusion of another type of landmark that does not require the dense deployment of infrastructure (such as Bluetooth beacons) could contribute to the improvement of that proposed system. Another study to highlight is [19], in which 12 activities are recognized with 80% accuracy. In that study, a smartphone is used with an IPS that uses infrared IR motion sensors. The other studies classify simple activities and a few ADLs, leading to a high level of accuracy.

Study	Group	Type of activities	Number of activities recognized	Number of devices worn by person	IPS	IL precision	HAR method	Supervised method?	HAR precision	Data fusion method
[10]	HAR	simple, ADL	7	1	UWB-TOA		ELM	yes	93,33	Extreme learning machine
[11]	HAR	simple, ADL	8	3	camera			yes	85	Viterbi
[12]	HAR	simple	3	1	PDR			yes	91	RF, HMM
[13]	HAR	simple	4	1	camera		NN, HMM	yes	89	HMM
[14]	HAR	simple, health	7	2	IR			yes	72	Bayes net, SVM, rules
[15]	HAR	ADL	9	1	WIFI RSSI		HMM	yes	95,8	HMM
[16]	HAR	ADL	8	2	PDR	1.2m	Templates	yes	82	particle filter
[17]	HAR	simple, ADL	12	1	IR	75%	best-first-tree	yes	80	HMM
[18]	HAR	ADL	9	0	House's electric system and ultrasonic		Random forest	yes	79,39	RF
[19]	HAR	ADL	23	1	BLE RSSI		Random forest	yes	99,58	RF
[20]	HAR	simple, ADL	5	1	Camera SLAM		ADABOOSTM2	yes	80	no
[21]	HAR	simple	6	1	BLE RSSI	0.4m	Ensemble	yes	91	Rules
[22]	HAR	simple	6	0	UWB		CNN	yes	87	CNN
[23]	HAR	simple	6		simulated		SVM	yes	89,3	no
[24]	HAR	simple, health	5	1	ZigBee fingerprinting	2m	SVM	yes	100	SVM
[25]	HAR	simple, ADL	0	1	wifi, GPS, sound		Ensemble	yes	90	Ensemble

[26]	IPS	simple, ADL	5	1	WIFI fingerprinting	3m	naive Bayes	yes	81,7	Particle filter
[27]	IPS	simple, ADL	4	1	PDR	0.52m	KNN	yes	98,98	HMM
[28]	IPS	simple	4	2	PDR + EMG	1.2m	Linear Discrimination Analysis	yes	98	no
[29]	IPS	simple	4	1	WiFI RSSI	2.8m	Threshold	no		no
[30]	IPS	simple	4	1	WIFI fingerprinting	0.59m	J48	yes	97	Particle Filter
[31]	IPS	simple	4	1	PDR	3m	fuzzy associative classifier	yes	80	HMM
[32]	IPS	simple, ADL	4	0	PIR, RFID, sound					Bayes framework of Set-Membership Filtering (SMF)
[33]	IPS	simple, ADL	7	2	SLAM ROBOT	82%	HMM, NN	yes		HMM
[34]	IPS	simple	3	1	PDR	7 m	J48	yes	91,4	no
[35]	IPS	simple	2	1	BLE RSSI		threshold	no	94	no
[36]	IPS	ADL, work	9	0	Wifi fingerprinting		DTW	no	99,95	DTW
[37]	IPS	simple, ADL	9	1			CNN	yes	95,21	no
[38]	IPS	simple, ADL	9	1	wifi and magnetic fingerprinting	2,4m	Conv LSTM	yes	73	Conv LSTM
[39]	HAR + IPS	simple, ADL, work	23	3	PDR	90%-100%	Templates	yes	89	Particle filter
[40]	HAR y IPS	simple, health	7	1	WIFI fingerprinting	94,11%	KNN3	yes	97,48	no
[41]	HAR + IPS	simple, ADL	8	0	WIFI RSSI	65%		yes	85	deep learning
[42]	HAR y IPS	simple	3	1	BLE RSSI		multilayer perceptron	yes	95,25	no
[43]	HAR + IPS	simple	3	1	BLE RSSI	80,60%	Random forest	yes	73,8	no
[44]	HAR y IPS	simple	4	0	IR	0,85 m	RF	yes	92,51	RF

[45]	HAR + IPS	ADL	6	0	WIFI fingerprinting	95,68%	NN	yes	88,13	Conv. NN
[46]	HAR + IPS	simple, health	8	1	WiFi RSSI	94,16%	NN	yes	94,73	NN
[47]	HAR + IPS	simple, ADL	8	4	PDR	~2m-12m	Random forest	yes	89	RF
[48]	HAR + IPS	simple	2	0	WiFi RSSI	99,70%	Conv. LSTM	yes	90,2	PCA
[49]	HAR + IPS	simple	5	4	UWB	0,19%	SVM	yes	80,2	SVM
[50]	HAR + IPS	simple, health	3	1	WIFI RSSI	2,15m	rules	no	97,5	no

Table 2.4 Summary of the studies of the systematic review.

2.3 Research gaps

As a result of the analysis of the state of the art, it is possible to declare the following gaps:

There is a well-defined current interest in exploiting the potential provided by the relationship between what is done (HAR) and where it is done (IL) for the AAL - and indoor environments in general. This requires that the HAR be supported in IL and vice versa since these two research fields have been frequently addressed separately.

- Of the 12 studies focused on HAR and IL (see the second column of Table 2.4), 8 have used a data fusion technique. The proposed system by Hardegger et al. [39] is the system that recognizes the most activities (23). However, the system uses three devices (IMU in the wrist and foot and smartphone in the pocket). Its IL accuracy was in the range of 90% to 100%, and its HAR accuracy was 89%. Therefore, improving these results through a less invasive solution is desirable.

- To track the location in an indoor environment, it is first necessary to obtain a map. The scenarios for the AAL require getting that map to avoid additional deployment of sensors or an exhaustive training phase. Therefore, the relationship between locations, objects, and activity recognition should be maximized.

- Within existing machine learning techniques for the recognition of activities, the personal models (model trained with data of the person who will use it) require little data per activity, and the collection process of those data and its labeling remains an arduous task, even more if it is considered the number of activities that an older adult could perform in a AAL scenario. For this reason, it is necessary to search for strategies that eliminate or substantially reduce the labeling work for each activity.

- All the studies have used some traditional supervised machine learning methods (Table 2.4), which means that their resulting models are static, and therefore, the complete systems that use them are static. This means that some change in the environment or, even more likely, a change in how a person executes an activity would cause the model to become obsolete. The latter is particularly critical in AAL scenarios because the performance in the execution of ADLs is deteriorated due to natural aging or some neurodegenerative disease such as Alzheimer's or Parkinson's. Therefore, it is necessary to explore semi-supervised or unsupervised methods and incremental or evolving system methods that allow having updated the model for both HAR and IL.

- The evaluation of the studies included in the systematic review is usually done with a small group of people. As Calvaresi and collaborators conclude in their systematic review called "exploring the ambient assisted living domain " [54], due to the small number of people testing the studies included, their lack of rigorous evaluation and validation is evident. Also, the people evaluating the studies have not been older adults. This constitutes a lack of evaluation for systems intended to be used in AAL environments [54].

2.4 Summary

This chapter presented the state of the art related to the research topic addressed. The answers to the research questions posed in the planning of the systematic review allowed the researchers to obtain a broad overview of the current state of knowledge regarding solutions that take advantage of the relationship between HAR and IL. The chapter ends by exposing the gaps that lead to the establishment of the research question and the objectives of this dissertation.

Chapter 3

Indoor localization strategy

This chapter introduced a pipeline for human trajectory reconstruction. Pedestrian dead-reckoning with a zero-velocity update algorithm is the backbone of the pipeline. The pipeline only uses one IMU on the person's foot to get accelerometer and gyroscope data. With that data, it can reconstruct the trajectory of the person. A comprehensive pipeline evaluation is presented at the end of the chapter.

3.1 Indoor localization estimation techniques

Indoor localization has been widely discussed in recent years. This is mainly due to the need for better location accuracy in those environments, where satellite positioning systems, such as GPS, Glonass, and Galileo, are not accurate enough due to the nature of the radio frequency signals. These signals have to travel from outside the planet, suffering high attenuation and also experimenting with the multipath phenomenon [55]. These two characteristics do not represent a problem in locating a target when it has a line of sight to the sky. However, these systems pose a problem when the target is inside indoor environments such as houses or buildings [56].

The development of ubiquitous devices has generated the development of different techniques for estimating or calculating location in indoor environments. Specifically for locating people in those environments, many location-based services (LBS) have been explored. Among them are the monitoring people in hospitals and homes, support in rehabilitation therapies, navigation for blind or visually impaired people, and navigation in shopping centers [55–58].

There is a wide variety of Indoor Location systems (ILS). The deployment of a particular system depends on factors such as privacy, cost, and required accuracy [58].

The calculation or estimation of the position of a person is usually carried out with the help of data that allow the estimation of the position. These can be divided into three groups:

- Wireless: Methods that involve wireless communication technologies such as WIFI, Bluetooth, RFID, Ultra-Wide Band infrared, and ultrasound.

- Pedestrian Dead-Reckoning: Based on the person's last known position, their current position is calculated from their body movement data.

- Video analysis: Technologies that use video or image analysis to detect the person and/or labels or landmarks in the environment to locate the person.

3.1.1 Wireless Technologies

3.1.1.1 Proximity

The proximity technique consists of estimating the position of the person by consulting the known location of nearby devices. In this case, the person must wear a transmitting or receiving device capable of communicating with the devices deployed in the indoor environment. Common examples of this technique are IPSs that use WIFI nodes while the person to be located carries a Smartphone. The proximity of the Smartphone to a specific WIFI node can be estimated based on the Received Signal Strength Indicator (RSSI) received by the Smartphone from the WIFI nodes.

The position estimated by this technique is known as a symbolic position, that is, geometric coordinates of the person's position are not obtained, but an idea of how close he/she is to a certain node. In this way, in cases in which it is sufficient to know where the person is in the house (for example in the kitchen, bathroom, living room, etc.), an IPS based on proximity would be sufficient.

3.1.1.2 Fingerprinting

It is a technique similar to proximity. It consists of two phases: offline and online. In the offline phase, a RSSI map is created. For this, the indoor environment is usually divided into a grid. In each grid cell, the RSSI values received from previously deployed nodes are collected and stored. The receiving device must remain for a certain time in each cell while collecting the RSSI. The person can already be located in the indoor environment in the online phase while carrying the receiving device. This is done by comparing the signals received in real-time with those stored in the offline phase.

Another approach to this method is to have one or more signal emitting nodes. Those signals are affected as the person moves through the indoor environment. Using machine learning techniques, it is possible to train an algorithm that relates the fluctuations in the signals with specific positions of the person.

3.1.1.3 TRIANGULATION

This technique uses the triangle geometry theory to calculate the target's position. The key to this technique is to calculate the distance between two or more nodes and the object to be located. Those distances can be obtained using different methods: Time of Flight (TOF), Time of Arrival (TOA), Time Difference of Arrival (TDOA), and Angle of Arrival (AOA). The most common way to use this technique is to use at least three RF or ultra-sound signal receiving or transmitting nodes to triangulate the position of the target. In that case, since the absolute position of the three nodes is known, the signal measurements of each node can be used to obtain an estimated distance to the target. With the three node-target distance estimates, a much more precise location estimate is obtained by applying the trilateration method.

3.1.2 Pedestrian dead-reckoning

Unlike the previous techniques, Pedestrian dead-reckoning (PDR) does not require the deployment of devices in the indoor environment. In theory, the location of the person can be calculated solely from acceleration and angular velocity data taken with an Inertial Measurement Unit (IMU). Often the person's position is updated when the person takes a step. For this, the position immediately before the step taken is used as the starting point. The length of the step is calculated by integrating the acceleration data twice. The direction of the movement is obtained from both the angular velocity data and the acceleration data.

3.1.3 Video analysis

The location of a person in an indoor environment can also be obtained from the analysis of images or videos. There are two options: deploy cameras around the indoor environment or that the person to be located carries a camera. This method often involves obtaining a map of the environment and subsequently analyzing the raw video to calculate the person's position. Privacy is, therefore, an issue of concern when using this method.

A method born in robotics, known as Simultaneous Location and Mapping (SLAM), is a widely known alternative that avoids previously obtaining the indoor environment map. In SLAM, the person usually carries a camera, and with the collected images, preset landmarks are detected. Landmarks can be elements in a house such as doors, stairs, windows, etc. As the person walks through the indoor environment, SLAM defines the position of the landmarks and simultaneously calculates the position of the person. It is important to mention that SLAM is not limited to the use of video cameras. The automatic generation of the map and the person's location can be obtained with other data sources; for example, using a combination of PDR with detection of landmarks such as RFID tags or WIFI or Bluetooth nodes.

3.2 Pedestrian dead-reckoning-based method for indoor localization

The method chosen to perform IL in this work is based on PDR. Bearing in mind that the intention is to develop a system that tracks the position of older adults in their homes, PDR seems to be an appropriate method due to its low intrusiveness, low cost, and minimal security

risks in terms of the type of data necessary for their functioning. PDR uses body motion data collected by inertial measurement units (IMU) to estimate the change in position of a person based on their last known position [59]. Although modern IMUs often contain an accelerometer, gyroscope, and magnetometer, this latter sensor was not used in the proposed method. This decision was made because the alterations or fluctuations of the magnetic field in indoor environments make it unreliable [60]. Additionally, the system is intended to be as simple as possible and use the fewest devices and sensors to reduce the impact on battery consumption.

PDR methods usually estimate the person's displacement by double integration of the acceleration data. When this operation is carried out, the noise and the intrinsic errors derived from the production of accelerometers and gyroscopes (there are no perfect sensors; they all have a margin of error) are raised to the third power. This makes indoor localization using only double integration of acceleration data impractical [61–63]. Foot-mounted PDR, along with zero-velocity update (ZUPT) algorithms, has been the most widely and successful method used to reduce the drift in estimating the person's location [61]. Most of the foot-mounted PDR systems have been evaluated with normal walking. Natural movements that occur in daily life like swinging legs while sitting, side steps, stopping, or avoiding obstacles, have rarely been considered. Dealing with these kinds of natural movements in an AAL environment is essential, but no studies that evaluate the IL taking into account the aforementioned natural movements in AAL were found. While collecting a dataset with these characteristics, it was decided to propose a pipeline for trajectory reconstruction based on PDR ZUPT and evaluate it using the dataset of Martindale et al [64]. This dataset contains data collected from a foot-mounted IMU while people were performing activities involving side steps, swinging feet while sitting, stopping, and avoiding obstacles. It also contains activities that involve walking, running, and jogging. Therefore, performing trajectory reconstruction using that dataset poses a huge challenge.

To deal with walking and running activities, threshold-based and machine learning-based foot-mounted PDR approaches have been proposed [65–69]. The foot-mounted PDR systems are usually evaluated in closed-loop trajectories by measuring the return position error (RPE). The RPE indicates the distance between the final position of the person obtained by the system and the actual physical final position of the person at the end of the trial [60]. Li et al. [65,66] proposed a threshold-based stance-phase detector that consists of one footstep detector and two zero-velocity detectors, one for walking and another for running. One pedestrian walked and ran in two closed-loop trajectories, one square-shaped (195.7 m), and the other eight-shaped path (292.1 m). For the square-shaped path, the RPE was 0.24% for walking and 0.42% for running. For the eight-shape path, the RPE was 0.2% for walking and 1.01% for running. Wagstaff et al. [68] proposed an adaptive zero-velocity detector that selects an optimal threshold for zero-velocity detection depending on the movement of the person (walking or running). Five people evaluated this system. They walked and ran 130 m in an "L" shaped path. The RPE was 1% for walking and 3.24% for running.

Wagstaff et al. [69] proposed a method for zero-velocity detection by using a long short-term memory neural network (LSTM) [16]. The advantage of this method is that machine learning-

based zero-velocity detection is free of threshold-tuning. The evaluation of this method consisted of five people walking and running a 220-m “L” shaped path. The RPE in walking was 0.49% and running 0.93%. Similarly, Ren et al. proposed a zero-velocity detection algorithm based on HMM [67]. The system was evaluated by one person in an oval-shaped sports field of 422 m. The RPE when walking and running were 0.6% and 1.61%, respectively.

In the described studies, good results have been obtained in the trajectory reconstruction. However, these only contain continuous sequences of walking and running, they do not include natural movements that occur in ADLs. In addition, they were evaluated with very few people. The proposed pipeline for personal trajectory reconstruction closes these two gaps. It is divided into 4 modules (Figure 3.1). The data flow is from left to right. In the first module is the data collection device, in this case, an IMU. This device must be worn by people on one of their feet. This is with the aim of implementing a method based on PDR ZUPT. In the second module, the accelerometer and gyroscope data collected with the IMU are processed. First, the type of movement of the person is classified: walking, jogging, or running. Then, the data for each stride are obtained separately and two gait events are detected for each stride: mid-stance and toe-off. With these gait events detected it is possible to calculate the length and orientation of each stride in the third module. Finally, using the stride length and orientation, the trajectory of the person is updated.

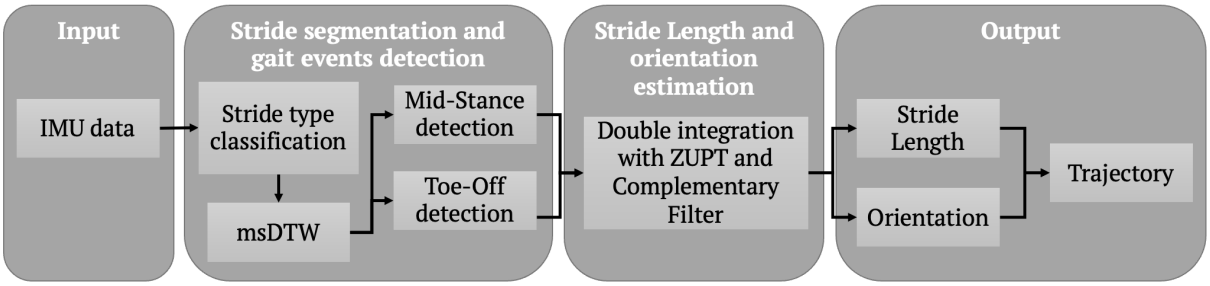

Figure 3.1 Pipeline for indoor localization

This pipeline is based on the work of Hanning et al. [70]. The toe-off and mid-stance detection algorithms were adapted to deal with non-walking strides. Stride-type classification and double integration process with ZUPT and complementary filter were added. The process for trajectory reconstruction through the proposed pipeline is detailed below.

3.2.1 IMU

The same alignment and position of the IMU are used in all of our experiments. The IMU is glued on one side of the shoe at ankle height (Figure 3.2). The IMU set up for data collection is as follows: sampling rate: 200Hz, acceleration range ±16 g, angular velocity range ±2000 DPS. The IMUs used are usually from Shimmer (Shimmer sensing, Dublin, Ireland). Before each data collection session, the IMU is calibrated. The calibration process is simple and runs using the manufacturer's software. Accelerometer calibration consists of letting the IMU rest on each of its six sides. Gyroscope calibration consists of rotating the IMU completely around each of its axes.

(a) (b)

Figure 3.2 IMU placement and sensor axis alignment. (a)Accelerometer (b) Gyroscope.

3.2.2 Stride segmentation and gait events detection

The two primary phases of the gait cycle are the swing phase and the stance phase. The stance phase consists of the entire time that a foot is on the ground. The swing phase consists of the entire time that the foot is in the air (Figure 3.3).

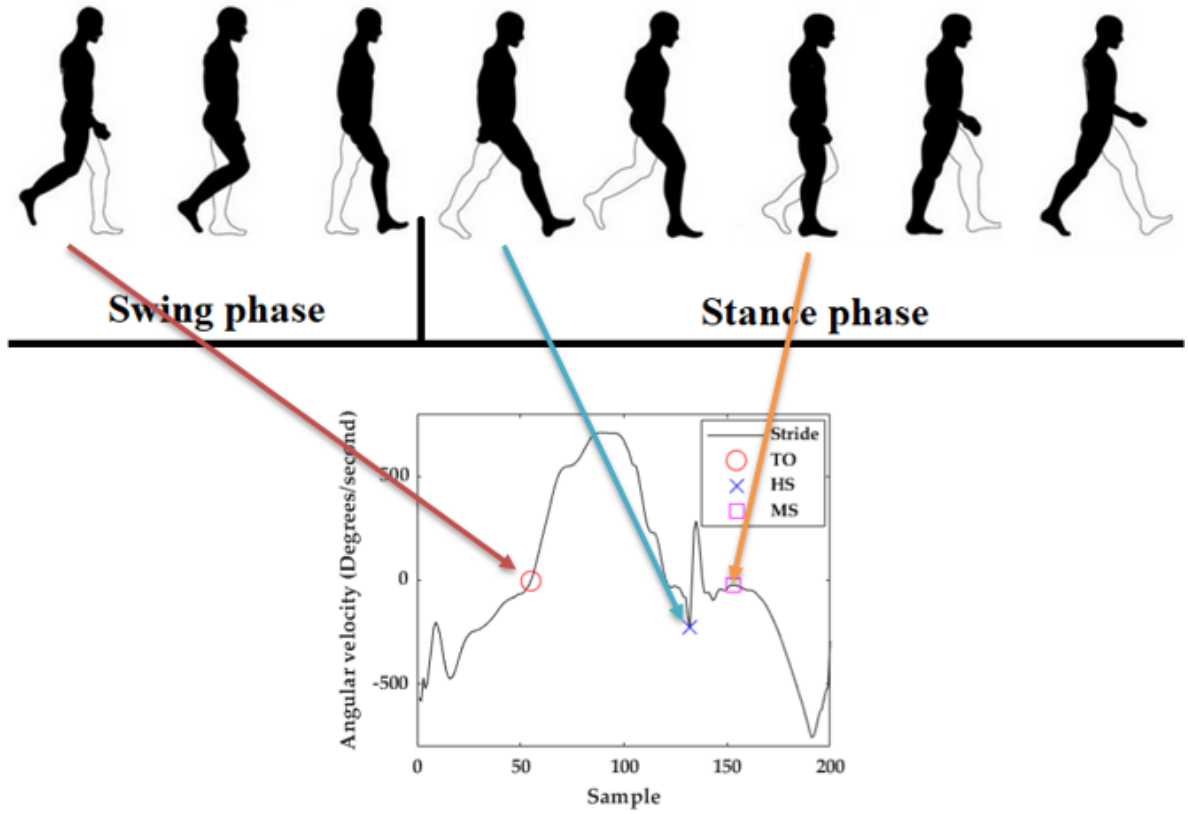

Figure 3.3 Gait cycle and signal generated.

The start of the swing phase is known as the toe-off (TO) event. This event occurs just as the foot leaves the ground. The end of the swing phase is when the heel hits the ground, an event called heel strike (HS). During the stance phase, the mid-stance (MS) event occurs when the person's foot is fully supported on the floor. At that moment the speed of the foot is zero and

therefore the energy of the acceleration and gyroscope signals is equal to zero. [71,72] (Figure 3.3).

3.2.2.1 Multi-dimensional subsequence dynamic time warping (msDTW)

msDTW is a template-matching method. It is used to find a subsequence of continuous signal sequences similar to a given reference pattern. It has been proven that using foot-mounted IMU and msDTW is a robust method for stride segmentation of healthy people, older adults, and Parkinson's patients [73]. In the context of stride segmentation, that pattern consists of a template of one stride. Figure 3.4 shows the gyroscope z-axis signal for the three types of motion. As can be seen, although the shape of the signal is similar in all three cases, there are peculiarities at some specific points. For example, a walking stride would be expected to be longer than a running stride. It is also logical that the magnitude of the running stride signal is greater than the others due to the rapid movement involved in running. Since msDTW looks for similarities in the continuous signal concerning a template, the differences in the walking, jogging, and running patterns make it necessary to have a unique template for each of them.

The strategy followed to obtain the three templates consisted of developing a MATLAB script that obtained all the walking, jogging, and running strides from the dataset of Martindale et al. [64] (described in detail in section 3.2.3.2 Dataset 2). A total of 8,724 walking, 1,688 jogging, and 1,360 running strides were obtained from 20 people. In [73–75] only straight strides were included for the generation of their templates. Unlike them, we include both straight and turning strides. The process of obtaining each template consisted of taking each stride and interpolating it to a fixed size of 200 samples. Finally, the signal magnitude of each of the 200 samples of all strides was averaged. This process was done by the aforementioned MATLAB script. The result of this process for the gyroscope z-axis signal is displayed in Figure 3.4.

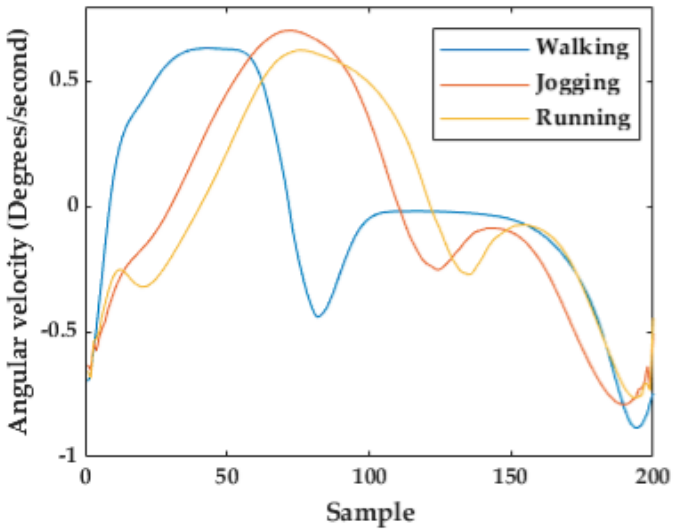

Figure 3.4 Walking, jogging and running templates (Gyroscope z-axis).

With the generated templates, the segmentation of the strides was carried out using the msDTW implementation written in MATLAB by Hannink et al. [76]. An example of the result obtained of the segmentation of a sequence of running strides is shown in Figure 3.5.

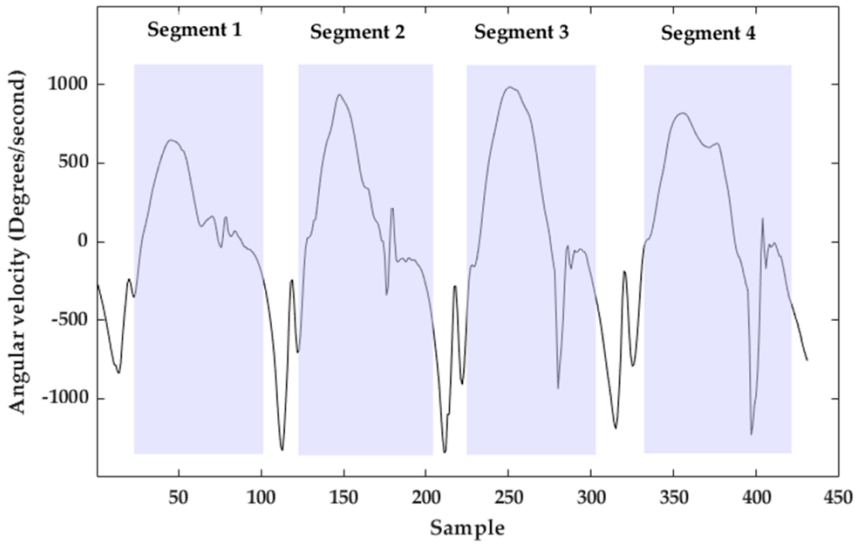

Figure 3.5 Example of stride segmentation using msDTW.

Each of the segments is a possible stride. It can be seen that there are spaces between the segments although the four strides were consecutive; that is, the person did not stop during the march. This problem was solved using the TO event detection explained in section 3.2.2.3. The first gait event that occurs in each segment (from left to right) is the TO. The start of a stride was defined as its TO event and for consecutive strides, the end of the stride is the TO event of the next stride. In this way, the segments obtained correspond more closely to the strides that occurred in the performance of each activity in Figure 3.6.

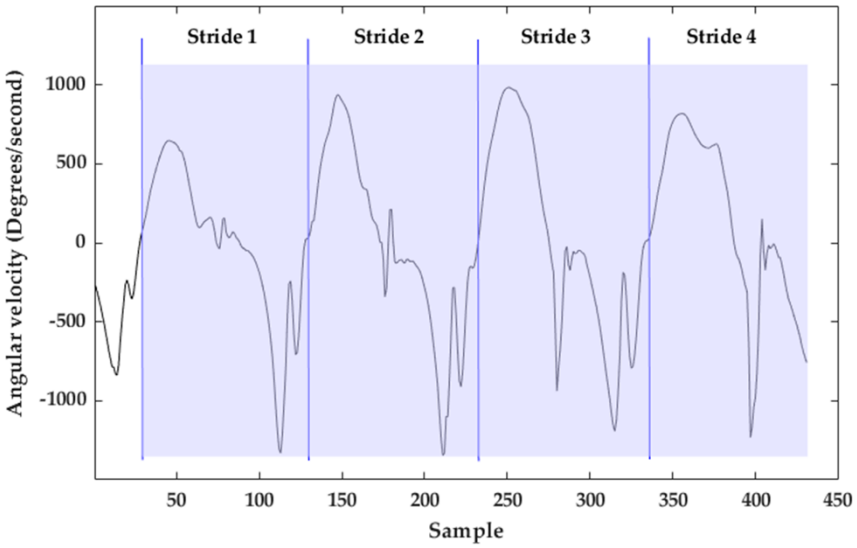

Figure 3.6 Final stride segmentation using msDTW and TO detection

The precision and sensitivity of the stride segmentation using msDTW can be tuned using a threshold. The threshold needed to detect a stride indicates the similarity between that stride and the template used; that is, a large threshold indicates a large difference between the template and the segmented stride [23]. Therefore, with a very small threshold, the number of false-negative strides would increase, and a very large threshold would generate false positives strides. Thresholds from 0 to 100 in steps of 5 were tested on the training dataset. As a result, it was found that a fixed threshold of 65 maximizes the F-score of the stride segmentation in walking, jogging, and running activities (Figure 3.7).

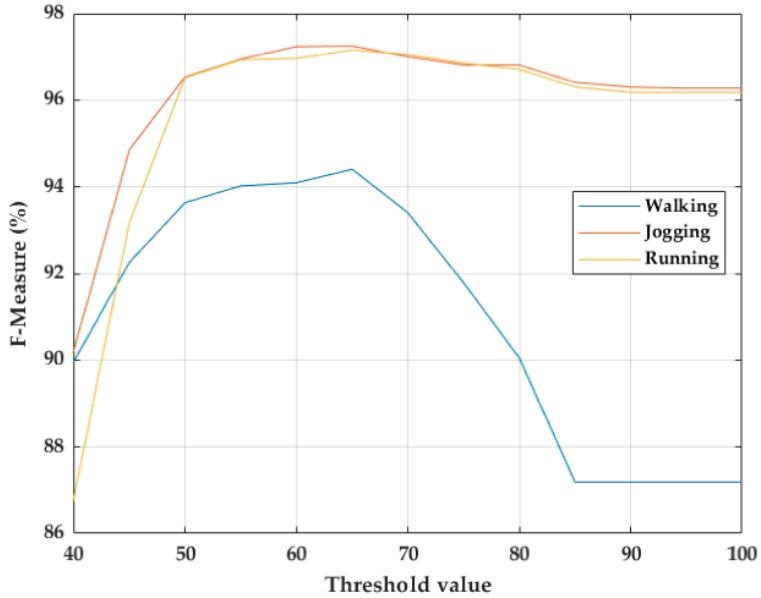

Figure 3.7 Threshold choice for stride segmentation of walking, jogging, and running strides using msDTW.

3.2.2.2 STRIDE TYPE CLASSIFICATION

The stride segmentation process with msDTW requires the correct template to be used based on the person's type of movement. For this reason, before executing the stride segmentation, it is necessary to know which of the three templates to use. In order to automatically select the walking, jogging, or running template that will be used in the stride segmentation process, some machine learning algorithms included in the MATLAB classification learner app were evaluated using the Martindale dataset (Section 3.2.3.2 Dataset 2). A window size of 200 samples (1 second of data) and an overlap of 100 samples were used for feature extraction. The features extracted were velocity (by integrating accelerometer readings), angular velocity, and energy of accelerometer and gyroscope axes (square root of the sum of the signal of the three axes of the sensor). Using the majority vote rule, the most frequent value in the result was chosen as the final classification. The evaluation was performed using ten-fold cross-validation. As a result, the highest accuracy was achieved by the SVM classifier with a polynomial kernel function of third-order (98.1%).

3.2.2.3 TOE-OFF DETECTION

When the ankle joint changes from plantar flexion to a dorsal extension position in the sagittal plane, the gyroscope z-axis describes a zero-crossing [73]. The algorithm included in [76] for TO detection consists of detecting the first zero-crossing in the gyroscope z-axis. Due to the abrupt movements in jogging and running strides, in a few cases, a peak located at the beginning of the stride causes a zero crossing. This would lead to a wrong TO detection (red circle in Figure 3.8). Consequently, the adapted algorithm for TO detection (Table 3.1) find the maximum peak of the signal and then finds the nearest zero crossing before it (blue circle in Figure 3.8). After the detection of all the TOs that belongs to the activity, all the portions corresponding from TO to TO are considered as strides (Figure 3.6). The longer stride time is a walking stride. Considering that it lasts around one second [64], if one TO to TO portion is greater than 2 s (400 samples), only the signal of the first 1.5 s was considered to calculate the length and orientation of the stride. A TO to TO segment greater than 400 samples usually indicates that the person stopped walking, jogging, or running.

1: xMP ← getMaximumPeak(stride-gyro-z)

2: xZC ← getZeroCrossing(stride-gyro-z(1 : xMP))

3: TO ← getNearestZCtoMP(xZC, xMP)

Table 3.1 Toe – off (TO) detection algorithm.

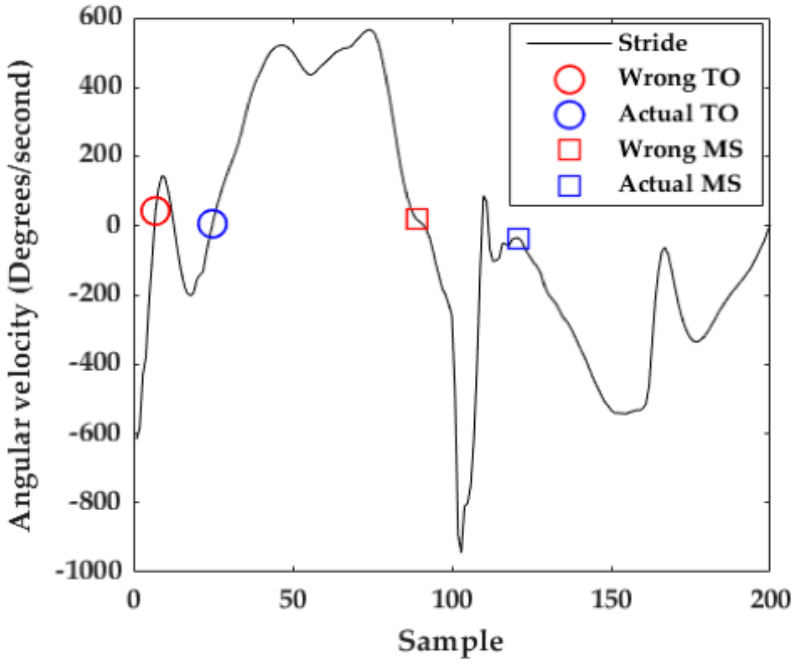

Figure 3.8 Example of TO and MS detection.

3.2.2.4 MID-STANCE DETECTION

At Mid-Stance (MS) the foot is entirely stationary on the ground [73,74], which means that its velocity is zero. The gyroscope z-signal is minimal at that moment. The stance-phase time decreases as the speed of movement increases from walking to running (Figure 3.3). This makes MS detection more difficult for jogging and running strides [62]. The algorithm proposed in [76] for MS detection in walking strides consists of calculating the middle of the window with the lowest energy in the full stride's gyroscope z-signal [73,74,76]. That algorithm often does not detect properly the MS for jogging and running strides, because it confuses the MS with other parts of the signal, like the valley just before the HS or the peak before the next TO (red square in Figure 3.8).

The adaptation of the MS detection algorithm (Table 3.2) consisted of (1) taking only the stride portion from HS to 80% of the stride. This portion was chosen taking into account that the stance-phase of walking strides is approximately the last 60% of the stride and for jogging and running strides is approximately the last 40% of the stride [77]. (2) Calculating the middle of the window with the lowest energy within that portion—to this end, a window size of 20 samples (100 ms) and a window overlap of 10 samples (Blue square in Figure 3.8) are used.

```
1: windowSize ← 20
2: overlap ← 10
3: stride ← interpolateStrideTo200Samples(stride-gyro-z)
4: xMP ← getMaximumPeak(stride)
5: stride ← stride(xMP : 160)
6: xHS ← getMinimumPeak(stride)
7: stride ← stride(xHS : end)
8: MS getMinimumEnergy(stride, windowSize, overlap)
```

Table 3.2 Mid-Stance detection algorithm

3.2.2.5 STRIDE LENGTH AND ORIENTATION ESTIMATION

The zero-velocity update (ZUPT) method was used to mitigate the drift due to the use of an IMU. Zero-velocity detection was done by supervising the magnitude of the gyroscope rate of turn of each measurement. If the measurement is less than a threshold of 0.6 DPS, that measurement is considered a zero-velocity measurement. It has been proved that this simple approach works properly in walking strides [63,71]. However, this approach does not work correctly in jogging and running strides due to the abrupt signal variations. The solution to this problem is the use of the MS detection algorithm proposed (Table 3.2 Mid-Stance detection algorithm). Considering that the average stance-phase time in running strides is around 100 ms (20 samples using a sample rate of 200 Hz), it was empirically found that taking 5 samples to each side of the MS (which corresponds to 50 ms) leads to better zero-velocity detection in jogging and running strides.

After zero-velocity detection, a Complementary Kalman Filter (CF) was used in order to model the error in velocity and position estimates using the ZUPTs as measurements. When zero-

velocity is detected, but the estimated velocity is different from zero, the CF adjusts the velocity and the corresponding displacement. The CF used in this work is based on the proposed work by Fischer et al. [63].

Three parameters have to be set up for the CF initialization: accelerometer and gyroscope noise (σ_a and σ_w) and the ZUPT detection noise (σ_v). Accelerometer and gyroscope noise were set to an equal value (σ_a = 0.01 m/s2 and σ_w = 0.01 rad/s). ZUPT detection noise depends on the velocity of the participant. That parameter was established by evaluating from σ_v = 0.001 m/s to σ_v = 0.05 m/s in steps of 0.001 m/s. The σ_v chosen was the one that produced the least error in the final distance evaluated.

The initialization of the Complementary Filter (CF) implies establishing a series of matrices. First, the state of the CF is described with a matrix that includes the errors in orientation, position, and velocity. Equation 3.1 shows the state in an array representation. Each array element is a 1x3 array containing the errors in the three-axis.

$$E = [E_o \; E_p \; E_v] \qquad \text{Equation 3.1}$$

The error covariance matrix accumulates the error in orientation, position, and velocity produced in each sample k:

$$P_k = [0_{9x9}] \qquad \text{Equation 3.2}$$

The state transition function (Equation 3.3) is a matrix that is multiplied by the state matrix to get the next state of the filter. 'S' is the Skew-symmetric cross-product operator matrix formed from the n-frame accelerations and Δt is the time step equal to 0.005 seconds, which results from dividing 1 second between the IMU data collection frequency (200Hz).

$$F_k = \begin{matrix} I_{3X3} & 0_{3x3} & 0_{3x3} \\ 0_{3x3} & I_{3X3} & I_{3X3}\Delta t \\ -S\Delta t & 0_{3x3} & I_{3X3} \end{matrix} \qquad \text{Equation 3.3}$$

The process noise covariance matrix is calculated for each sample by multiplying the accelerometer and gyroscope noise by Δt:

$$Q_k = \left[\left(\sigma_{w_x} \; \sigma_{w_y} \; \sigma_{w_z} \; 0 \; 0 \; 0 \; \sigma_{a_x} \; \sigma_{a_y} \; \sigma_{a_z}\right)\Delta t\right] \qquad \text{Equation 3.4}$$

The uncertainty in velocity during each ZUPT is represented using the measurement noise covariance matrix (Equation 3.5). It is a diagonal matrix because no correlation in velocity is supposed to exist between axes.

$$R = \begin{matrix} \sigma_{v_x}^2 & 0 & 0 \\ 0 & \sigma_{v_y}^2 & 0 \\ 0 & 0 & \sigma_{v_z}^2 \end{matrix}$$ Equation 3.5

The measurement function matrix is used to move from the state variables space to the measurement variables states. In this implementation, the measurements are the ZUPTs that are recorded when velocity is supposed to be zero. That way, the measurement function has to contain an identity matrix in the position of the velocity error state as follows:

$$H_k = [(0_{3x3}\ 0_{3x3}\ I_{3x3})]$$ Equation 3.6

Before running the CF, the gyroscope bias has to be removed. Gyroscope bias is obtained by calculating the mean of the gyroscope readings while IMU is not moving, just before the beginning of the activity. The resulting value is subtracted from all gyroscope readings.

After gyroscope bias subtraction, the CF is executed. It has two phases: Prediction and update. In the prediction phase, the error covariance matrix (P_k) is propagated using Equation 3.7:

$$P_k = F_k P_{k-1} F_k^T + Q_k$$ Equation 3.7

Only when a sample k is a ZUPT, the Update phase is executed. In this case, the Kalman gain is calculated with Equation 3.8.

$$K_k = P_k H^T (H P_k H_T + R)^{-1}$$ Equation 3.8

After the Kalman gain is calculated, the errors in orientation, position, and velocity are obtained using Equation 3.9.

$$E = \left[E_o\ E_p\ E_v\right] = K_k V_k$$ Equation 3.9

Finally, the velocity and position estimates are corrected, as well as the error covariance matrix P_k:

$$V_k = V_k - E_v$$ Equation 3.10

$$Pos_k = Pos_k - E_p$$ Equation 3.11

$$P_k = (I_{9x9} - K_k H) P_k$$ Equation 3.12

The stride length and orientation estimation are obtained using the position increments in each zero-velocity update (MS events). Stride length, where ∇P_k is the position increment from stride k-1 to stride k, is calculated as follows:

$$SL_k = \sqrt{\nabla P_k(x)^2 + \nabla P_k(y)^2} \qquad \text{Equation 3.13}$$

3.2.3 Evaluation of the pipeline for trajectory reconstruction.

The proposed pipeline has the ability to reconstruct the trajectory of people regardless of the speed of their movement. This was evaluated using the two datasets described below.

3.2.3.1 Dataset 1

This dataset was collected by the author of this work at the University of Cauca, Popayán, Colombia. Ten pedestrians (with a mean age of 30 ± 3 years) walked, jogged and ran a closed-loop P-shaped path of approximately 150 meters. They wore an IMU attached to the lateral side of the left shoe with a Velcro strap. Jogging was described to the participants as "if one would jog for exercise in the evening" and running as "if one is late for a bus". Figure 3.9 shows a map of the path. The IMU was a Shimmer3 GSR+ (Shimmer Sensing, Dublin, Ireland). Acceleration (range: ±16 g) and angular velocity (range: ±2000 DPS) were collected at a frequency of 200 Hz. At the beginning of each trial, the participant was asked to remain standing without moving the IMU for at least 10 seconds for gyroscope bias calculation.

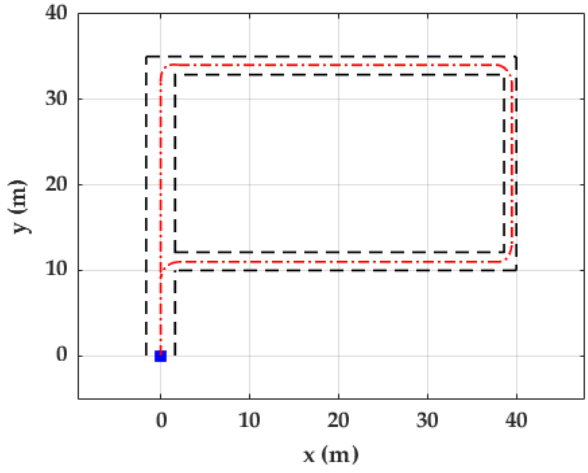

Figure 3.9 Top view of the trajectory followed in dataset 1.

3.2.3.2 Dataset 2

This dataset was collected by Martindale et al. to evaluate a method for smart labeling of cyclic activities [64]. It is publicly available at www.activitynet.org. The dataset provides gait data in a relatively natural setting. Its protocol consisted of the execution of 12 different task-driven activities performed in random order for each participant. It has data from 80 healthy participants with a mean age of 27 ± 6 years. Data were collected from 56 participants at the

Friedrich-Alexander University Erlangen-Nürnberg (Germany) and 24 participants at the University of Ljubljana (Slovenia). Data from 20 of these 24 participants were used only for template generation (Figure 3.4) and msDTW threshold definition (Figure 3.7). In this work, only the data collected from the IMU worn on the left foot was used for trajectory reconstruction of the ten activities shown in Table 3.3. The acceleration (range: ±8 g) and angular velocity (range: ±2000 DPS) were collected at a frequency of 200 Hz. The big advantage of this dataset is that it contains the swing and stance phases (on-ground and off-ground phases) of each stride labeled. The data were acquired in an indoor environment with chairs and tables as shown in Figure 3.10.

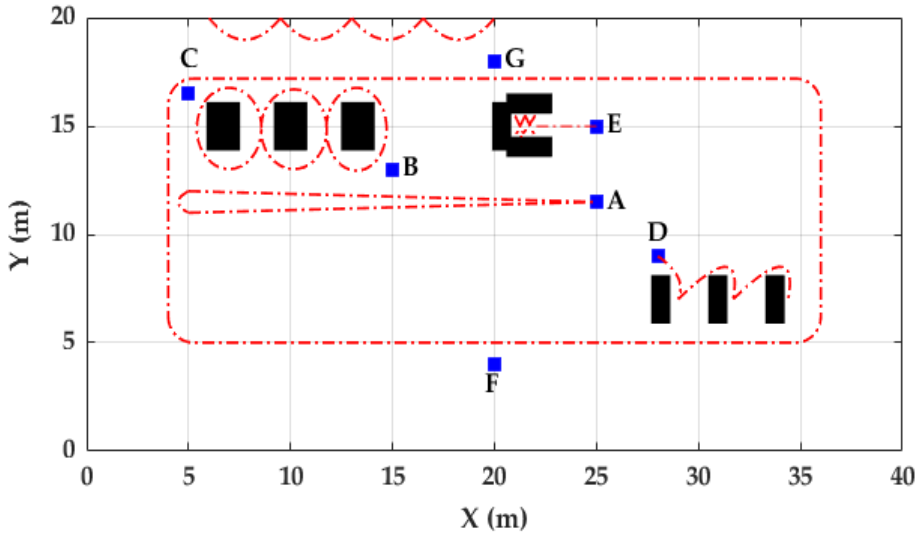

Figure 3.10 Top view of the indoor environment of dataset 2.

Activity	Description	Start → end Position	Approximated traveled distance (m)
W-Slalom	Walk slalom through 3 tables	B → B	31
W-Posters	Sign name on 5 posters on the wall	C → G	21
W-Tables	Perform tasks at 3 different tables while sitting	D → D	20
W-Cards	Perform task on a table while standing	E → E	6
W, J, R-20	Walk, jog, run 2 times 20m	A → A	40
W, J, R-Circuit	Walk, jog and run half a circuit each	F, G → G, F	43

Table 3.3 Activities in dataset 2.

3.2.3.3 EVALUATION RESULTS WITH DATASET 1

Classification of the type of activity.

There were only three errors in the classification of the person's activity (Figure 3.11). Two running activities were classified as jogging and one jogging activity was classified as running. The overall accuracy in the activity classification was 90%

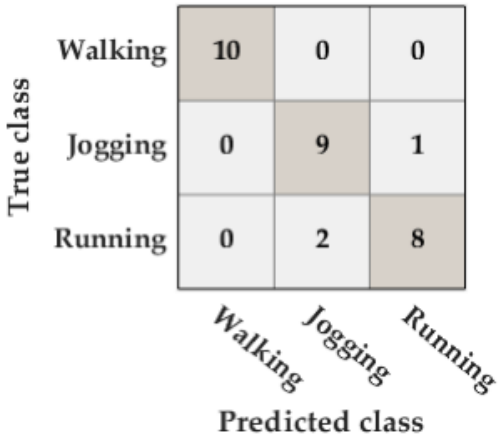

Figure 3.11 Confusion matrix of the classification of type of activity dataset 1.

Toe-off and mid-stance detection.

TO and MS were manually labeled in dataset 1. A TO or MS event is considered as a true positive (TP) if it is located within 15% of the total number of samples of the stride to the right and left of the TO/MS ground truth. A false positive (FP) occurs when a TO/MS is detected outside this range. A false negative (FN) indicates that a TO or MS for a stride was not detected.

Having in mind that 40% and 60% of the stride corresponds to the stance-phase of walking and running strides, respectively [77], the TO detection performance was evaluated in the training dataset using error ranges from 5% to 21% of the total stride in steps of 3% (Figure 3.12). As a result, 15% was chosen as an acceptable error range for TP calculation.

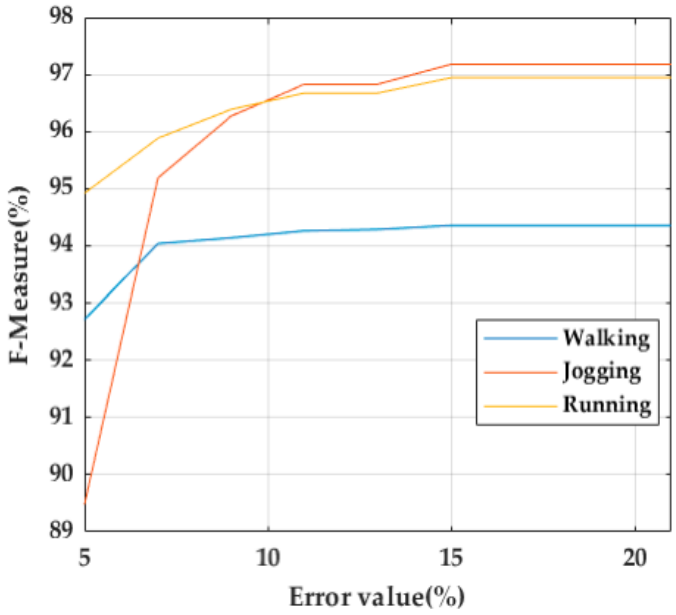

Figure 3.12 TO performance evaluation using different errors ranges.

The performance of the proposed algorithms for the detection of TO and MS included in the pipeline (Table 3.4) were compared with the algorithms previously proposed in [76] (Table 3.5).

	Toe-Off					Mid-Stance				
Activity	TO GT	TP	FP	FN	F-Score (%)	MS GT	TP	FP	FN	F-Score (%)
Walking	105.5	105.4	0.1	0.1	99.9	104.5	104.4	0.1	0.1	99.9
Jogging	75.4	39.4	37.1	36.2	51.5	74.4	41.2	34.2	33.3	54.9
Running	59.6	21.7	37.5	37.1	36.4	58.6	25.8	31.5	30.7	45.3

Table 3.4 TO and MS detection results for dataset 1. Algorithms in [76].
TO GT: ground truth TO rate. MS GT: ground truth MS rate. TP: true-positive rate. FP: false-positive rate. FN: false-negative rate.

	Toe-Off					Mid-Stance				
Activity	TO GT	TP	FP	FN	F-Score (%)	MS GT	TP	FP	FN	F-Score (%)
Walking	105.5	105.5	0	0	100	104.5	104.5	0	0	100
Jogging	75.4	75.2	0.1	0.2	99.8	74.4	74.4	0	0	100
Running	59.6	59.3	0.3	0.2	99.7	58.6	58.5	0.1	0.1	99.8

Table 3.5 TO and MS detection results for dataset 1. Proposed algorithms.
TO GT: ground truth TO rate. MS GT: ground truth MS rate. TP: true-positive rate. FP: false-positive rate. FN: false-negative rate.

The F-score achieved for the proposed TO and MS detection algorithms outperformed that achieved for the previous algorithms for all jogging and running activities. In the case of walking activities, the results are very similar for both the proposed and former algorithms. As a conclusion, for dataset 1, the proposed algorithms can detect TO and MS events in walking, jogging, and running strides.

The amount of FP and FN in the detection of TO and MS leads to the conclusion that the choice of the threshold (Figure 3.7) was appropriate. It is important to remember that the threshold was established with the data of 20 people (from Slovenia) from dataset 2.

Trajectory reconstruction in dataset 1.

Two measures were used to evaluate the trajectory reconstruction:

(1) Return position error (RPE): it is the distance between the coordinates of the actual final point of the activity (for this dataset these coordinates are (0, 0)) and the coordinates of the participant's final stride calculated using the pipeline.

(2) Strides out of trajectory (SOT): All strides of the reconstructed trajectory should be within the boundaries of the corridors represented by black dotted lines (Figure 3.9). Otherwise, those strides will be counted as out of trajectory.

In general, the higher velocity the higher SOT and RPE. Although on average 5.7 % of the strides are out of trajectory in the running trial, the RPE remains less than 1.0% (Table 3.6). Trajectories of the three trials are mostly within the boundaries. Trajectory reconstruction for the ten participants of dataset 1 formed a P-shaped path in the three cases (Figure 3.13, Figure 3.14, and Figure 3.15). Black dotted lines show outer edges (walls) of the possible path. Gray lines are the trajectories reconstructed of the ten participants by using the proposed pipeline.

Sometimes the RPE is small, but the reconstructed trajectory does not fit the actual trajectory performed by the person. As a consequence, the number of strides out of the trajectory was proposed as an additional evaluation metric. The RPEs obtained with the pipeline proposed for the three trials collected in dataset 1 are less than 1%. This result is similar to the obtained in [65–69].

Activity	SOT				RPE			
	[76]		P. A		[76]		P. A	
	#	%	#	%	meters	%	meters	%
Walking	1.7	1.6	1.7	1.6	0.8	0.5	0.8	0.5
Jogging	6.6	8.6	2.9	3.8	2.2	1.4	1.4	0.9
Running	5.3	9.2	3.3	5.7	2.6	1.6	1.4	0.9

Table 3.6 Trajectory reconstruction results. Dataset 1. (#: number of SOT. %: percentage of SOT)

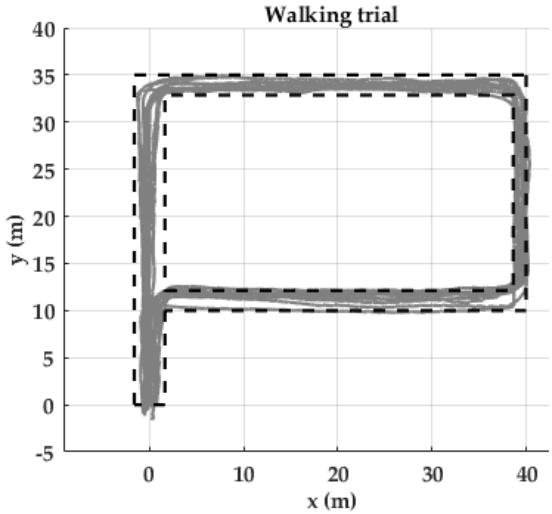

Figure 3.13 Trajectory reconstruction result. Dataset 1. Walking

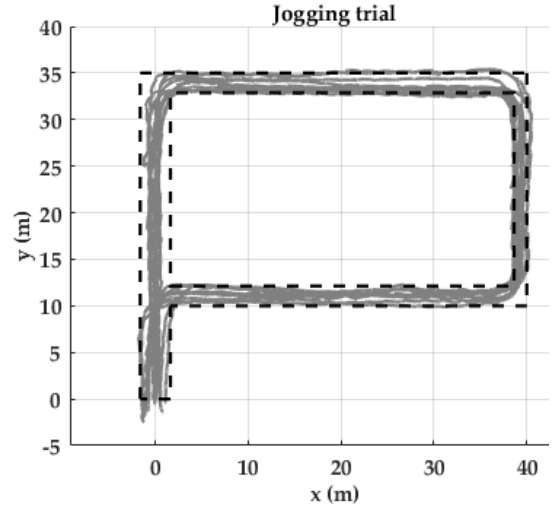

Figure 3.14 Trajectory reconstruction result. Dataset 1. Jogging

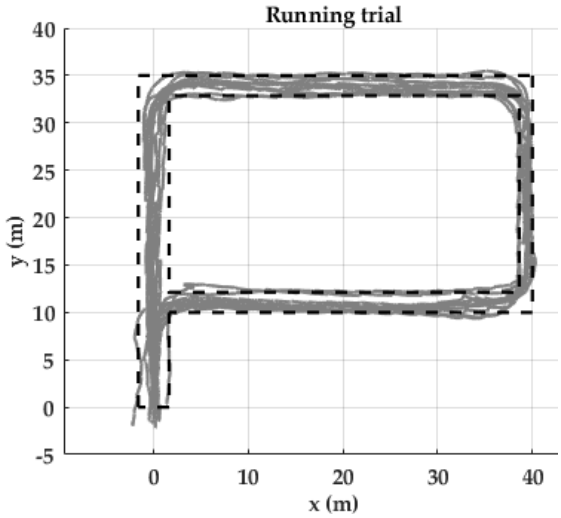

Figure 3.15 Trajectory reconstruction result. Dataset 1. Running

3.2.3.4 EVALUATION RESULTS WITH DATASET 2

Only the data collected from the 56 participants at the Friedrich-Alexander University Erlangen-Nürnberg (Germany) were used to evaluate TO detection and trajectory reconstruction.

Classification of the type of activity.

The results obtained in the classification of the type of activity for dataset 2 using the SVM algorithm are similar to those obtained in dataset 1. This confirms that the most frequent classification errors occurred between jogging and running activities. Fourteen activities were classified as running and were jogging activities. Similarly, 17 running activities were misclassified as jogging (Figure 3.16). It is possible that these misclassifications occurred because the running and jogging speeds of some of the people in both datasets were very similar. The use of personal models could be a solution. These models based on machine learning are trained with data from the same person who is going to use them.

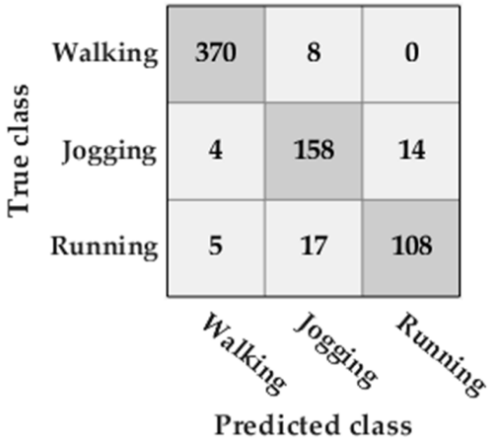

Figure 3.16 Confusion matrix of the classification of type of activity dataset 2.

Toe-off mid-stance detection.

It was not possible to evaluate MS detection in dataset 2 because it does not have ground-truth information for mid-stance. Therefore, only TO detection was evaluated. In dataset 2 the beginning and end of the stance and swing phase are labeled. The last sample of the stance-phase of each stride was used as ground truth for the evaluation of the TO detection algorithm.

The data collected from the 56 participants at the Friedrich-Alexander University Erlangen-Nürnberg (Germany) were used to evaluate TO detection. The same criteria used in dataset 1 for TP, FP, and FN calculations were used. The average results of TO detection for each type of activity performed by the 56 participants using the previous and the proposed algorithms are shown in Table 3.7.

Activity	TO	TP		FP		FN		F-Score (%)	
		[76]	P. A	[76]	P. A	[76]	P. A	[76]	P. A
W-Slalom	21.5	21.2	21.2	0.8	0.8	0.4	0.3	97	97
W-Posters	13.0	10.6	10.6	3.6	3.5	2.3	2.3	77	78
W-Tables	11.9	9.5	9.5	3.7	3.7	2.4	2.4	75	75
W-Cards	4.33	3.7	3.7	1.6	1.6	2.4	0.6	71	71
W-20	28.4	28.2	28.2	1.3	1.0	0.4	0.2	99	98
J-20	22.3	13.7	21.6	9.7	1.1	8.6	0.7	56	96
R-20	18.4	8.1	17.0	12.3	2.1	10.6	1.3	48	90
W-Circuit	28.2	27.6	27.7	0.7	0.7	0.4	0.3	98	98
J-Circuit	21.9	11.8	21.3	10.8	0.7	10	0.5	49	97
R-Circuit	17.7	7.6	17.3	10.7	0.8	10.2	0.4	40	96

Table 3.7 Toe-Off detection results. Dataset 2.

W-Posters, W-Tables, and W-Cards are the three activities with the lowest F-Score values. This is very likely to happen since those activities involve non-stride movements such as stopping, sitting, lateral and backward steps. This means that the signal generated for those foot movements is different from the three generated templates. This could be accounted for by using templates generated by those specific movements, as previously demonstrated in [75], where specific templates were generated for each specific activity such as ascending and descending stairs. Unfortunately, the wide range of possible natural foot movements makes this alternative difficult to implement. Other types of methods need to be evaluated. For example, a hierarchical hidden Markov model (hHMM) approach has proved to be a robust method for stride segmentation of walking activities that include non-stride movements in Parkinson's patients [67] and for stride segmentation of jogging activities [69]. Furthermore, hHMM is a threshold-free approach; therefore, it should be explored in order to improve the results obtained for the walking activities that include non-stride movements such as W-Posters, W-Tables, and W-Cards, as well as for stride segmentation of jogging and running activities.

For all the activities, the number of false positives (FP) was always higher than the number of false negatives (FN). This did not occur in dataset 1. In this case, this could indicate that the

threshold used for stride segmentation with msDTW might have been overestimated since a large threshold implies that there is a large difference between the template used and the segmented strides. This generates FP strides. However, it was confirmed that by reducing that threshold, the number of FN increased, causing a decrease in the F-score. Threshold-free methods based on machine learning techniques such as those used by Ren [67] and Wagstaff [69] would make the stride segmentation process straightforward by avoiding to set any threshold.

Trajectory reconstruction in dataset 2.

It is important to note that the start and end activity positions were defined by chairs in the indoor environment. For that reason, the actual positions where the participants started and finished the activities were not precisely the same as the chairs' positions since participants began each activity near the corresponding chair and did not necessarily return to the exact point where they started the activity. Based on the videos of the data collection, participants started and finished the activities within a radius of 1.5 m around the chairs. This has to be taken into account while analyzing the trajectory reconstruction results in Table 3.8. Moreover, it was not possible to subtract the gyroscope bias in all activities performed in dataset 2 because the activities were performed continuously. A prerequisite for bias computation is that the person stands still for a few seconds for the calculation of the mean of the gyroscope readings and then subtracts it from the entire movement sequence. These two limitations of dataset 2 may be the cause of the higher RPE compared to dataset 1.

Activity	Activity distance	SOT				RPE			
	(meters)	[76]		P. A		[76]		P. A	
		#	%	#	%	meters	%	meters	%
W-Slalom	31	1.1	5.2	1.1	5.2	1.7	5.5	1.7	5.5
W-Posters	21	1.0	8.0	1.0	8.0	1.9	9.0	1.8	8.8
W-Tables	20	3.1	25.9	3.1	25.9	2.8	14.1	2.8	14.1
W-Cards	6	1.3	30.5	1.3	30.5	1.6	27.4	1.6	27.4
W-20	40	3.7	13.1	3.7	13.1	1.7	4.2	1.7	4.2
J-20	40	7.5	34.2	3.9	17.9	5.5	14.2	2.0	5.1
R-20	40	4.1	22.5	3.1	17.0	5.2	13.9	2.5	6.0
W-Circuit	43	4.1	14.4	4.1	14.4	2.9	6.7	3.0	6.7
J-Circuit	43	6.4	30.2	4.5	20.4	14.5	33.7	3.6	8.8
R-Circuit	43	5.1	29.9	3.9	22.4	16.2	37.7	3.7	8.7

Table 3.8 Trajectory reconstruction results. Dataset 2.

Figure 3.17 shows the trajectory reconstruction of non-circuit activities for all 56 participants of dataset 2. Black, blue, and orange lines denote R-20, J-20, and W-20, respectively. Red, green, violet, and light green lines represent W-Cards, W-Slalom, W-Posters, and W-Tables, respectively. Light blue in Figure 3.17 and gray rectangles in Figure 3.18, Figure 3.19, and Figure 3.20, indicate the path where all the strides related to a certain activity should take place. If a stride is out of this path, it is considered as a Stride Out of Trajectory (SOT). A SOT can be

caused by the accumulative error of stride lengths and angle calculation of previous strides. These zones were defined taking into account the coordinates of the chairs and tables and the boundaries of the indoor environment.

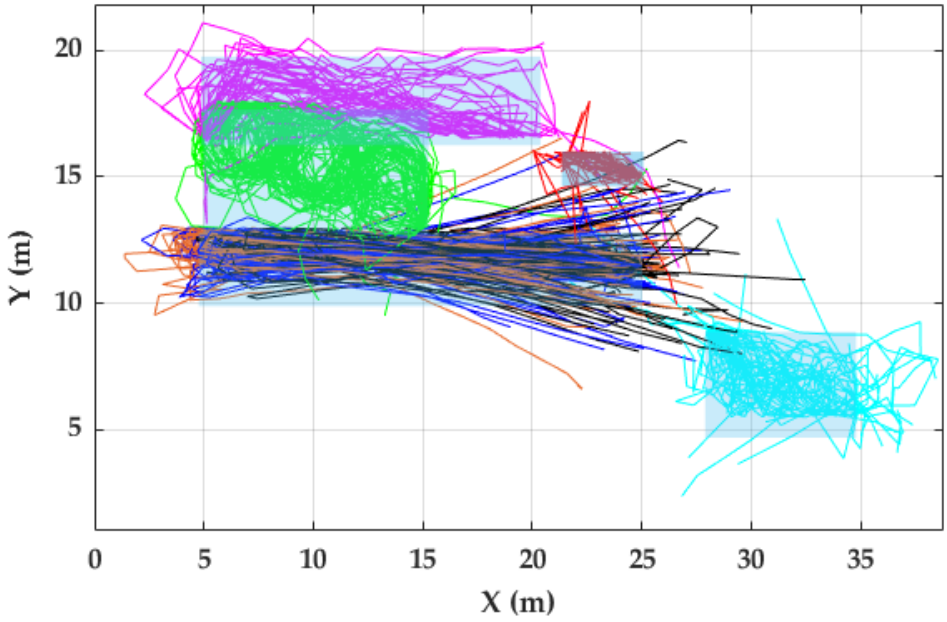

Figure 3.17 Trajectory reconstruction dataset 1. Non-circuit activities.

The number of strides out of trajectory is directly related to the RPE obtained; the more strides out of the acceptable path range, the higher the RPE. When observing the trajectory reconstruction of the activities W-20, J-20, R-20, and W-Circuit, J-Circuit, R-Circuit, it appears that the difficulty in trajectory reconstruction increases with stride velocity (from walking to jogging and running). This also occurred in the five aforementioned papers that performed the trajectory reconstruction of walking and running activities [65–69]. In those papers, the evaluations were performed with very few people. From our study, we can confirm that there is still a gap in trajectory reconstruction using foot-mounted IPDR systems of jogging/running activities regarding the trajectory reconstruction of walking activities.

The trajectory reconstruction of circuit activities for all 56 participants of dataset 2 is shown in Figure 3.18, Figure 3.19, and Figure 3.20. Black lines denote the trajectory followed by the participants. Gray zones represent the zone where all the strides should take place.

In both circuit and non-circuit activities, most of the trajectories were inside the zones where the strides have to be. The trajectory reconstruction of activities W-20, J-20, and R-20 describes two straight trajectories, joined by a 180-degree turn. The trajectory reconstruction of W-Slalom allows the identification of the area where the tables are located. The W-Posters activity includes non-straight strides, which are well described in the trajectory obtained. Regarding the circuit activities, although most of the strides are inside the activity zones, some trajectories lead towards the outer part of the activity zone and others lead towards the internal part of the circuit.

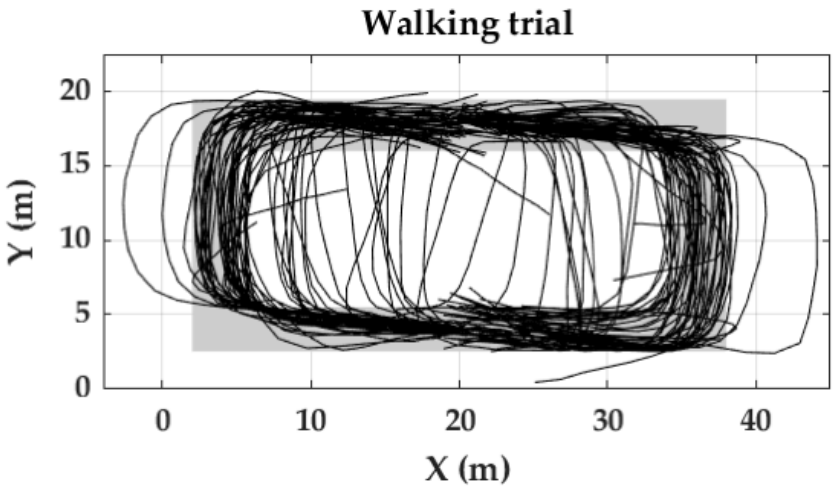

Figure 3.18 Trajectory reconstruction result. Walking trial. Dataset 2.

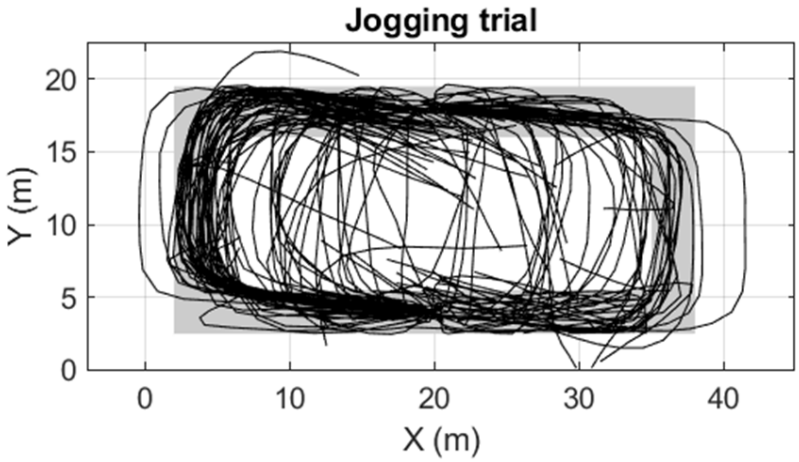

Figure 3.19 Trajectory reconstruction result. Jogging trial. Dataset 2.

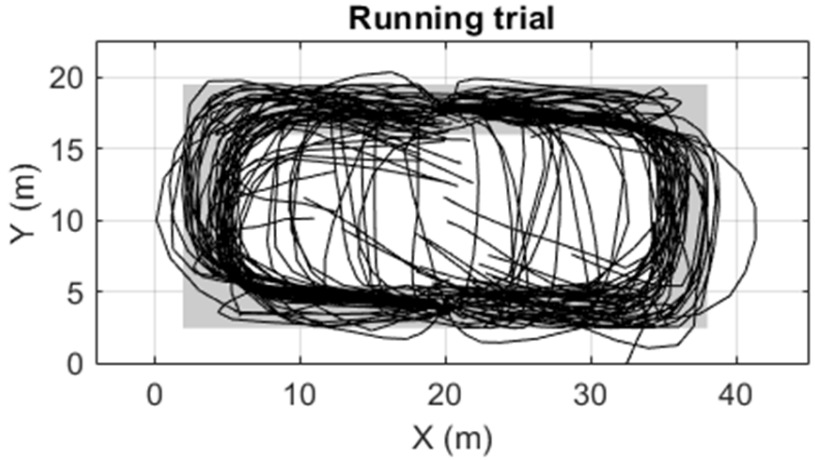

Figure 3.20 Trajectory reconstruction result. Running trial. Dataset 2.

3.3 Summary

In this chapter, a pipeline for trajectory reconstruction was introduced. The pipeline is based on PDR ZUPT, a method that only needs an IMU on the person's foot to follow their trajectory. The choice of this method, as well as the choice of msDTW and the proposed algorithms for toe-off and mid-stance detection, were made while keeping in mind that the goal is to perform indoor localization in AAL environments. Chapter 4 details the final proposal for IL in those types of environments and Chapter 5 shows its evaluation.

Chapter 4

Framework for Simultaneous Indoor Localization, Mapping, and Human Activity Recognition.

Both indoor location (IL) and Human Activity Recognition (HAR) have been widely studied. Many studies have addressed IL and HAR in an isolated way [78]. However, few studies have taken advantage of the IL and HAR relationship. For example, in the context of a house, people usually carry out certain activities in specific places: cook in the kitchen, watch television in the living room or bedroom, wash hands in the bathroom sink, etc. Knowing the exact location of the person might improve the classification of the activity performed. Also, information about the action being performed can improve the identification of the individual's physical location.

A novel method for Simultaneous Pedestrian Indoor Localization, house mapping, and Human Activity Recognition is introduced in this chapter. Movement data of the person is acquired from an IMU. The positioning estimates of PDR are improved by fusing them with human activity data (proximity and activity-related data from BLE beacons). The proposed method was designed to reduce configuration, deployment, and maintenance efforts, and to be capable of adapting to changes that may happen in the indoor environment, such as relocation of furniture and to changes in performing activities of daily living. These features make the proposed method promising to obtain both accurate indoor localization and activity recognition in a smart home or ambient assisted living scenario.

4.1 SLAM Background

Nowadays there is a diversity of IPS. Their characteristics change according to the technologies they use [60,79,80]. Choosing an IPS should be made considering seven aspects: the characteristics of the indoor environment, the accepted level of precision, budget limitations, obtrusiveness, system complexity, robustness, and privacy [56–58]. When choosing the type of IPS to use in an ambient-assisted living (AAL) scenario, these aspects need to be considered. In addition, the indoor localization and Human Activity Recognition of older adults should be carried out to assist them in their daily life tasks. In these types of scenarios, privacy and obtrusiveness are fundamental aspects. Consequently, it is desirable to avoid using IPSs that work with camera-based methods or require the person to wear multiple devices on their body. Under these considerations and taking into account the results obtained in the previous chapter, simultaneous indoor localization and mapping (SLAM) [81] was chosen as the backbone of the proposed framework for IL and HAR for AAL scenarios.

When using SLAM to map people, it is usually used to estimate the person's position in an indoor environment. SLAM combines data from proprioceptive sensors like IMUs attached to the body, with exteroceptive sensors like cameras, RFID tags, Bluetooth beacons, and laser range sensors deployed in the indoor environment. A unique feature of SLAM compared with other IL methods is that it allows the automatic creation from scratch of the map of the IL. The map is built from the observation of landmarks. These can be objects, devices, or characteristics of the indoor environment.

4.1.1 Related works to PDR ZUPT SLAM.

The proposed framework uses the pipeline presented in Chapter 3. Therefore, the intention is that only a single IMU be used on the person's foot. Previous works have also used one single IMU on the foot to perform simultaneous localization and mapping.

Son Gu et al. proposed a method for corner detection based on motion data captured with one IMU attached to one foot [82]. The corridors and corners of the indoor environment were used as landmarks. They evaluated their method in two settings: an office environment (20 m x 20 m) and a library (70 m x 70 m). The error in the indoor localization was 1.34 m and 0.8 m, respectively. This error shows that the complexity of the indoor environment is related to the precision obtained

FootSLAM, in conjunction with PlaceSLAM [83], implements a Rao-Blackwellized Particle Filter, where each particle contains an instance of the person trajectory and its related map. The landmarks used were RFID tags. The PDR open-loop position error was corrected when the proximity to RFID tags was detected. These tags were put in places such as corridors or doors. A position error of 2 m at two reference points was achieved.

In Wifi GraphSLAM [84], Wifi antennas were used as landmarks. The received signal strength indicator (RSSI) from the Wifi antennas deployed in the indoor environment was used to

estimate the distance between the person and the antennas. The reported precision was 2.23 m in a 60 m x 10 m environment.

A Graph-based optimization method that solves the SLAM problem is proposed in Zuo et al. [85]. It combines PDR and Bluetooth fingerprinting. That method was evaluated using 48 BLE beacons in an office context. The RSSI readings from the beacons were received in a smartphone carried by the person. The beacons were installed approximately evenly covering the complete area (90 m × 37 m). The positioning error was 3.25 m. The mean positioning error of the beacons was 1.27 m. A second evaluation was performed using only 24 beacons. In that case, the position error was 4.69 m, and the mean position error of the beacons was 2.26 m.

In ActionSLAM [86], the landmarks were activities: sitting, standing, opening, or closing doors and windows. The precision achieved was 1.16 m. The main disadvantage of this method is the need to use two IMUs in addition to the one worn on the foot: one on the waist to detect when the person sits or stands, and another on the hand to detect opening or closing doors or windows. This is the only study where human activities have been used as landmarks in SLAM.

4.2 Proposed framework for simultaneous indoor localization, mapping, and Human Activity Recognition for AAL scenarios.

To the best of our knowledge, the proposed framework for simultaneous indoor localization, mapping, and Human Activity Recognition is the first to use a combination of BLE beacons and HAR data as landmarks. The main components of the proposed framework are described in Figure 4.1. The “IMU and beacons data processing” block receives the IMU and beacons data, executes the pedestrian dead-reckoning with zero velocity updates algorithm, initializes the beacon's location, and recognizes the human activities. The “trajectory and beacons location estimators” block implements the three phases of a particle filter algorithm: prediction, up-date, and resample. As a result, the person and beacon's indoor location is obtained. Each of the components of the framework is explained in detail below.

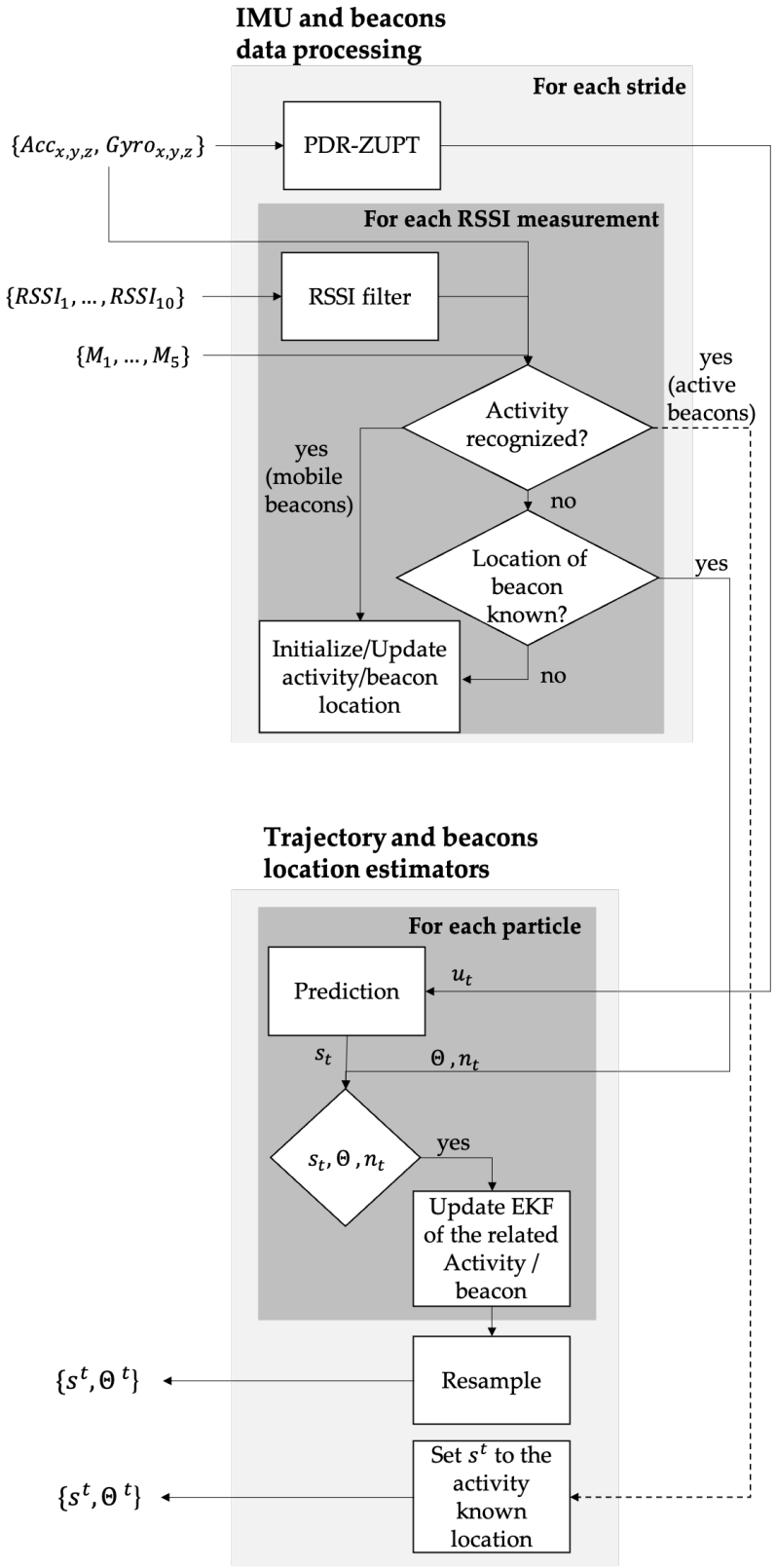

Figure 4.1 Proposed framework for simultaneous indoor localization, mapping, and Human Activity Recognition.

4.2.1 IMU and beacons data processing block

In this block the data of the IMU and the beacons are processed, the initial estimate of the position of the beacons is made, and the recognition of the activities begins. With the results obtained in this block, the "Trajectory and beacons location estimators" block is in charge of updating the map of the house and the position of the person in it.

As in the previous chapter, acceleration and angular velocity data are collected with a foot-mounted IMU. (Figure 3.2). BLE beacons are used to get proximity and activity-related data. BLE beacons are small devices (Figure 4.2) that emit a BLE signal that can be received and interpreted by devices such as a smartphone.

Figure 4.2 BLE beacon. (Taken from www.estimote.com)

Estimote beacons were used in the experiments carried out in this project (Estimote Proximity Beacons, Estimote Inc, San Francisco, CA, USA, https://estimote.com/). These beacons have built-in accelerometers. They were set up to send the raw acceleration data within telemetry packets (TLM packets) at a frequency of 10 Hz. Each TLM packet contains the universally unique identifier (UUID) of the beacon that emits it, the three-axis acceleration raw data, the movement state of the beacon (moving or still), and the duration of the current state of movement. Along with each packet, the received signal strength indicator (RSSI) was received as an indicator of proximity.

Unfortunately, the IMU used did not allow the reception of BLE signals. For that reason, it was necessary to develop a mobile application to collect the data from the beacons. Python scripts were developed to synchronize the data from the IMU and the beacons. All scripts and applications developed in this project are available at: https://github.com/jesusceron.

Beacons were categorized as:

1. Stationary: beacons that will always be still. They are only used to provide proximity data to reference points of the house. Data movement of these types of beacons is not used.
2. Active: The movement of these beacons indicates certain activity related to the object to which they are attached. For example, a movement of the beacon attached to the toilet

lid (accompanied by proximity detection to it) could indicate the action of using the toilet.

3. **Mobile:** These are a special type of active beacons. They are attached to objects that can change their position when used (Broom, pitcher, and hairbrush).

4.2.1.1 PDR-ZUPT

This component implements the pipeline described in Chapter 3 and published in [87]. The acceleration and gyroscope data collected from the IMU attached to the person's foot are the income variables of the algorithm that implements the pedestrian dead reckoning technique with zero-velocity update. Foot-mounted PDR ZUPT has been proven to be an excellent strategy to reduce the drift in PDR [61]. This module generates an estimate of the length and orientation of each stride called the motion measurement u_t. With these data, an estimate of the person's current position in the Cartesian plane is obtained. Finally, u_t is sent to the prediction module of the "Trajectory and beacons location estimators." block.

4.2.1.2 RSSI FILTER

A smartphone receives the RSSI readings from the beacons deployed in the indoor environment. The relationship between the RSSI and the distance between a beacon and the smartphone is given by Equation 4.1. This equation is known as the log-distance path loss model:

$$RSSI = 10n\left(\frac{d}{d_{1m}}\right) + RSSI_{1m}\,, \qquad \text{Equation 4.1}$$

Usually, 1 m is taken as distance reference $d_{1m} = 1\,m$. $RSSI_{1m}$ is the RSSI reading measured at 1 m between the emitter and receiver. In ideal conditions, given any RSSI value, the exact distance between the beacon and the smartphone could be calculated with Equation (5). However, it is widely known that this relationship is not exact, mainly due to multipath propagation phenomena. Furthermore, the BLE signal is broadcast on 2 MHz bandwidth channels in the 2.4 GHz band, causing the BLE signal to be affected by fading, even more so than WIFI signal [88]. For that reason, before using Equation 4.1 to calculate the distance between the smartphone and a specific beacon, it is necessary to filter the RSSI signal. A one-dimensional Kalman Filter was used for that purpose. The filter design procedure has the three steps described below:

1. The state variable is the signal to be filtered:

$$x = RSSI\ readings \qquad \text{Equation 4.2}$$

2. Prediction Phase.

Two equations compose the one-variable Kalman filter prediction step. These described the parameters needed to perform the Kalman filter prediction's phase:

$$\bar{x} = x + dx \quad \text{Equation 4.3}$$

$$\bar{P} = P + Q \quad \text{Equation 4.4}$$

The current state $\underline{x}$ is equal to the previous state (x) plus a value given by the process model (dx). That model should describe how the state variable changes from the previous state to the current state. It was assumed that the current value will be equal to the previous one by making $dx = 0$. The above is true because it is not possible to establish a mathematical function that estimates the current RSSI value based on the previous one.

The variance of the current state $\underline{P}$ depends on the variance of the previous state (P) plus the uncertainty (variance) that the process model introduces, known as the process noise (Q). At the beginning, P is unknown. It is then assumed that P is a large value indicating a lot of uncertainty in the initial estimate. Therefore, its initial value was set to $P = (24\ dBm)^2$. More precisely, P was initialized as double the variance of the z measurements. The process noise was established as $Q = (0.55\ dBm)^2$ empirically.

3. Update phase.

There are four equations in this step:

$$y = z + \bar{x} \quad \text{Equation 4.5}$$

$$K = \frac{\bar{P}}{\bar{P} + R} \quad \text{Equation 4.6}$$

$$x = \bar{x} + Ky \quad \text{Equation 4.7}$$

$$P = (1 - K)\bar{P} \quad \text{Equation 4.8}$$

The residual, or innovation (y), is equal to the measurement (z) plus the current state ($\underline{x}$). the residual, represents the error between the received RSSI measurement and the estimate made with the transition function, namely, the previous RSSI measurement. The parameter to be set in this phase is the measurement noise R. This value is the estimated variance of the z measurements. $R = (12\ dBm)^2$ was used because it was observed that the RSSI readings fluctuate with a standard deviation of around 12 dBm when the beacon and smartphone are separated at a fixed distance. Figure 4 shows a real example of the use of the RSSI filter. The raw RSSI signal is in gray. The filtered RSSI signal is in red.

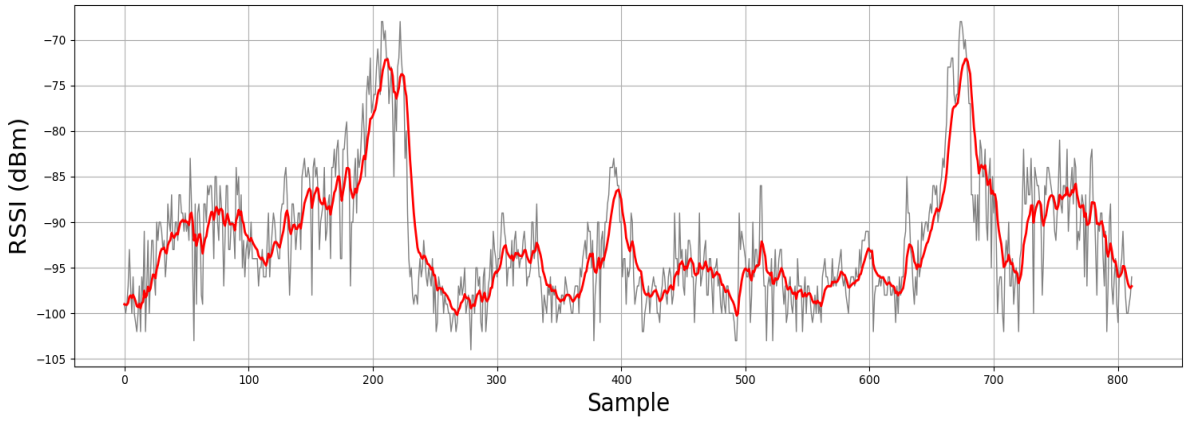

Figure 4.3 Example of RSSI filter result.

4.2.1.3 BEACONS POSITION INITIALIZATION

Using Equation 4.1 and assuming that the beacon's signal propagation pattern is spherical, all points belonging to that sphere with a radius equal to the estimated range are possible points at which a beacon could be located. This makes the uncertainty of the beacon's position very large. A Kalman filter is used to estimate the beacons position, but it cannot deal with a very large uncertainty as just mentioned. The Kalman filter covariance matrix would tend to be very large, causing non-convergence. Two measures were taken to address this problem:

1. The establishment of a small distance range to start and update the position of the beacons.

If the transmission power of a beacon is increased, its coverage area increase. However, the RSSI readings becomes more unstable as the power goes up. To avoid that problem, a maximum range of around 3.5 m was setup. Based on the manufacturer specifications, to get that range, the transmission power of the beacons must be configured at –20 dBm. Additionally, it was empirically found that the RSSI readings are stable up to an approximate range of 2.5 m. This range is equivalent to an RSSI value of −88 dBm. Therefore, if the received RSSI value is less than −88 dBm, that value is not considered either for initialization or for updating the beacon location.

2. The initialization of beacon's location by using particle filters.

By using a particle filter the initial position of a beacon can be obtained. As many particles can be created in a sphere in the approximate range of radius equal to the distance calculated with the Log-distance path loss model (Equation 4.1). As new beacon RSSIs are received, the particulate filter is updated and converges on a single possible position.

Initialization of location for stationary and active (non-mobile) beacons.

Once the first RSSI reading higher than -88 dBm is received, the distance between the beacon and the smartphone (z = radius) is obtained through the Log-distance path loss model (Equation 4.1). The measurement noise (R) of z is assumed to be 10% of z. For example, if the resulting distance estimation using Equation 4.1 indicates that a beacon is in a radius of 2 m, R confirms that the location of the beacon is on a disk of inner radius equal to 1.8 m and outer radius equal to 2.2 m.

The next step is to create $n = 2000$ uniformly distributed particles inside that disk. Each particle represents a possible beacon location. The largest disc occurs when $z = 2.5\ m$. In that case, the density of particles is $2.54\frac{particles}{cm^2}$.. The particle distribution was performed as described in Cook using the following equations:

$$x = \sqrt{r}\ cos\ cos\ \theta \quad \text{Equation 4.9}$$

$$y = \sqrt{r}\ sin\ sin\ \theta \quad \text{Equation 4.10}$$

With $r \in [radius - (radius \times 0.1), radius + (radius \times 0.1)]$ and $\theta \in [0, 2\pi]$. Each particle has an associate weight (w), which is proportional to the probability of being the particle representing the true beacons' position. When the first z is estimated, the weights of all the particles are initialized with a value $w = \frac{1}{n}$.

1. Prediction

When a new stride is detected, the new position of each particle is given by:

$$pos_x = pos_x + (stride_{length_x} + rand \times Q) \quad \text{Equation 4.11}$$

$$pos_y = pos_y + (stride_{length_y} + rand \times Q) \quad \text{Equation 4.12}$$

The particles move the amount traveled by the person plus an amount given by the process noise (Q). It was established at $0.01\ m^2$. $randn$ is a random decimal number and $randn \in [0,1]$.

2. Update

From the second estimated z onwards, the particle weights are updated using the following equation:

$$w_t = w_{t-1} \times p(z|distance, R) \quad \text{Equation 4.13}$$

$p(z|distance, R)$ is the probability density function of the measurement z given the distance between the particle and the person and the measurement noise R.

3. Resampling

In this phase, the particles that have very low weight (w) are replaced with copies of particles that have a high weight. After having updated the weights of all the particles, the number of effective particles is calculated using:

$$\widehat{N}_{eff} = \frac{1}{\sum_{i=1}^{N}(w^i)^2} \qquad \text{Equation 4.14}$$

When$\widehat{N}_{eff}$ is less than half of the total particles (n=1000), the sampling process is activated. There are different methods for this purpose, such as multinomial, residual, stratified, and systematic resampling [89]. Stratified and systematic resampling have been shown to outperform the other methods in resolving several problems. Systematic resampling ensures a uniformed sampling from all the particle space while ensuring larger weights are proportionality resample more often. Stratified resampling ensures that particles with larger weights are resampled more often [90]. Both approaches were tested with the proposed method. Since no relevant performance differences were identified, systematic resampling was used for all further experiments.

4. Initial position estimate

After the update phase is done, it is possible to estimate the position of the beacon by calculating the sum of the weighted values of the particles:

$$pos_x = \frac{1}{N}\sum_{i=1}^{N} w^i x^i \qquad pos_y = \frac{1}{N}\sum_{i=1}^{N} w^i y^i \qquad \text{Equation 4.15}$$

In the same way, the mean of the variance of all the particles can be estimated. When the value of the variance of both coordinates reaches a value of less than $0.01\ m^2$, the beacon position initialization phase is finished.

Initialization and re-initialization of mobile beacons

When a person uses an everyday item such as the broom, the pitcher, or the hairbrush, that element changes its position not only concerning the x-y coordinates but also likely changes its position with respect to the z coordinate. Besides, the items may not be returned to the same point from which it was taken. Consequently, its position has to be reset every time its use is detected. A particle filter was also used for this purpose. The difference with the method described for locating the stationary and other non-mobile beacons is that, instead of creating a disk and generating 2000 particles inside within it, in this case, the upper half of a sphere is built, and 10,000 particles are distributed uniformly into it. The measurement noise (R) was also set to 10% of z, then, the external and internal radius of the sphere is given by $r \in [z - R, z + R]$. The azimuth and polar coordinates were calculated using:

$$azimuth = 2\pi \times u \quad \text{Equation 4.16}$$

$$polar = (1 - v) \quad \text{Equation 4.17}$$

Variables u and v are random decimal numbers such that $u, v \in [0,1]$. The polar coordinates of each particle generated with the previous equations were transformed into Cartesian coordinates. The minimum density of particles is reached with the maximum z allowed (2.5 m). For that case, the density of particles is $2.53 \frac{particles}{cm^3}$. The prediction, update, and sampling phases are the same as those described above. The estimate of the moving beacon's final position is given when it is detected that the beacon has stopped moving. The estimates of the x-y coordinates of that instant are established as the new position of the beacon.

4.2.2 Trajectory and beacons location estimators block

On one hand, the estimation of the person's location is carried out utilizing a particle filter. At the beginning of each session, 600 particles are created. The current state s^t of each particle represents a possible x-y position, so the history of the particle's states makes up a probable trajectory followed by the person $S^t = \{s_1, s_2, \dots, s_t, \}$. With N = 600, there are 600 possible paths at each time step: $S_n^t = \{s_1^n, s_2^n, \dots, s_t^n, \}$ such that $n \in [600]$.

On the other hand, the estimation of the position of the beacons must be done separately for each particle, since the estimate of the positions of the beacons depends on the position of the person. To achieve this, each beacon's position was estimated with an independent extended Kalman filter (EKF), as proposed by Montemerlo et al. [91].

4.2.2.1 Prediction

The length and direction of a new stride detected are sent to the prediction phase. In this phase, the new state of the 600 particles is estimated. The equations involved in this process are the same as those described in the previous section (Equation 4.11 and Equation 4.12). The standard deviation of the stride length was set to 0.1 m. This means that the process error Q is assumed to be a fixed value equal to $0.01\ m^2$.

4.2.2.2 Update

Once the first estimate of the location of a beacon is obtained through the initialization module, the estimate and its covariance matrix are used as the initial state of the respective EKF. Beacons do not provide orientation information; consequently, the used EKF implements an update phase that relies only on range information. It was adapted from the range-only SLAM method proposed by Menegatti et al. [92]. The state and covariance matrix of its EKF must be updated when a new distance measurement is received from a beacon. For this, the transition function is given by the distance between the current estimate of the person's position and the current estimate of the beacon's position:

$$h_n(x_b^n, y_b^n) = \sqrt{\left(x_{s_t}^n - x_b^n\right)^2 + \left(y_{s_t}^n - y_b^n\right)^2} \quad \text{Equation 4.18}$$

The residual represents the error between the received distance measurement to the beacon z, and the estimate made with the transition function:

$$y = z - h(\underline{x}) \quad \text{Equation 4.19}$$

Since $h(\underline{x})$ is not a linear function, it must be linearized by calculating its Jacobian. The SciPy Python library was used for this purpose. The result is:

$$H = \left[\frac{x_{s_t}^n - x_b^n}{h_n}, \frac{y_{s_t}^n - y_b^n}{h_n}\right] \quad \text{Equation 4.20}$$

With the calculated residual and Jacobian, the state and its respective covariance matrix can finally be updated using the Kalman filter equations:

$$K = \bar{P}H^T(H\bar{P}H^T + R)^{-1} \quad \text{Equation 4.21}$$

$$x = \bar{x} + Ky \quad \text{Equation 4.22}$$

$$P = (I - KH)\bar{P} \quad \text{Equation 4.23}$$

Finally, the weight of each particle is updated using:

$$w_t^n = w_{t-1}^n \times p(z|h_n, R) \quad \text{Equation 4.24}$$

4.2.2.3 Resampling

Since each of the 600 particles generated has an associated weight representing the probability of tracking the actual person's trajectory, it is desired that the particles with a very low weight be replaced by others that have a high weight for the filter to converge. After the weight of all the particles has been updated, the number of effective particles $\widehat{N}_{eff}$ is calculated using Equation 4.14. In case this is less than half of the total particles used (300 for this case), sampling is carried out using the systematic resampling method [90].

4.3 Initial evaluation of the proposed framework

4.3.1 Dataset

An apartment was simulated in a room of the Machine Learning and Data Analytics lab at the University of Erlangen-Nuremberg, Germany (Figure 4.4). Eight participants (mean age: 29.4 ± 3.7 years) carried out the activities described in Table 4.1. Human movement, proximity, and action-related data were collected for each participant. Each session had an average duration of 6.21 ± 1.17 min.

Main Activities	Sub-Activities
Enter the apartment	Go down the stairs, go to the door and open it.
Take off jacket	Go into the room and leave the jacket there.
Serve something to eat and go to the dining room to eat.	Go to the kitchen and serve some drinks (using the pitcher) and take something to eat. Go to the table and eat what was served.
Sweep	Go to the bathroom, take the broom, go to the living room, and sweep it. Return the broom to the place where it was taken.
Combing	Go to the bathroom, take the comb, and comb your hair.
Use the toilet	Go to the bathroom, lift the seat cover that simulates the toiler lid, and sit in it.
Leave the apartment	Go for the jacket left in the room. Put on the jacket and leave the house. Finish the activity at the same starting point.

Table 4.1 Activities performed for the participants for the initial framework evaluation.

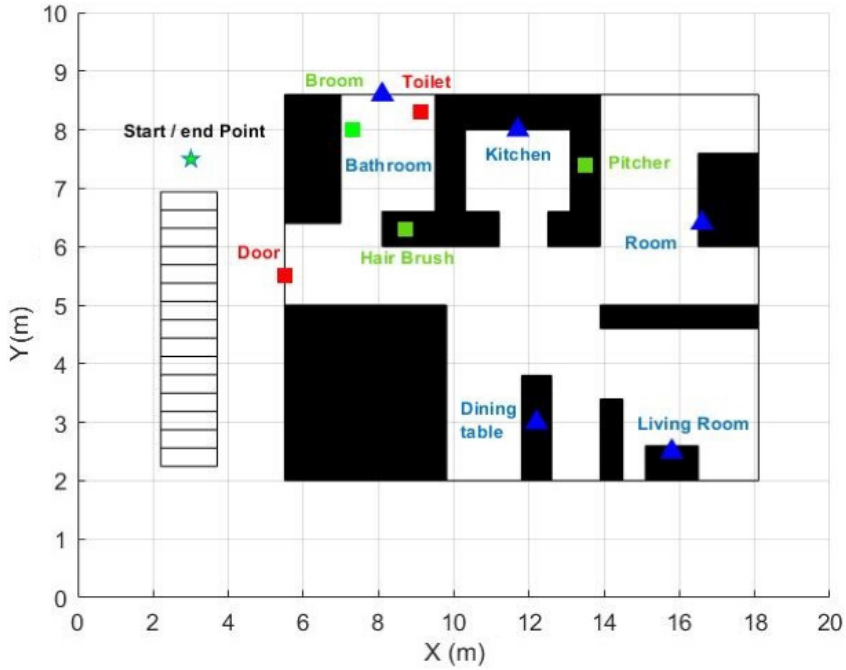

Figure 4.4 Map of the simulated apartment.

4.3.1.1 HUMAN MOVEMENT DATA

Each participant used four Inertial Measurement Units - IMUs (Portabiles GmbH, Erlangen, Germany https://portabiles.de/) placed on each wrist and foot. The IMUs continuously communicate with each other to synchronize their clocks. The sampling frequency used was 204.8 Hz, and the variables collected were acceleration (range: ± 16 g) and angular velocity (range: ± 2000 DPS).

Since the IMU does not receive the BLE signals from beacons, a smartphone (Motorola G6 Plus) was carried in one of the participant's pockets to receive those signals. The smartphone's

acceleration (range: ± 8 g) and angular velocity (range: ± 2000 DPS) data at a sampling frequency of 204.8 Hz were also collected. A mobile application for Android devices was developed to receive the TLM packets from the ten beacons. The application was executed in the background during data collection on the smartphone carried in the participant's pocket. The data collected from the IMUs and the smartphone was synchronized using a python script that matched each data point's timestamps. All sessions were recorded in video. The videos were used as a reference for the evaluation process.

4.3.1.2 PROXIMITY AND MOVEMENT OBJECT DATA

Ten beacons were deployed in the simulated apartment (red and green squares and blue triangles in Figure 4.4). The configuration and deployment were done following the recommendations of Castillo-Cara et al. [93]. They studied the beacon setup parameters such as transmission power, density, and topology. As a result of their study, they recommend splitting the target area into sectors, keeping gaps between them to avoid a beacons' signal overlapping. They also suggest using low or medium transmission power to avoid large RSSI fluctuations. The transmission power was set at −20 dBm, with which the manufacturer indicates that a range of around 3.5 m radii is reached.

Five beacons are stationary (Bathroom, kitchen, room, living room, and dining table) and five are active. Of those five actives, three are mobile (hairbrush, pitcher, and broom) and two are only active (door and toilet) (Figure 4.4). A picture of beacons used is presented in Figure 4.5 (Two active beacons in red squares and one stationary in a blue square)

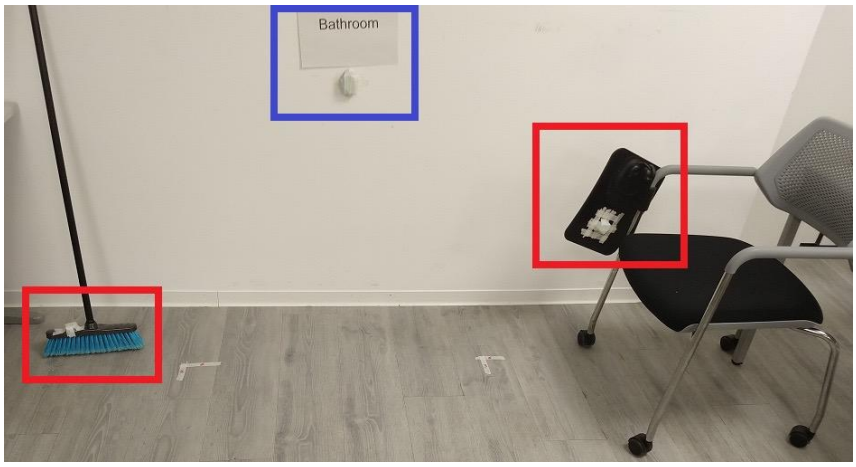

Figure 4.5 Beacons deployed in the simulated apartment.

4.3.2 Beacons localization evaluation-House mapping

The position of the beacons is unknown at the beginning of the first activity's execution.

The initialization process for the localization of a beacon starts when the person enters the radius of coverage of the beacon (around 3.5 m). Once the beacon position is initialized, the RSSI

measurements of that beacon are used to refine the participant's position using the particle filter. Simultaneously, the beacon's position is refined with its respective EKF utilizing the participant's position. The evaluation metric for beacons localization is the Euclidean distance (in two dimensions) between the beacon's ground-truth position and its estimated position.

The prediction phase in all the particle filters involves the addition of a random error (Equation 4.11 and Equation 4.12) to produce different filter state options that possibly capture the actual state of the system. Due to the random nature of these errors, the evaluation of the location of the beacons and the participants varies in each execution for the same participant. As a strategy for evaluation, it was decided to execute the process 10 times for each participant and get the average of the 10 runs

The average localization error of the ten beacons was 0.82 ± 0.24 m. The average localization error of the stationary beacons was 0.96 ± 0.65 m (Table 4.2). Keeping in mind that the largest radius allowed was established as 2.5 m, this average error is equivalent to 38.4% of the aforementioned maximum range. This result shows how difficult it is to locate a Bluetooth beacon even using low transmission power and filtering the RSSI signal with a Kalman filter. The effects of the multipath phenomenon on Bluetooth signals are the cause of the difficulty of estimating the distance between the beacon and the receiving device using the Log-distance path model.

Participant	Bathroom	Kitchen	Room	L. Room	D. Room
1	1.42	0.30	0.18	0.65	0.72
2	0.52	0.40	0.83	1.75	0.67
3	1.14	0.78	0.49	0.73	0.23
4	0.62	1.57	0.73	0.88	0.83
5	0.92	0.90	0.74	5.98	1.67
6	0.47	0.46	0.88	0.25	0.36
7	0.91	1.30	0.67	1.03	0.82
8	1.06	1.50	1.18	0.43	1.56
Avg. error (m)	0.88 ± 0.30	0.9 ± 0.47	0.71 ± 0.27	1.46 ± 1.75	0.86 ± 0.48

Table 4.2 Localization error of stationary beacons.

The error of the active beacons was 0.67 ± 0.29 m (Table 4.3). For the mobile beacons, the actual position was considered as the position before the beacon started moving and the estimated position as the position after the beacon was moving. This result is lower than that obtained for the stationary beacons. More RSSI values were received from active beacons than from stationary beacons. This may be the cause of that result. This makes sense because the participants interacted with the active beacons, and for that reason, they were closer and longer compared to the stationary beacons. That allows the particle filter to converge quickly by processing more reliable range measurements.

As a possible solution to that issue, it is suggested to carry out a simple training phase to obtain a more precise location of the beacons. That phase would consist of the person addressing each

beacon deployed in the environment and staying as close as possible to each beacon for at least ten seconds so that the particle filter converges by processing enough measurements taken at a short distance and, therefore, a more reliable one.

Participant	Door	H. Brush	Broom	Toilet	Pitcher
1	0.48	0.57	0.11	0.78	0.49
2	0.15	0.70	0.27	0.81	0.59
3	0.81	0.49	1.01	0.26	0.75
4	0.21	0.45	0.73	0.44	1.59
5	0.94	0.86	1.14	0.35	0.76
6	0.66	1.12	0.85	0.25	0.87
7	0.88	0.67	0.98	1.13	0.65
8	0.38	0.61	0.86	0.34	0.93
Avg. error (m)	0.56 ± 0.28	0.68 ± 0.20	0.74 ± 0.34	0.55 ± 0.30	0.83 ± 0.31

Table 4.3 Localization error of active beacons.

Beacons' localization results are also presented graphically (Figure 6). The ground-truth and estimated locations of each beacon were drawn with the same color to visualize how much the estimates varied from the actual beacons' positions. Each point corresponds to the average of the 10 location estimates of a beacon for each participant. The ground-truth location and the location estimates for each beacon share the same color.

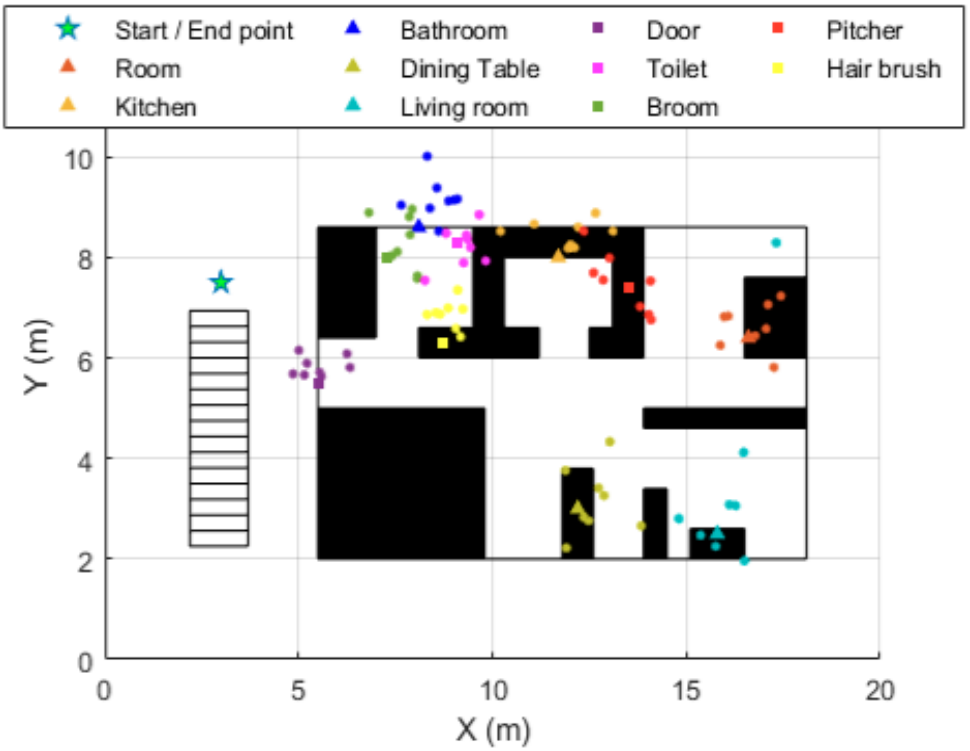

Figure 4.6 Graphic results of the beacons localization.

The process for locating the active beacons attached to the door and the bathroom was the same as for the stationary beacons. The remaining three beacons were considered mobile beacons. For them, 10,000 particles were uniformly distributed in the upper half of a sphere with an upper and lower radius calculated in the same way as for the disk. Although the number of particles per unit area was similar when the disk or sphere was used, the error of the mobile beacons' localization was greater in all cases compared to the active non-mobile beacons. Increasing the number of particles for the mobile beacons' localization could reduce the error obtained, but this would depend on the maximum threshold of the processing capacity of the device in which the proposed method would be executed.

Another important aspect to be discussed is the number of beacons to be used. The greater the number of beacons deployed in the environment, the smaller the error of their location reading [94]. When using 48 beacons, the error was 1.27 m; using 24, the error increased to 2.26 m. Although the average localization error of the 10 beacons used in our work was 0.82 ± 0.24 m, the area of the evaluation environment in [85] was 24 times greater than the area of the environment used in our work. For that reason, although the average error obtained by our proposed method is less, it cannot be established that it improves the result obtained in [94].

The complexity and robustness of the proposed method were fundamental characteristics taken into account in its design. SLAM is a very robust recursive algorithm since it continually updates both the landmarks and the person's position. Therefore, if there is any kind of change in the position of furniture or obstacles, the IPS can adapt to it automatically. Without prior knowledge of the environment, the method can obtain a map of the environment. The map is represented through the location of the beacons. The complexity of the proposed method is minimal since it would allow the user to place the beacons at home in the same way that they were used in this work. After the filters converge, the person can be located using the map generated automatically.

4.3.3 Evaluation of the pedestrian indoor localization

The movement of an active beacon indicates the interaction of the person with a specific object. This interaction is used as a landmark. After the position of the active beacon is initialized, it is used to reset the participant's position with respect to that beacon. At that moment, the loop is closed, which means that the participant's location is reset, and the localization error is evaluated (for example, when the participant goes from the start point to the entrance of the simulated apartment). When movement is detected in the beacon placed at the door, the localization of the person is established to the position of the beacon and the error in the localization is obtained. The location error is calculated as the Euclidean distance (in two dimensions) between the ground truth (real) beacon's position and the participant's estimated position.

The total trajectories in all the tests have the same starting and ending point. Thus, the localization error was also calculated at the end of each test, using as ground truth the real coordinates of the starting/ending point.

The average localization error for all the participants was 1.05 m ± 0.44 m (Table 4.4).

Participant	Error (m)
1	0.79 ± 0.28
2	1.24 ± 0.56
3	1.16 ± 0.49
4	1.34 ± 0.52
5	1.38 ± 0.85
6	0.95 ± 0.34
7	0.71 ± 0.26
8	0.77 ± 0.26
Avg:	1.05 ± 0.44

Table 4.4 Average localization error for each participant (ten executed runs).

This localization error is smaller than the obtained in the related works [82–86]. However, a direct comparison between the studies is not possible because all the works have been evaluated in different scenarios, with different shapes and sizes, and using different transmitting/receiving devices. Therefore, it is not fair to conclude that the proposed method is better than the related works.

The shorter the distance traveled by the person, the less the drift suffered due to the estimation of the position with PDR [57]. This seems to be the key to the proposed framework. The localization error was measured every time the movement of an active beacon was detected. At the same time, the person's position was reset to the last established position of that beacon. In the related works, the localization error was measured only at one reference point, which is usually the same point where the person begins to walk. It is also important to highlight that the data collected included activities in which the person was standing or sitting. The non-stride movements involved in those activities make location tracking even more difficult as they lead to stride detection errors and loss of orientation. The key to handling the possible errors produced by such movements is the fusion of the PDR method's data with the range of distance to the beacons.

The person's trajectory is made up of the sum of the estimated locations of each of their strides. The trajectories were aligned with the map only at the beginning of the first activity, taken as a reference to the first participant's strides while descending the stairs. The blue lines in Figure 4.7 are the 10 trajectories reconstructed for each participant (ten executed runs of the framework for each participant). The description of each image has the sequence of activities followed by the participant.

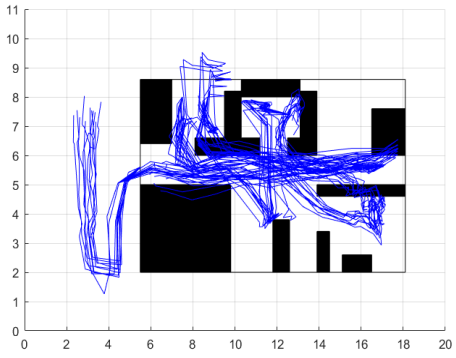

(**a**) Participant 1: Start, door, room, kitchen (a pitcher), dining room, bathroom (hair-brush), bathroom (broom), living room, bathroom (toilet), room, door, end.

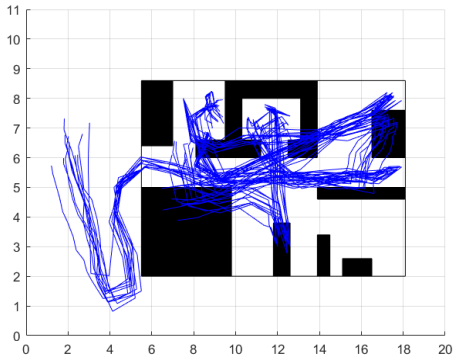

(**b**) Participant 2: Start, door, room, kitchen (a pitcher), dining room, bathroom (broom), living room, bathroom (toilet), bathroom (hairbrush), room, door, end.

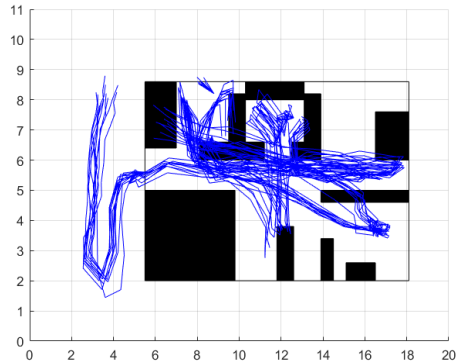

(**c**) Participant 3: Start, door, room, kitchen (a pitcher), dining room, bathroom (toilet), bathroom (hairbrush), bathroom (broom), living room, room, door, end.

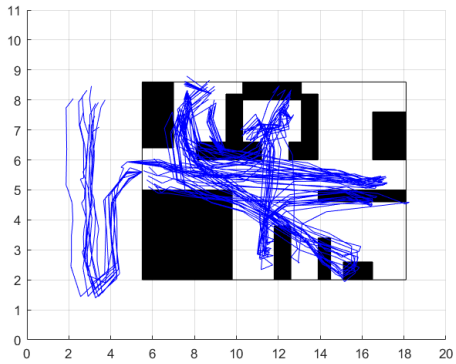

(**d**) Participant 4**:** Start, door, room, bathroom (hairbrush), bathroom (toilet), bathroom (broom), living room, kitchen (a pitcher), dining room, room, door, end.

(**e**) Participant 5**:** Start, door, room, bathroom (broom), living room, bathroom (hairbrush), kitchen (a pitcher), dining room, bathroom (toilet), room, door, end.

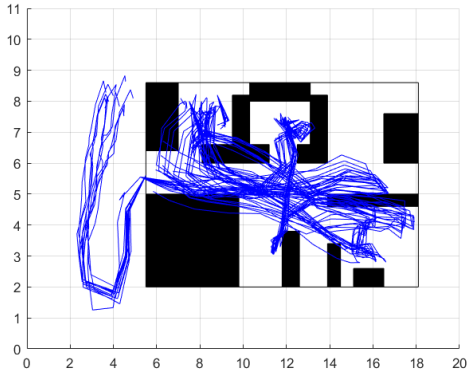

(**f**) Participant 6: Start, door, room, bathroom (toilet), bathroom (hairbrush), bathroom (broom), living room, kitchen (a pitcher), dining room, room, door, end.

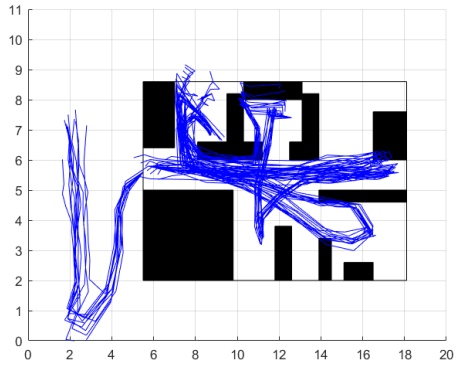

(**g**) Participant 7: Start, door, room, bathroom (toilet), bathroom (broom), living room, bathroom (hairbrush), kitchen (a pitcher), dining room, room, door, end.

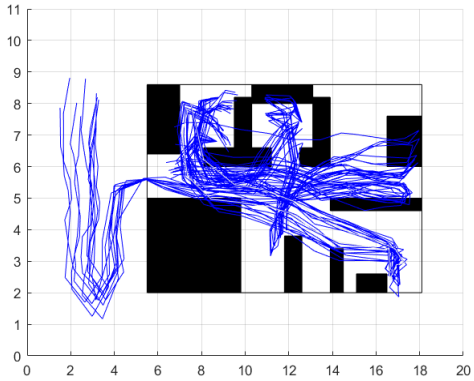

(**h**) Participant 8: Start, door, room, bathroom (toilet), bathroom (broom), living room, bathroom (hairbrush), kitchen (a pitcher), dining room, room, door, end.

Figure 4.7 Results of participant's localization.

The reconstructed trajectory for participants 2 and 5 was not as good as the others. An orientation error seriously affected the trajectory from the beginning. That caused the location of the beacons to be erroneously initialized or updated. Since the mapping and trajectory are continuously updated, this would lead to an exhaustive analysis of how often the person should visit the different places in their home in such a way that the SLAM-based method can correct a large orientation error. Instead of going in depth on that analysis, there are two possible and more direct solutions: the first is to include in the data fusion the orientation data given by a magnetometer, a sensor with which it is possible to obtain the orientation with respect to the magnetic poles of the earth. The second possible solution is to increase the transmission power of the stationary beacons to have more range measurements to correct the error.

The particle filter used to estimate the person's location (4.2.2 Trajectory and beacons location estimators block) used 600 particles, which correspond to 600 possible locations that are evaluated every time a distance measurement to a beacon is available. The greater the number of particles, the higher the processing capacity and time necessary to execute the proposed method. Hardegger et al. [39,86], performed an analysis of the relationship between the number of particles and the processing time required for updating and resampling. They concluded that 1000 particles were sufficient to achieve adequate precision and their set of algorithms was able to run on a smartphone. In the case of the proposed framework in this project, an analysis of the indoor localization precision regarding the number of particles was performed using 10 different quantities of particles, starting at 100 and ending at 1,000, increasing by steps of 100. The result indicates that 600 particles are enough to get adequate precision.

4.4 Summary

The proposed framework involves the use of one IMU at the user's foot. This enables PDR implementation with Zero-Velocity-Updates. This strategy is recognized for providing higher precision in the calculation of stride size and, therefore, in location tracking compared to others that use the IMU on other parts of the body [62]. Furthermore, the use of the IMU at the foot could be useful for Ambient Assisted Living scenarios, where obtaining gait parameters are useful for the early detection and monitoring of diseases like Parkinson's disease [86].

To the best of our knowledge, this is the first method that includes the beacons' data movement as activity-related events in a method for pedestrian Simultaneous Localization and Mapping (SLAM). Enabling the reception of the Bluetooth signal from beacons in the IMU would be an important step towards deploying an IPS method in a real environment. In this way, the use of the smartphone for solely receiving Bluetooth signals from the beacons would be avoided. If the beacon signal is received by the IMU placed on the foot, relocating the stationary beacons at ground level should be considered to get a line of sight and simplify the distance estimation.

Chapter 5

Evaluation of the proposed framework in an AAL scenario

The feasibility of the framework presented in Chapter 4 is evaluated in a home environment with older adults. As the framework was intended to be used in AAL scenarios, it is minimally intrusive and opportunistic since, in addition to tracking the person's location and type of activity performed, it has the potential to analyze gait parameters in older adults, as shown in our previous work [87]. The method is very useful for the early detection of gait disorders such as those derived from Parkinson's disease.

This chapter also describes in detail the module for activity recognition of the framework. It is based on the data stream paradigm. This paradigm was created in response to the need to deal with a continuous stream of data sampled in real-time [95]. The most important characteristic of algorithms written for data streams is updating their model by inspecting each training example. This means that the model can be updated without splitting a static dataset into training and test sets. Besides, as they inspect each training example once, there is no risk of memory overflow, and usually, the processor load is very low. The characteristics of this type of algorithm are appropriate for HAR because: (1) they can work in real-time, i.e., processing and classifying the examples that arrive one by one. (2) They optimize the data processing, reducing memory use. Therefore, they can efficiently run on mobile and wearable devices with reduced memory and battery capacity. (3) Unlike traditional classification algorithms, data stream algorithms can maintain up-to-date classification models. This feature is particularly important in AAL settings, in which the way older adults perform activities of daily living may change over time.

Previous to this work, Khannouz et al. [96] compared the performance of 5 data stream algorithms using two real [97,98] and three synthetic HAR datasets. The real datasets used by Khannouz et al. do not contain activities of daily living and only include data from IMUs. As a result, the Mondrian Tree and Naive Bayes algorithms obtained the best F1 measures. It is important to mention that the algorithms of the StreamDM-C ++ [99] and OrpailleCC [100] apps were used in that work.

5.1 Dataset

The data used in this research were collected in a house in Popayán, Colombia (Figure 5.1). Twenty-two people performed nine different activities as described in Table 5.1. Eleven people were older than 60 years (older adults' group) with an average age of 70.72. The average age of the remaining eleven people was 41.81 (control group). Three types of data were collected: data of the movement of the person's foot, the person's proximity to Bluetooth beacons deployed in the house (Figure 5.1), and the motion of the beacons attached to daily objects. The average duration of data collection for each participant was 7.4 minutes. The ethics committee approved the collection protocol of this dataset of the University of Cauca. Before data collection, the participants signed informed consent. All participants are able to perform activities of daily living based on their answers to the Katz Index (measuring independence in activities of daily living).

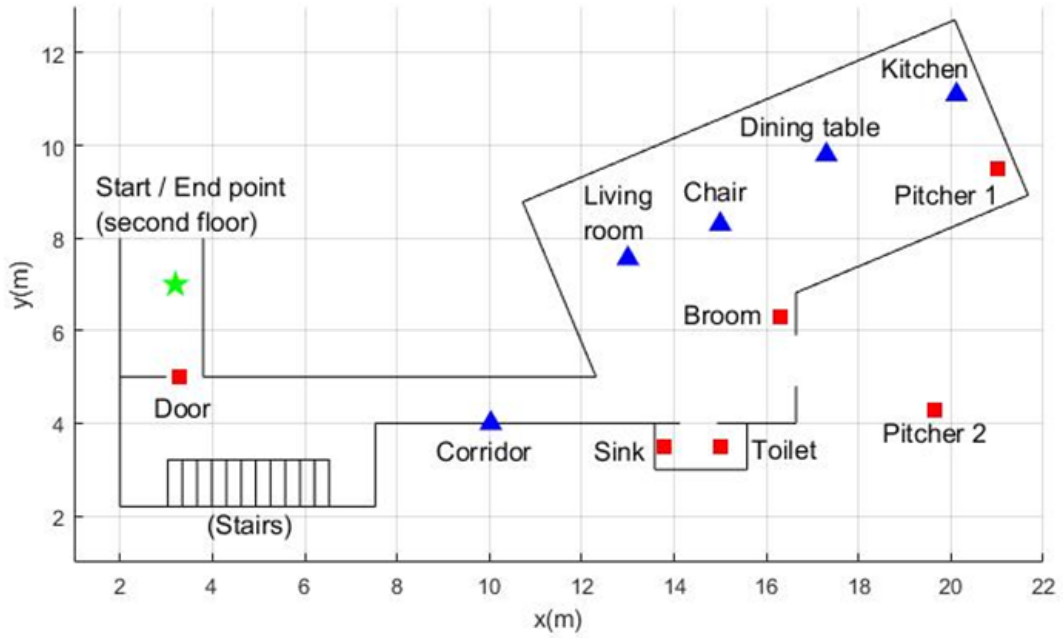

Figure 5.1 Top view of the house used for data collection.

Activity	Description
Enter the house	The session begins on the second floor of the house.
Serve something to eat.	Go down the stairs, go to the kitchen and use a jug to serve something to drink
Eat at the dining table	Take what was served to the dining room and drink it. Food is also available at the dining table if desired.
Wash hands	Go to the bathroom and wash hands in the bathroom sink
Watch TV	Go to the living room, sit on the couch, and watch TV for at least two minutes
Water a plant	Go to the garden, take the jug, and water a plant
Sweep the floor	Take the broom and sweep for at least one minute
Use the toilet	Go to the bathroom and use it or pretend to use it (lift the toilet lid, wait a few seconds, and lower it)
Leave the house	Head towards the same starting point on the second floor.

Table 5.1 Activities performed in data collection.

5.1.1 Foot movement data

The person's foot movement data collected was their acceleration and angular velocity. For this, an IMU (Shimmer sensing, Dublin, Ireland) was attached to each participant's lateral part of the right shoe. The IMU was previously calibrated, and sensitivity of ± 16 g was used for acceleration and ± 2000 °/s for angular velocity. The sampling frequency used was 204.8 Hz.

5.1.2 Proximity data

Ten BLE beacons (Estimote proximity beacons, Estimote Inc, San Francisco, USA, https://estimote.com) were used (Fig. 5.1). A mobile application was developed to run in the background on a smartphone that each participant carried in each session to receive the data streamed by the beacons. The beacons were configured to transmit 10 packets per second. Each telemetric packet contains the received signal strength indicator (RSSI) and the acceleration of the beacon.

The transmission power used in all beacons was -20 dBm. According to the manufacturer, this power coverage is achieved in a radius of 3.5 m. After experimenting with the beacons, we conclude that the RSSI at a distance of one meter is approximate -80 dBm. Therefore, $d_{1m} = 1\ m$ and, $RSSI_{1m} = -80$. The n term depends on the signal transmission medium. To obtain a consistent relationship between RSSI and distance in equation 1, n = 0.6 was used. The variable d is the distance between a given beacon and the smartphone that the person carries.

5.1.3 Motion data from beacons

In addition to RSSI, the packets sent by the beacons contain three-dimensional acceleration signals of the beacon. This functionality allows the movement of the beacon to be directly related to the use of the object to which it is attached.

As a summary, depending on its purpose, a beacon can be categorized as stationary, active, or mobile (Figure 5.2):

1. Stationary beacons: Beacons intended to be stationary in a defined place, for example, on the table or in the kitchen. Their movement is not of interest. They are only used to estimate proximity.

2. Active beacons: An active beacon is attached to an item related to a daily life activity, for example, the Toilet and the bathroom sink. In this way, the movement of an active beacon can indicate that the person is carrying out the activity related to that beacon. For example, if it is detected that the beacon placed on the bathroom sink is moving, this could indicate that the person is washing their hands.

3. Mobile beacons: Beacons that are also attached to an object of daily use, whose movement indicates an activity. Still, unlike active beacons, the position of mobile beacons can change drastically since they are attached to elements such as the broom and a jug.

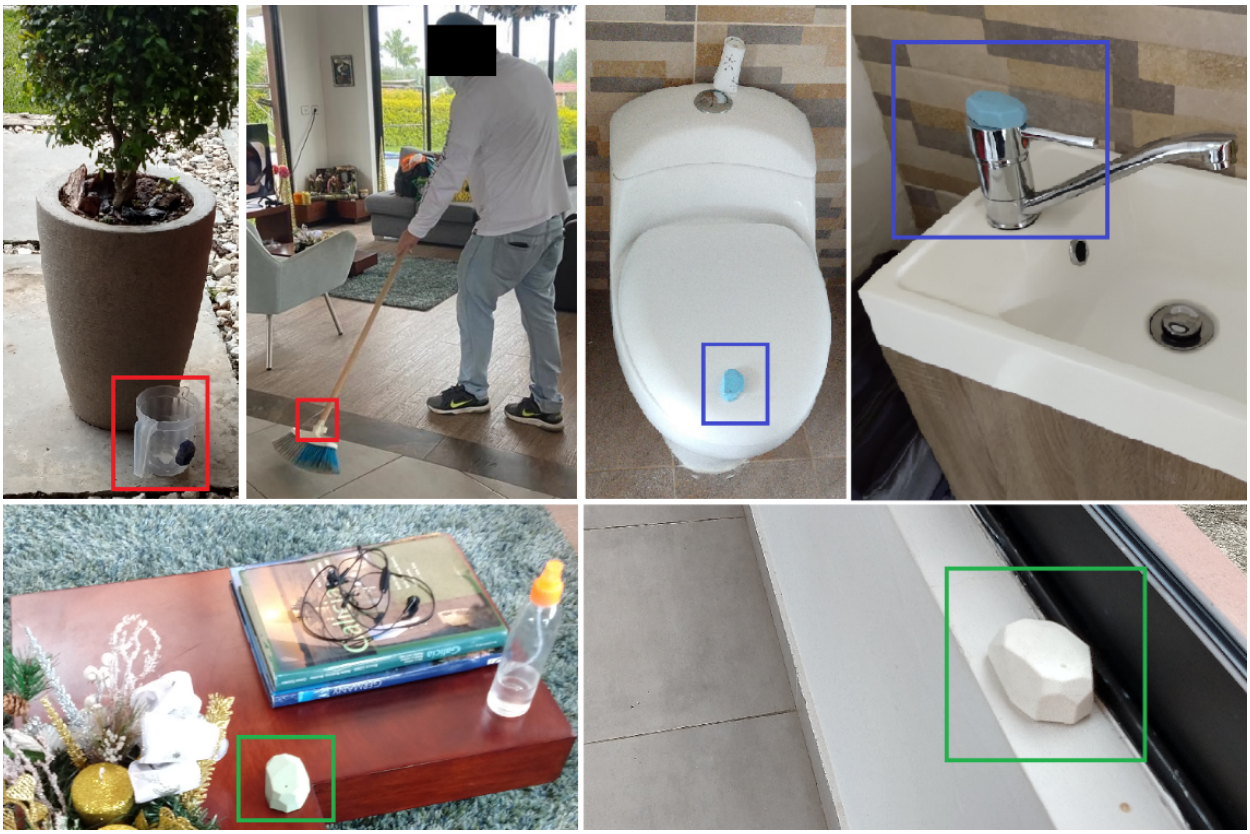

Figure 5.2 Pictures of the beacons used for data collection.

5.2 Human Activity Recognition module

The SLAM method mitigates the error derived from calculating the motion measurement u_t obtained with the PDR ZUPT method by observing landmarks [101]. Furthermore, the set of all landmarks detected at time t $\theta = \{\theta_1, \theta_2, \ldots, \theta_t, \}$ represent the map through which the person is moving. In this work, the ten beacons described above were used as landmarks. There is a particularity with active and mobile beacons since their movement is related to specific activity. In [102], we established a simple rule to relate the motion of beacons to an activity: if the movement was detected in a beacon, it was presumed that the person was using that beacon and, consequently, was carrying out the activity related to it. However, this assumption can cause false positives in multi-inhabited environments since the cause of a beacon's movement might not be the person who is using the system. For that reason, there is a need to classify human activity more rigorously, taking as input the data from the beacons and the movement data collected with the IMU.

Because the specific problem of recognizing human activity involves dealing with data that comes from a dynamic system, that is, that changes or evolves over time, the technique to perform the recognition of the human activity should be able to deal with this problem. That is why data stream algorithms were chosen.

The data collected from the IMU and the beacons were synchronized using scripts written in Python. Four of the activities to be classified are directly related to active and mobile beacons (Table 5.2).

	Activity	Beacon related	Type of beacon
1	Walking	NA	NA
2	Climbing/descending stairs	NA	NA
3	Being still	NA	NA
4	Using jug	Beacon in pitcher	Mobile
5	Sweeping	Beacon in broom	Mobile
6	Using bathroom sink	Beacon in bathroom sink	Active
7	Using toilet	Beacon in toilet	Active

Table 5.2 Human activities to be recognized.

The labeling of each dataset sample with its corresponding activity was carried out manually with an application developed in MatLab that allows synchronizing the previously synchronized data with the video of its collection.

After the RSSI data has been filtered $\{RSSI_1, RSSI_2, \dots, RSSI_{10},\}$, it is used together with the motion data of the beacons $\{M_1, M_2, M_3, M_4\}$ and the acceleration and angular velocity data {Acc, Gyro} to perform the feature extraction process. This process consisted of taking 5-second windows of data (1024 samples) and extracting features from them. Forty features were initially extracted, which included:

1. The maximum and minimum value for each axis of the accelerometer and gyroscope (n = 12)

2. Mean, median, and standard deviation of the acceleration and angular velocity, respectively, for each accelerometer axis (n = 18)

3. The mean of the square root of the sum of the values of each axis squared (mean of the Energy of the accelerometer and gyroscope signal, n = 2)

4. The ID of the four closest beacons detected (n = 4)

5. State of movement of beacons: binary variables that indicate if the active and mobile beacons are in movement (n = 4)

The correlation-based feature subset selection algorithm was used to select the most relevant features. This algorithm detects the subset of highly correlated features with the class while having low intercorrelation [103]. As a result, nine features were selected by the algorithm using ten-fold cross-validation in all the datasets:

1. Maximum acceleration value of the x-axis

2. Median acceleration of the z-axis
3. Median angular velocity of the z-axis
4. Gyroscope energy
5. Movement status of the active and mobile beacons
6. The ID of the closest beacon.

These nine features were used to train and evaluate three data stream classification algorithms: Naive Nayes, Hoeffding tree, and K-nearest neighbor (KNN). The algorithms Hoeffding tree and KNN are adaptations of the original algorithms to fulfill the conditions of the data stream classification. On the other hand, the original Naive Bayes algorithm does not need to be adapted for data stream classification because it is trained incrementally based on Bayes' theorem, and its memory requirements are low.

Summary of the functioning of the Human Activity Recognition module:

For each $RSSI_x$ reading (coming from beacon x) greater than -85dbm, it is checked if beacon x is in motion or if the reading belongs to a 5-second window classified as one of the activities 4, 5, 6, or 7 (Table 5.2). If so:

1. If the RSSI comes from a mobile beacon in motion, its position is updated in the "update activity/beacon location" module. If the RSSI comes from an active beacon in motion, the person's position at time t (S_t) is set equal to the known location of the beacon.

2. If the RSSI comes from a stationary beacon, it is checked whether the location of beacon x is known.

    a. If so, the set of landmarks at time t $\theta = \{\theta_1, \theta_2, \dots, \theta_t, \}$ is sent to the block "trajectory and beacons location estimators" together with the array of IDs of the beacons detected at the time (n_t).

    b. If not, its position is updated in the "update activity/beacon location" module.

5.3 Final framework evaluation

The evaluation process for the Human Activity Recognition and indoor localization modules is detailed below. In addition, all the software developed in Python and MatLab for the acquisition and processing of data and the dataset used for the evaluation is publicly available at: https://github.com/jesusceron.

5.3.1 HAR module evaluation

The software "Massive Online Analyzes" (MOA) [95] was used for the evaluation of the Human Activity Recognition module. This software, written in Java, contains a pool of data stream classification algorithms and offers an API that provides many features, including training and evaluation, obtaining evaluation metrics, and exporting the created models for later use.

The evaluated algorithms were used with their default parameters. For example, the number of activities to be recognized was 7. Consequently, K was set to 7 in KNN.

The evaluation method used is called interleaved Test-Then-Train. In this, each example is used to evaluate the model before it is used to train it. In this way, the model is continuously assessed with unseen examples, ensuring the model's generalization. In addition, this method enables obtaining updated statistics with each example that the algorithm processes, thus drawing its learning curve.

We used the F1 score to evaluate the performance of the classifiers. This metric is a measure that gives equal importance to precision and recall and is frequently used to assess the performance of models generated from unbalanced datasets such as the one collected in this study:

$$F1 = 2\frac{precision * recall}{precision + recall} \qquad \text{Equation 5.1}$$

In total, 3716 examples were extracted from the data of the 22 participants. On average, there were 169 examples per participant. The evaluation process was similar to the leave-one-subject-out method. As the data stream classification algorithm is trained example by example, an arff file was created in which the examples of the participant were placed at the end of the file, after the examples of the other 21 participants. In addition, the examples of the 21 participants were randomized in each file to obtain results that showed the variance of the F1 measure between participants and hindered the algorithms' learning process.

5.3.2 Indoor trajectory reconstruction

The complete trajectory followed by each participant during data collection can be divided into six sub-trajectories:

1. From the main entrance to the kitchen (where a drink is served with the jug)
2. From the kitchen to the sink (person washes his/her hands in the sink)
3. From the sink to the garden (water the plant with a jug)
4. From the garden to the living room (sweep the living room with the broom)
5. From the living room to the bathroom (use or pretend to use the toilet)
6. From the bathroom to the main entrance

Except for the initial and final activity, the rest of the sub-trajectories begin and finish where an activity is detected. Thus, the start and end coordinates of data collection are the same. In

addition, the exact starting and ending coordinates of each sub-trajectory are known. Therefore, it is possible to calculate the error of the estimated trajectory by calculating the Euclidean distance between the coordinates of the last step of the sub-trajectory estimated and the true coordinates where the activity started.

It was important to demonstrate that the proposed framework can work appropriately for adults and older adults. Therefore, a student t-test was performed to compare the means of the location errors between the two groups. The null hypothesis states that there is no significant difference between the means of the indoor localization errors of the older adults and control groups. A 95% confidence interval was used.

5.4 Framework evaluation results

5.4.1 HAR module

To evaluate the three data stream classification algorithms' overall performance, Table 5.3 shows the precision, F1 score, and processing time to process the 3716 examples. The data in each column corresponds to the average of all participants. The main evaluation metric used to evaluate HAR was F1.

Algorithm	F1 score (percent)	Evaluation time (CPU seconds)	Classifications correct (percent)
KNN	88.01	45.68	89.92
Naive Bayes	86.78	0.51	89.70
Hoeffding tree	83.76	0.73	87.56

Table 5.3 General performance of algorithms.

The percentage of the examples correctly classified using these three algorithms was high. KNN and NB reached almost 90%, and HT reached 87.56%. However, the results of the F1 measure were a little lower, but the order of algorithms concerning their performance was preserved: the best F1 is KNN (88.01%), followed by NB (86.78%) and finally HT (83.76%) (Table 5.3). In Khannouz's work [96, 100], the level of F1 was much lower, although a direct comparison of the performance of the algorithms cannot be made because the datasets used are different. For example, their real datasets do not contain data from BLE beacons, and the activities carried out in them are different.

Table 5.4 shows in detail the average value of this metric for each sub-trajectory.

Activity	KNN	Naive Bayes	Hoeffding tree
Walking	82,24	82,21	79,63
Climbing/Descending stairs	49,87	31,29	29,71
Using pitcher	99,41	99,58	97,28
Being still	94,60	95,13	93,82
Using bathroom sink	91,57	91,53	85,06
Sweeping	99,50	99,61	98,27
Using toilet	96,84	98,27	92,52

Table 5.4 Performance of the algorithms in the classification of each activity.

The activity of going up or down the stairs produced a low F1 in all cases. On a closer inspection, the reason for this is that algorithms classified many examples labeled as "climbing/descending stairs" as "walking." Consequently, the number of false positives affects the F1 measure of the "walking" activity. This phenomenon seems to affect the older adult group more. Consequently, there was a significant difference in recognition of the walking activity between older adults and control groups (Table 5.5). There are ways to handle the low F1 obtained for the "Climbing / descending stairs" activity. The simplest solution is to merge the activities "walking" and "Climbing / descending stairs." In that case, when looking at the results in Table 5.4, it is foreseeable that KNN and NB would have a very similar F1. Another option would be to look for features that help classify that activity and include them in the learning phase. It would also be possible to place two stationary beacons at both sides of the stairs, which in addition to helping to refine the location, would help to classify the activity in question. Finally, including the data from a barometer is a viable option. Some IMUs have a built-in barometer, and it has already been proven a valuable sensor for measuring changes in height in indoor environments [104,105].

A t-test was carried out to test for any significant difference in the F1 measure of the older adults and control group for each activity. There was a significant difference between the two groups only in the case of the recognition of the walking activity.

	CG	OAG	Difference	p-value
Walking	82.41	82.06	-0.35	0.05
Climbing/ descending stairs	49.82	49.91	0.09	0.91
Using pitcher	99.42	99.39	-0.02	0.49
Being still	94.56	94.63	0.07	0.45
Using bathroom sink	91.48	91.65	0.16	0.39
Sweeping	99.50	99.49	-0.01	0.71
Using toilet	96.71	96.95	0.23	0.14
All activities	88.02	88.00	-0,01	0.90

Table 5.5 T-student test result. Comparison of F1 measure between older adults (OAG) and control group (CG).

The interleaved Test-Then-Train evaluation method allows the learning curve of the data stream algorithms to be obtained (Figure 5.3). Each example that the algorithm receives evaluates the model created so far and then uses the same example to train and update the model.

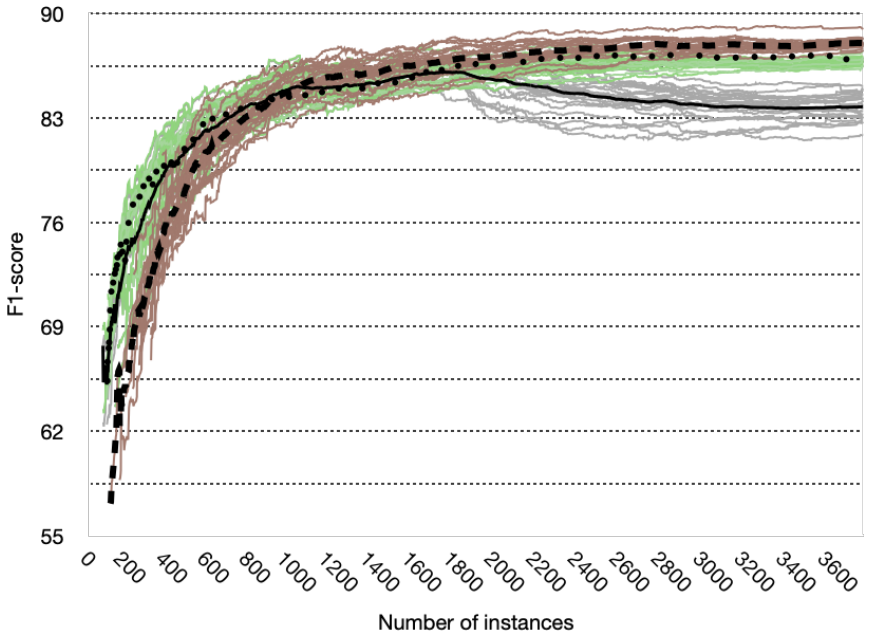

Figure 5.3 Learning curves for all participants and their average. NB: green lines, average on the dotted line. HT: gray lines, average on the solid line. KNN: red lines, average in broken line.

While the learning curves for the KNN and NB algorithms maintain an upward trend after 1800 examples, the learning curve for the HT algorithm has a downward behavior that stabilizes approximately at example number 3000. Consequently, we chose to include the KNN and NB algorithms in our framework. Furthermore, the learning curve of the KNN algorithm is lower than the curves of the NB and HT algorithms up to approximately 1000 examples. This behavior is expected since KNN must base its classification on the most similar examples previously classified. Still, since it is a data stream algorithm, it does not save all the history of the examples when performing the comparison. Instead, it stores only some [95].

The evaluation of a data stream algorithm includes calculating the time it takes to process each example. The processing time of the three algorithms has a linear behavior through time. Therefore, the time it takes for the algorithm to process an example corresponds to dividing the total time it took to process the 3716 examples by the total number of examples. The nearest neighbor search performed in KNN and the need to store a set of examples to compare the similarity with unknown examples are costly computational tasks compared to the tasks required in NB and HT. However, KNN processes each sample in 12.9 ms, and the proposed framework needs to classify an example every 5 seconds. In addition, the classification model obtained with KNN could be quickly executed on a device with a very low memory capacity, since it only uses 0.69 kB.

5.4.2 Indoor localization

The generation of particles in the prediction phase is a random process. This means that the proposed method must be executed several times to have a reasonable estimate of the indoor location error for each participant. Therefore, the proposed method was run ten times for each participant. Table 5.6 and Table 5.7 show the average location error in each sub-trajectory for the older adults and control group, respectively.

The total average localization error was 1.023 m for the older adults group participants and 0.986 m for the control group. These results are similar to those obtained in our previous work [102]. The novelty of this study is the comparison of the results between the groups.

Participant	1	2	3	4	5	6	7	8	9	10	11	Average
Door to kitchen	1.92	1.75	1.98	0.45	1.2	0.63	1.67	2.09	1.24	1.29	1.06	1.39
Kitchen to the bathroom sink	1.5	1.3	1.49	1.02	0.93	1.13	3.05	3.27	1.36	0.76	0.17	1.45
Bathroom sink to plant	0.49	1.22	0.4	1.99	0.63	0.72	0.31	0.29	0.55	1.38	1.01	0.82
Plant to room	1.56	1.49	0.74	0.62	3.05	0.22	0.53	0.15	0.28	0.9	0.22	0.89
Broom to toilet	0.44	1.37	0.44	1.05	0.3	0.68	0.68	0.47	0.15	0.39	0.59	0.6
Toilet to door	0.56	1.68	0.75	0.9	1.18	0.78	0.83	0.88	0.59	0.68	1.69	0.96
Total average error	1.08	1.47	0.97	1.02	1.22	0.69	1.18	1.19	0.7	0.9	0.79	1.02

Table 5.6 Average error (in meters) of the location for each sub-trajectory (older adults' group).

Participant	1	2	3	4	5	6	7	8	9	10	11	Average
Door to kitchen	0.91	1.06	0.99	1.13	0.71	1.41	1.04	1.23	1.73	0.95	2.95	1.28
Kitchen to the bathroom sink	0.87	0.36	1.51	0.90	2.13	1.91	1.14	1.25	2.42	1.32	1.71	1.41
Bathroom sink to plant	0.30	0.34	1.51	0.64	2.91	0.54	1.36	1.59	2.15	1.51	1.14	1.27
Plant to room	0.61	0.47	0.85	0.44	0.23	0.46	0.60	1.13	1.35	0.16	1.10	0.67
Broom to toilet	0.18	0.23	0.97	0.28	0.19	0.25	1.07	0.26	1.07	0.34	0.22	0.46
Toilet to door	0.22	0.36	0.94	0.28	2.76	0.88	0.94	0.79	0.24	0.41	0.86	0.79
Total average error	0.51	0.47	1.13	0.61	1.49	0.91	1.03	1.04	1.49	0.78	1.33	0.98

Table 5.7 Average error (in meters) of the location for each sub-trajectory (control group).

There is no significant difference in the location error between older adults and control groups (Table 5.8). This result, along with the results obtained in the HAR section, indicates that the proposed framework to perform simultaneous indoor localization, mapping, and Human Activity Recognition works adequately with older adults, and therefore is suitable to be implemented in ambient assisted living scenarios. It is important to note that this result implies

that the inclusion of the data stream classifier for HAR was successful since the proposed framework follows the location based on the results of the HAR module.

	CG	OAG	Difference	p-value
Door to kitchen	1.28	1.28	-0.00	0.90
Kitchen to the bathroom sink	1.41	1.41	0.18	0.60
Bathroom to plant	1.27	1.27	-0.49	0.11
Plant to broom	0.67	0.67	0.21	0.47
Broom to toilet	0.46	0.46	0.10	0.53
Toilet to door	0.79	0.79	0.21	0.40
Complete trajectory	0.98	0.98	0.03	0.78

Table 5.8 T-student test result. Comparison of errors between older adults and control group.

Going deeper into the comparison of the results of the two groups, the largest average error occurs for the sub-trajectory between going from the kitchen to the bathroom sink. That trajectory implied that the participant served something to drink in the kitchen, walked to the dining room, sat down and ate something, stood up, and went to wash his/her hands. It is known that sitting activities are likely to cause loss of heading; even more, when the person moves his/her feet when seated. One way to deal with heading drift is to deploy as many beacons as possible and position them to have a line of sight with the Bluetooth signal receiver device as much as possible. This design consideration must be considered if the receiving device is the same IMU as is put in the person's shoe. In that case, it would be preferable for the stationary beacons to be kept level with the ground.

Figure 5.4 to Figure 5.7 show the localization results for all the participants. The ten runs for each participant are in gray color and the average is in blue. There is a drift in reconstructing the final sub-trajectories of participants 1 and 5 of the control group (Figure 5.4) and participant 7 of the older adults' group (Figure 5.5). That drift results in a large error in the location of said sub-trajectory for the participants mentioned above. The activity consists of going from the bathroom to the main entrance on the second floor. The loss of heading occurs from the moment the sub-trajectory begins, just after using the toilet. As in the previous case, having more beacons to correct the orientation would be very useful. As proposed in section 4.1, placing a beacon at each end of the stairs would improve heading drift and classify the "climbing / descending stairs" activity.

The longest sub-path (around 20 m in length) is to go from the starting point to the kitchen. Although this activity involves going downstairs, the indoor location on the stairs was done very well for both groups (Figure 5.4 and Figure 5.5) However, the average location error for this sub-trajectory was 1,395 m for the control group and 1,287 m for the older adults group. Then, the cause of the error is in the correction of the position carried out by the particle filter. As in the case of heading loss, they have more beacons, especially stationary, that are at the same level as the receiving device of their signals, which would be the way to improve localization.

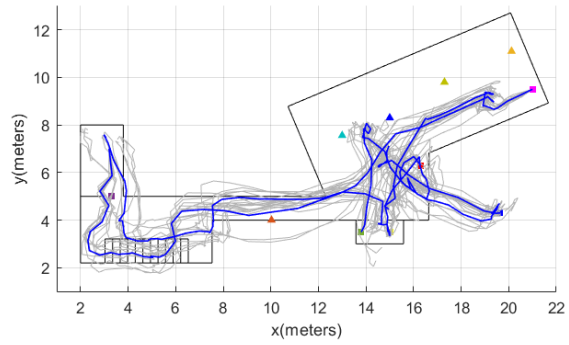

Participant 1

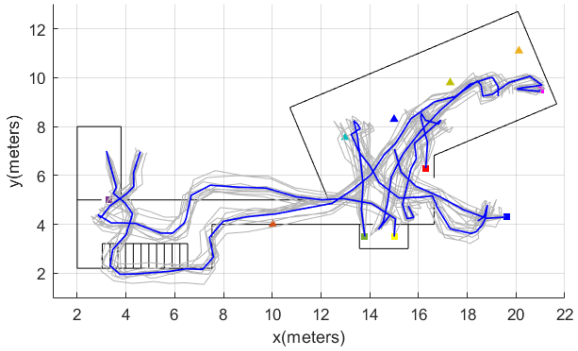

Participant 2

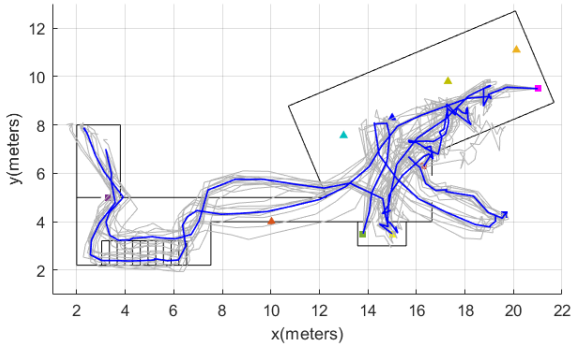

Participant 3

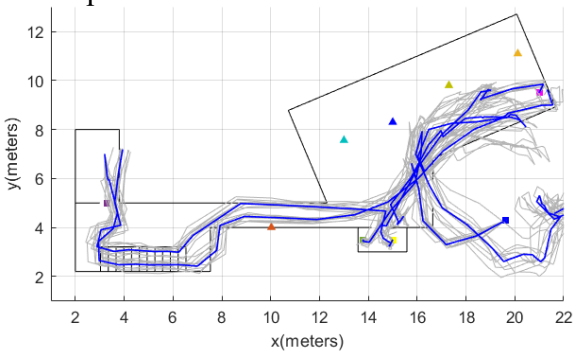

Participant 4

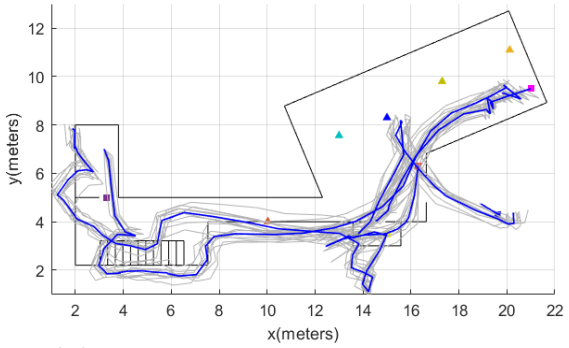

Participant 5

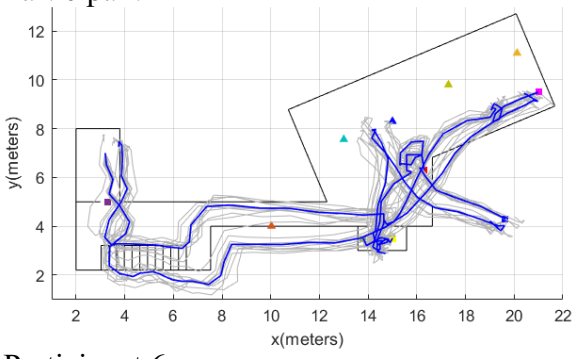

Participant 6

Figure 5.4 Indoor localization results (Older adults' group, participants 1-6).

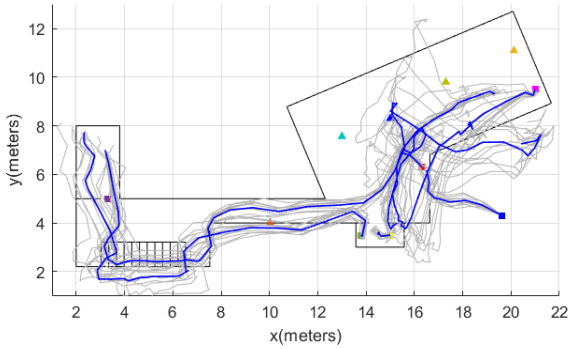

Participant 7

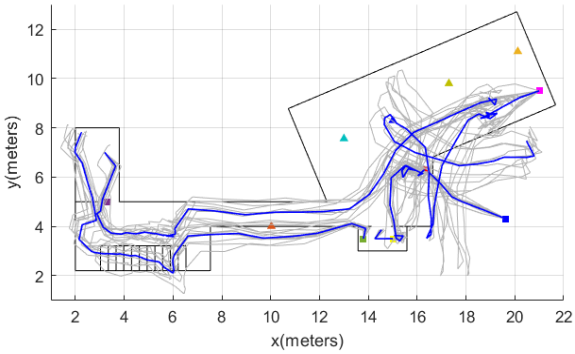

Participant 8

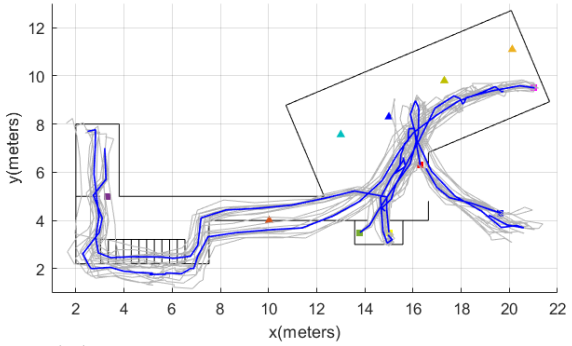

Participant 9

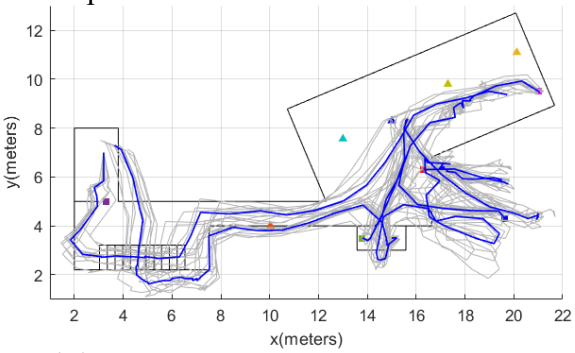

Participant 10

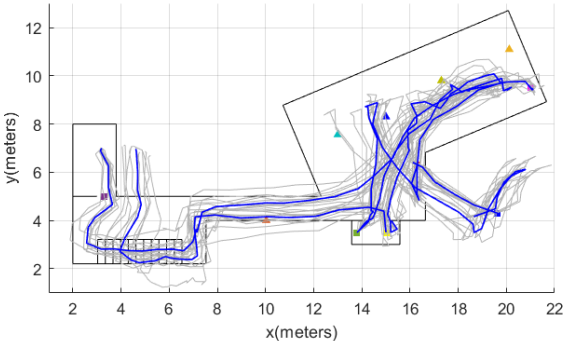

Participant 11

Figure 5.5 Indoor localization results (Older adults' group, participants 7-11).

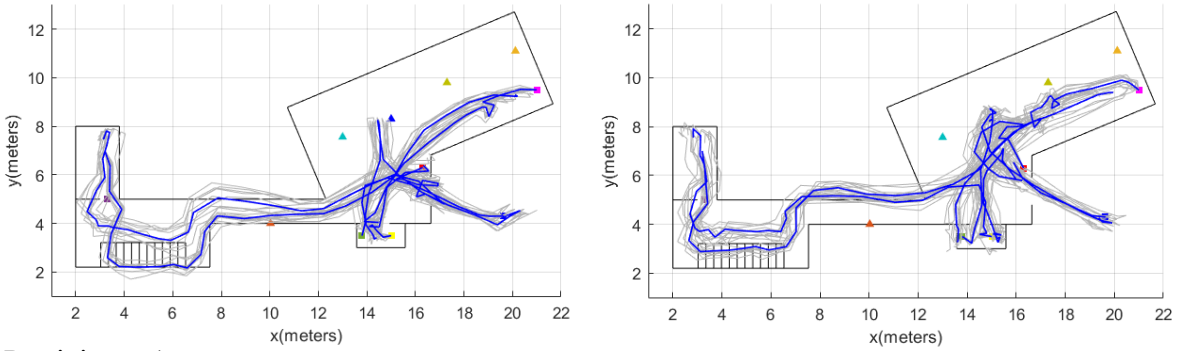

Participant 1

Participant 2

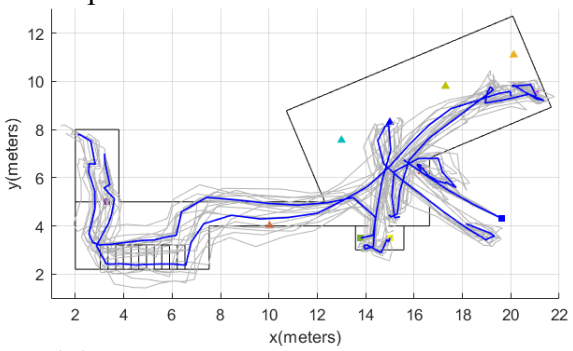

Participant 3

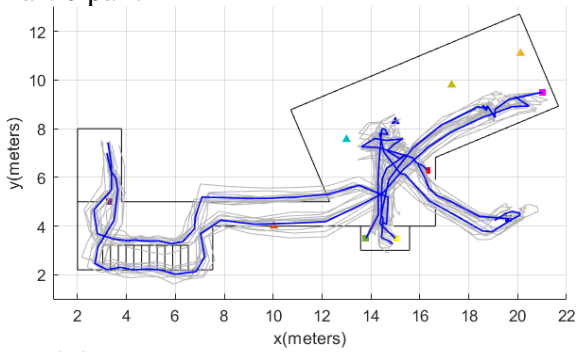

Participant 4

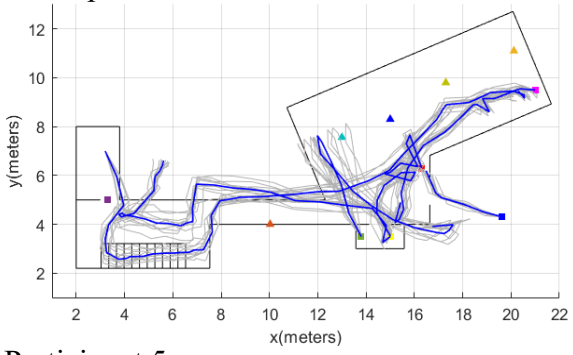

Participant 5

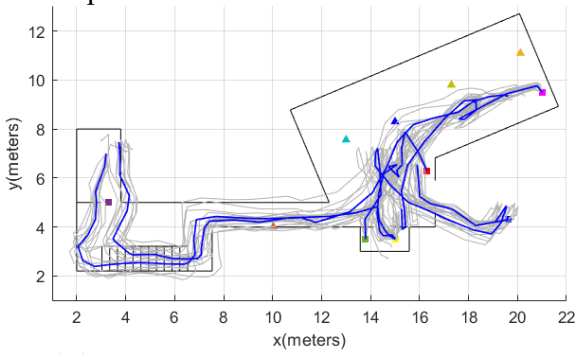

Participant 6

Figure 5.6 Indoor localization results (control group, participants 1-6).

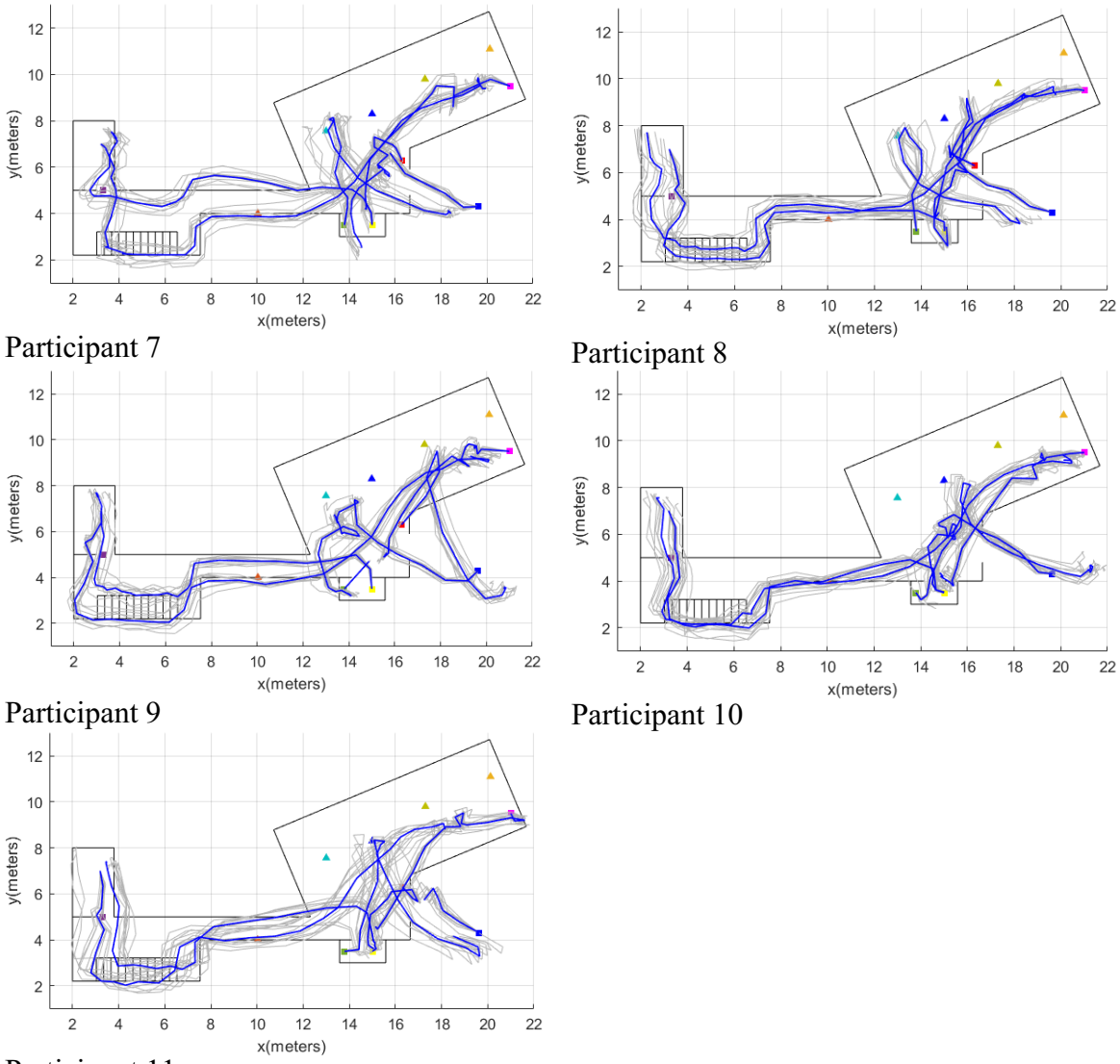

Figure 5.7 Indoor localization results (control group, participants 7-11).

5.5 Summary

This chapter presented the evaluation of the proposed framework that simultaneously and non-invasively performs indoor localization, mapping, and Human Activity Recognition in AAL scenarios. The framework fuses data from an IMU placed in the person's shoe with proximity and human activity-related data from BLE beacons. The feasibility of the framework was demonstrated in a home environment with adults and older adults performing simultaneous location, mapping, and recognition of daily life activities.

Chapter 6

Conclusions and future work

This chapter contains the main conclusions obtained from the development of this doctoral thesis. Subsequently, the recommendations and the proposed future work are presented.

6.1 Conclusions

In this work, a proposal for simultaneous Human Activity Recognition, mapping, and indoor localization for ambient assisted living scenarios has been presented. The work intended to take advantage of the existing relationship between the activity a person performs and the place where it is completed. The relationship between location and human activity is evident to anyone. If individuals know what activity a person is doing inside his/her house, it is probably somewhat intuitive to know where the person is located. People could also have an idea of what possible activities a person is doing if they know where the person is.

The rapid development of new ubiquitous technologies and the growing interest in Human Activity Recognition and Indoor Localization have enabled the emergence of new methods and systems able to tackle both HAR and IL simultaneously. The state-of-the-art (Chapter 2) shows that, so far, very few studies have taken advantage of the relationship between what is done by a person and where it is done in an indoor environment. The possible main benefit of taking advantage of the relationship is the increased accuracy of both HAR and IL.

HAR and IL in AAL environments are especially critical since an AAL scenario must be recognized as a dynamic system, for two main reasons: the first one is that the way an older adult executes specific daily activities can change due to natural aging or due to some disease such as dementia, Parkinson's, or Alzheimer's. The second is about IL since if the location of the furniture changes or a new obstacle is put in the indoor environment, the IPS will most likely

need to be recalibrated or retrained. According to the state of the art described in chapter 2, no study has considered the dynamic nature of AAL environments. Most IPS need a previous training phase. In this phase, the IPS learn the map of the indoor environment. In the context of AAL scenarios, it is desirable that this training phase is not needed or the time and effort required are minimized as much as possible.

Another important aspect to consider is that usually, the works aimed at supporting IL in HAR or vice versa have evaluated their proposals with very few people. Usually, those people are not older adults. As Calvaresi concludes in their systematic review [54], the lack of rigorous evaluation and validation is evident due to the small number of people testing the studies included.

Pedestrian Dead-Reckoning and Device-Free-based methods have emerged as the least intrusive solutions to carry IL and HAR simultaneously. This is especially important for AAL scenarios, where older adults need assistance. However, both methods have many challenges to overcome. In the case of PDR, some challenges are the heading error due to noise, bias, or misalignment of sensors, the loss of orientation, and the locations of the body in which the sensors can be placed. Also, if a magnetometer is used to get orientation data, it is necessary to deal with the noise of metallic objects or electronic devices. Device-Free based methods use wireless technologies. Besides having to face problems such as attenuation or multipath propagation, the person being tracked must be identified in multi-inhabited environments. Another problem with device-free methods is the fluctuations of the signal produced by other people or changes in the furniture. This leads to propagation models changing and thus requiring a system update.

The first approach with the IL was the proposal of a pipeline for trajectory reconstruction of walking, jogging, and running activities using a foot-mounted inertial pedestrian dead-reckoning system. The dynamic time warping method was adapted to segment walking, jogging, and running strides. Stride length and orientation estimation were performed using a zero-velocity update algorithm adapted for walking, jogging, and running strides and empowered by a complementary Kalman filter. This pipeline was incorporated in the final framework proposed. Several people comprehensively evaluated the pipeline. The results of this evaluation can serve as a baseline for comparing future systems. Future work will be focused on using hidden Markov models to improve stride segmentation and fusing symbolic location from an RSSI signal to update the indoor localization when possible.

The proposed framework for simultaneous Human Activity Recognition, indoor localization, and house mapping was built based on the SLAM framework. SLAM was born in robotics to get a map and locate a robot on it. SLAM has already been applied in other disciplines. Pedestrian localization is one of these disciplines. It was decided to get the pedestrian movement from a foot-mounted IMU. That way, a Pedestrian Dead-Reckoning Algorithm with zero velocity updates was implemented. The PDR algorithm obtained the person position estimates. The position estimates were improved by fusing them with proximity and human activity-related data from BLE beacons deployed in the indoor environment. The framework simultaneously estimates the position of the beacons using Extended Kalman Filters. Since the location of the

beacons is not known at the beginning of the data collection, the framework incorporates a method to initialize the position of the beacons from scratch. As a recommendation, it is suggested to carry out a simple training phase to obtain a more precise location of the beacons. That phase would consist of the person addressing each beacon deployed in the environment and staying as close as possible to each beacon for at least ten seconds so that the particle filter converges by processing enough measurements taken at a short distance and, therefore, a more reliable one.

The final results show that SLAM allows a dynamic indoor localization. The recognition of activities aided by the interaction with Bluetooth beacons constitutes an excellent alternative to landmarks in SLAM. This allows mapping of the area in which the person moves and refining the localization of the person in it. Although previous works have used BLE beacons for indoor localization, to the best of our knowledge, this is the first one that uses the movement of beacons as an input variable for classifying activities that are later used as landmarks in the SLAM framework. HAR was carried out with a KNN data stream algorithm, which can be executed on any wearable due to its low memory consumption.

No single dataset was found with data that allows the evaluation of the proposed framework. Therefore, the collected dataset constitutes a fundamental part of our research, and it is publicly available for other authors. It included synchronized data from the IMU that the participants carried on their right foot and the BLE beacons deployed in the indoor environment. In addition, each example was labeled with one of the seven activities that the participants performed. The collected dataset includes 22 people, of which 11 are older than 60 years. This allowed us to compare the framework's performance concerning HAR and IL with adults and older adults. Finally, the dataset was collected in Colombia, allowing the training of local models in low- and middle-income settings, and it has been widely recommended in the literature [106,107].

6.2 Future work

The proposed framework is the backbone for future projects to develop flexible systems for monitoring IL and HAR based on two non-intrusive components: an IMU and Bluetooth beacons. The IMU in the shoe and BLE beacons deployed in the house are the necessary devices for the operation of the proposed framework. A smartphone was required since the IMU used does not have the functionality to receive Bluetooth signals. However, it is possible to adapt or develop an IMU capable of receiving a Bluetooth signal, thus avoiding the use of the Smartphone. The use of the IMU at the foot, in addition to being slightly intrusive, is opportunistic because it facilitates the detection of gait parameters in older adults. It is beneficial for detecting gait disorders such as those derived from Parkinson's disease. As future work, developing a smart insole that contains one accelerometer and gyroscope and the capacity to receive the BLE signal from the beacons can be beneficial to increase the use comfort. If the beacon signal is received by the IMU placed on the foot, relocating the stationary beacons at ground level should be considered to get a line of sight and simplify the distance estimation.

Although the activity classification model updates automatically, labeled examples will eventually be needed to refine its accuracy. For this reason, it is necessary to carry out an exhaustive analysis of the behavior of the online learning algorithm used. To have the HAR classification model up to date, as future work, an automatic process to label the learning examples could be done based on the movement of the beacons and their proximity to them.

It has been concluded that the more beacons deployed in the indoor environment, the better the accuracy of the IL and HAR. An exhaustive analysis in this regard is necessary. Characteristics such as the size and type of house or apartment of the older adult, the number of beacons, and the number of activities to be automatically recognized must be studied to obtain a generalizable system.

As just mentioned, the proposed framework is the basis for projects that require obtaining IL and/or HAR data in AAL scenarios. Continuing with developing a monitoring system for the elderly would be an interesting future project. IL and HAR data can be used to monitor changes in the older adult's routine, abnormal events, falls, movement impairment, gait impairment, changes in sleep hours, etc. Proposing a kit-type system, in which the elderly is given a set number of beacons with instructions on where to put them and perhaps a template-type IMU, would present an attractive option due to its simplicity and low cost to provide services based on location and in the activity.

References

1. United Nations World Population Ageing 2015; 2015; ISBN 9789211515381.
2. Kleinberger, T.; Becker, M.; Ras, E.; Holzinger, A.; Müller, P. Ambient Intelligence in Assisted Living: Enable Elderly People to Handle Future Interfaces. In Universal Access in Human-Computer Interaction. Ambient Interaction: 4th International Conference on Universal Access in Human-Computer Interaction, UAHCI 2007 Held as Part of HCI International 2007 Beijing, China, July 22-27, 2007 Proceedings, Part II; Stephanidis, C., Ed.; Springer Berlin Heidelberg: Berlin, Heidelberg, 2007; pp. 103–112 ISBN 978-3-540-73281-5.
3. Christensen, K.; Doblhammer, G.; Rau, R.; Vaupel, J.W. Ageing Populations: The Challenges Ahead. The Lancet 2009, 374, 1196–1208.
4. Ministerio de Salud y Protección Social Envejecimiento Demográfico 1951-2020. Dinámica Demográfica y Estructuras Poblacionales Available online: https://www.minsalud.gov.co/sites/rid/Lists/BibliotecaDigital/RIDE/DE/PS/Envejecimiento-demografico-Colombia-1951-2020.pdf (accessed on 24 October 2017).
5. Ministerio de Salud Diagnostico Preliminar Sobre Personas Mayores, Dependencia y Servicios Sociales En Colombia. Ministerio de Salud 2013, 19.
6. Vodjdani, N. The Ambient Assisted Living Joint Programme. In Proceedings of the Electronics System-Integration Technology Conference, 2008. ESTC 2008. 2nd; 2008; pp. 1–2.
7. Wang, Z.; Yang, Z.; Dong, T. A Review of Wearable Technologies for Elderly Care That Can Accurately Track Indoor Position, Recognize Physical Activities and Monitor Vital Signs in Real Time. Sensors (Switzerland) 2017, 17.
8. Su, X.; Tong, H.; Ji, P. Activity Recognition with Smartphone Sensors. Tsinghua Science and Technology 2014, 19, 235–249, doi:10.1109/TST.2014.6838194.
9. Loveday, A.; Sherar, L.B.; Sanders, J.P.; Sanderson, P.W.; Esliger, D.W. Technologies That Assess the Location of Physical Activity and Sedentary Behavior: A Systematic Review. Journal of Medical Internet Research 2015, 17, doi:10.2196/jmir.4761.
10. Xie, Z.; Zhang, J.; Xiao, W.; Sun, C.; Lu, Y. Extreme Learning Machine Based Location-Aware Activity Recognition. In Proceedings of 2017 Chinese Intelligent Systems Conference: Volume II; Jia, Y., Du, J., Zhang, W., Eds.; Springer Singapore: Singapore, 2018; pp. 757–768 ISBN 978-981-10-6499-9.
11. Zhu, C.; Sheng, W. Realtime Recognition of Complex Human Daily Activities Using Human Motion and Location Data. IEEE Transactions on Biomedical Engineering 2012, 59, 2422–2430, doi:10.1109/TBME.2012.2190602.
12. Bobkov, D.; Grimm, F.; Steinbach, E.; Hilsenbeck, S.; Schroth, G. Activity Recognition on Handheld Devices for Pedestrian Indoor Navigation. In Proceedings of the 2015 International Conference on Indoor Positioning and Indoor Navigation, IPIN 2015; 2015.
13. Zhu, C.; Sheng, W. Realtime Human Daily Activity Recognition through Fusion of Motion and Location Data. In Proceedings of the 2010 IEEE International Conference on Information and Automation, ICIA 2010; 2010; pp. 846–851.
14. Hong, J.-H.; Ramos, J.; Shin, C.; Dey, A.K. An Activity Recognition System for Ambient Assisted Living Environments. In Evaluating AAL Systems Through Competitive Benchmarking: International Competitions and Final Workshop, EvAAL 2012, July and September 2012. Revised Selected Papers; Chessa, S., Knauth, S., Eds.; Springer Berlin Heidelberg: Berlin, Heidelberg, 2013; pp. 148–158 ISBN 978-3-642-37419-7.
15. Liu, X.; Liu, Q. Power Consuming Activity Recognition in Home Environment. In Cloud Computing and Security: Third International Conference, ICCCS 2017, Nanjing, China, June 16-18, 2017, Revised Selected Papers, Part I; Sun, X., Chao, H.-C., You, X., Bertino, E., Eds.; Springer International Publishing: Cham, 2017; pp. 361–372 ISBN 978-3-319-68505-2.

16. Hardegger, M.; Nguyen-Dinh, L.-V.; Calatroni, A.; Tröster, G.; Roggen, D. Enhancing Action Recognition through Simultaneous Semantic Mapping from Body-Worn Motion Sensors. In Proceedings of the Proceedings of the 2014 ACM International Symposium on Wearable Computers (ISWC '14); 2014; pp. 99–106.
17. Roy, N.; Misra, A.; Cook, D. Ambient and Smartphone Sensor Assisted ADL Recognition in Multi-Inhabitant Smart Environments. Journal of Ambient Intelligence and Humanized Computing 2016, 7, 1–19, doi:10.1007/s12652-015-0294-7.
18. Nakagawa, E.; Moriya, K.; Suwa, H.; Fujimoto, M.; Arakawa, Y.; Yasumoto, K. Toward Real-Time in-Home Activity Recognition Using Indoor Positioning Sensor and Power Meters. In Proceedings of the 2017 IEEE International Conference on Pervasive Computing and Communications Workshops, PerCom Workshops 2017; 2017; pp. 539–544.
19. Ceron, J.D.; Lopez, D.M.; Hofmann, C. A Two-Layer Method for Sedentary Behaviors Classification Using Smartphone and Bluetooth Beacons. Studies in health technology and informatics 2017, 237, 115–122.
20. Sundaram, S.; Mayol-Cuevas, W.W. What Are We Doing Here? Egocentric Activity Recognition on the Move for Contextual Mapping. In Proceedings of the Proceedings - IEEE International Conference on Robotics and Automation; 2012; pp. 877–882.
21. Vesa, A.V.; Vlad, S.; Rus, R.; Antal, M.; Pop, C.; Anghel, I.; Cioara, T.; Salomie, I. Human Activity Recognition Using Smartphone Sensors and Beacon-Based Indoor Localization for Ambient Assisted Living Systems. In Proceedings of the 2020 IEEE 16th International Conference on Intelligent Computer Communication and Processing (ICCP); IEEE, September 3 2020; pp. 205–212.
22. Li, J.; Guo, Y.; Qi, Y. Using Neural Networks for Indoor Human Activity Recognition with Spatial Location Information. In Proceedings of the Proceedings - 2019 11th International Conference on Intelligent Human-Machine Systems and Cybernetics, IHMSC 2019; 2019; Vol. 2.
23. Chen, L.; Zhao, Y.; Zhang, Y.; Fan, S.; Jia, Y. An Online Prediction and Trajectory Tracking Method for Human Activity Recognition. In Proceedings of the PervasiveHealth: Pervasive Computing Technologies for Healthcare; 2020.
24. Pan, Z.; Wei, C. Human Activity Monitoring Based on Indoor Map Positioning. Microsystem Technologies 2021, 27, doi:10.1007/s00542-020-05124-w.
25. Wu, J.; Feng, Y.; Sun, P. Sensor Fusion for Recognition of Activities of Daily Living. Sensors (Switzerland) 2018, 18, doi:10.3390/s18114029.
26. Radu, V.; Marina, M.K. HiMLoc: Indoor Smartphone Localization via Activity Aware Pedestrian Dead Reckoning with Selective Crowdsourced WiFi Fingerprinting. In Proceedings of the 2013 International Conference on Indoor Positioning and Indoor Navigation, IPIN 2013; 2013.
27. Guo, S.; Xiong, H.; Zheng, X.; Zhou, Y. Activity Recognition and Semantic Description for Indoor Mobile Localization. Sensors (Switzerland) 2017, 17, doi:10.3390/s17030649.
28. Gao, N.; Zhao, L. A Pedestrian Dead Reckoning System Using SEMG Based on Activities Recognition. In Proceedings of the 2016 IEEE Chinese Guidance, Navigation and Control Conference (CGNCC); 2016; pp. 2361–2365.
29. Giorgetti, G.; Farley, R.; Chikkappa, K.; Ellis, J.; Kaleas, T. Cortina: Collaborative Indoor Positioning Using Low-Power Sensor Networks. Journal of Location Based Services 2012, 6, 137–160, doi:10.1080/17489725.2012.690217.
30. Moder, T.; Hafner, P.; Wisiol, K.; Wieser, M. 3D Indoor Positioning with Pedestrian Dead Reckoning and Activity Recognition Based on Bayes Filtering. In Proceedings of the IPIN 2014 - 2014 International Conference on Indoor Positioning and Indoor Navigation; 2014; pp. 717–720.
31. Torok, A.; Nagy, A.; Kovats, L.; Pach, P. DREAR - Towards Infrastructure-Free Indoor Localization via Dead-Reckoning Enhanced with Activity Recognition. In Proceedings of the Proceedings - 2014 8th International Conference on Next Generation Mobile Applications, Services and Technologies, NGMAST 2014; 2014; pp. 106–111.
32. Becis, Y.; Aubry, D.; Ramdani, N. Indoor Human / Robot Localization Using Robust Multi-Modal Data Fusion. In Proceedings of the IEEE Conference on Robotics and Automation; 2015; pp. 3456–3463.
33. Li, G.; Zhu, C.; Du, J.; Cheng, Q.; Sheng, W.; Chen, H. Robot Semantic Mapping through Wearable Sensor-Based Human Activity Recognition. In Proceedings of the Proceedings - IEEE International Conference on Robotics and Automation; 2012; pp. 5228–5233.

34. Murata, Y.; Hiroi, K.; Kaji, K.; Kawaguchi, N. Pedestrian Dead Reckoning Based on Human Activity Sensing Knowledge. Proceedings of the 2014 ACM International Joint Conference on Pervasive and Ubiquitous Computing Adjunct Publication - UbiComp '14 Adjunct 2014, 797–806, doi:10.1145/2638728.2641305.
35. Bouchard, K.; Eusufzai, M.R.; Ramezani, R.; Naeim, A. Generalizable Spatial Feature for Human Positioning Based on Bluetooth Beacons. In Proceedings of the 2016 IEEE 7th Annual Ubiquitous Computing, Electronics and Mobile Communication Conference, UEMCON 2016; 2016.
36. Wu, B.; Ma, Z.; Poslad, S.; Li, Y. WiFi Fingerprint Based, Indoor, Location-Driven Activities of Daily Living Recognition. In Proceedings of the Proceedings - 2018 5th International Conference on Behavioral, Economic, and Socio-Cultural Computing, BESC 2018; 2018.
37. Yang, J.; Cheng, K.; Chen, J.; Zhou, B.; Li, Q. Smartphones Based Online Activity Recognition for Indoor Localization Using Deep Convolutional Neural Network. In Proceedings of the Proceedings of 5th IEEE Conference on Ubiquitous Positioning, Indoor Navigation and Location-Based Services, UPINLBS 2018; 2018.
38. Moreira, D.; Barandas, M.; Rocha, T.; Alves, P.; Santos, R.; Leonardo, R.; Vieira, P.; Gamboa, H. Human Activity Recognition for Indoor Localization Using Smartphone Inertial Sensors. Sensors 2021, 21, doi:10.3390/s21186316.
39. Hardegger, M.; Roggen, D.; Calatroni, A.; Tröster, G. S-SMART: A Unified Bayesian Framework for Simultaneous Semantic Mapping, Activity Recognition, and Tracking. ACM Trans. Intell. Syst. Technol. 2016, 7, 34:1--34:28, doi:10.1145/2824286.
40. Sukreep, S.; Mongkolnam, P.; Nukoolkit, C. Detect the Daily Activities and In-House Locations Using Smartphone. Advances in Intelligent Systems and Computing 2015, 361, 215–225, doi:10.1007/978-3-319-19024-2_22.
41. Wang, J.; Zhang, X.; Gao, Q.; Yue, H.; Wang, H. Device-Free Wireless Localization and Activity Recognition: A Deep Learning Approach. IEEE Transactions on Vehicular Technology 2017, 66, 6258–6267, doi:10.1109/TVT.2016.2635161.
42. Reyes, F.M.; Gurrola, L.C.G.; Estrada, H.V. Location and Activity Detection for Indoor Environments. In Proceedings of the Lecture Notes in Computer Science (including subseries Lecture Notes in Artificial Intelligence and Lecture Notes in Bioinformatics); 2015; Vol. 9414, pp. 574–582.
43. Kashimoto, Y.; Morita, T.; Fujimoto, M.; Arakawa, Y.; Suwa, H.; Yasumoto, K. Implementation and Evaluation of Daycare Report Generation System Based on BLE Tag. In Proceedings of the Proceedings of the 15th International Conference on Mobile and Ubiquitous Multimedia; ACM: New York, NY, USA, 2016; pp. 327–329.
44. Luo, X.; Guan, Q.; Tan, H.; Gao, L.; Wang, Z.; Luo, X. Simultaneous Indoor Tracking and Activity Recognition Using Pyroelectric Infrared Sensors. Sensors (Switzerland) 2017, 17, doi:10.3390/s17081738.
45. Wang, F.; Feng, J.; Zhao, Y.; Zhang, X.; Zhang, S.; Han, J. Joint Activity Recognition and Indoor Localization With WiFi Fingerprints. IEEE Access 2019, 7, 80058–80068, doi:10.1109/ACCESS.2019.2923743.
46. Kim, H.-G.; Kim, G.Y. Deep Neural Network-Based Indoor Emergency Awareness Using Contextual Information From Sound, Human Activity, and Indoor Position on Mobile Device. IEEE Transactions on Consumer Electronics 2020, 66, 271–278, doi:10.1109/TCE.2020.3015197.
47. Makela, M.; Rantanen, J.; Kirkko-Jaakkola, M.; Ruotsalainen, L. Context Recognition in Infrastructure-Free Pedestrian Navigation—Toward Adaptive Filtering Algorithm. IEEE Sensors Journal 2018, 18, 7253–7264, doi:10.1109/JSEN.2018.2847038.
48. Huang, J.; Liu, B.; Jin, H.; Yu, N. WiLay: A Two-Layer Human Localization and Activity Recognition System Using WiFi. In Proceedings of the 2021 IEEE 93rd Vehicular Technology Conference (VTC2021-Spring); IEEE, April 2021; pp. 1–6.
49. Cheng, L.; Zhao, A.; Wang, K.; Li, H.; Wang, Y.; Chang, R. Activity Recognition and Localization Based on UWB Indoor Positioning System and Machine Learning. In Proceedings of the 11th Annual IEEE Information Technology, Electronics and Mobile Communication Conference, IEMCON 2020; 2020.
50. Ponce Ortiz, K.J. Fall Detection, Location and Identification for Elderly Institution. In Proceedings of the PervasiveHealth: Pervasive Computing Technologies for Healthcare; 2020.

51. Ceron, J.D.; Lopez, D.M.; Ramirez, G.A. A Mobile System for Sedentary Behaviors Classification Based on Accelerometer and Location Data. Computers in Industry 2017, 92–93, 25–31, doi:10.1016/j.compind.2017.06.005.
52. Alzantot, M.; Youssef, M. UPTIME: Ubiquitous Pedestrian Tracking Using Mobile Phones. In Proceedings of the 2012 IEEE Wireless Communications and Networking Conference (WCNC); 2012; pp. 3204–3209.
53. Kitchenham, B.; Brereton, O.P.; Budgen, D.; Turner, M.; Bailey, J.; Linkman, S.; Pearl Brereton, O.; Budgen, D.; Turner, M.; Bailey, J.; et al. Systematic Literature Reviews in Software Engineering - A Systematic Literature Review. Information and Software Technology 2009, 51, 7–15, doi:10.1016/j.infsof.2008.09.009.
54. Calvaresi, D.; Cesarini, D.; Sernani, P.; Marinoni, M.; Dragoni, A.F.; Sturm, A. Exploring the Ambient Assisted Living Domain: A Systematic Review. Journal of Ambient Intelligence and Humanized Computing 2017, 8, 239–257, doi:10.1007/s12652-016-0374-3.
55. Zafari, F.; Gkelias, A.; Leung, K.K. A Survey of Indoor Localization Systems and Technologies. IEEE Communications Surveys and Tutorials 2019, doi:10.1109/COMST.2019.2911558.
56. Tariq, Z. bin; Cheema, D.M.; Kamran, M.Z.; Naqvi, I.H. Non-GPS Positioning Systems: A Survey. ACM Computing Surveys 2017, doi:10.1145/3098207.
57. Sakpere, W.; Adeyeye-Oshin, M.; Mlitwa, N.B.W. A State-of-the-Art Survey of Indoor Positioning and Navigation Systems and Technologies. South African Computer Journal 2017, doi:10.18489/sacj.v29i3.452.
58. Basiri, A.; Lohan, E.S.; Moore, T.; Winstanley, A.; Peltola, P.; Hill, C.; Amirian, P.; Figueiredo e Silva, P. Indoor Location Based Services Challenges, Requirements and Usability of Current Solutions. Computer Science Review 2017, doi:10.1016/j.cosrev.2017.03.002.
59. Mukti Susanti, R.; Maulana Adhinugraha, K.; Alamri, S.; Barolli, L.; Taniar, D. Indoor Trajectory Reconstruction Using Mobile Devices. In Proceedings of the Proceedings - International Conference on Advanced Information Networking and Applications, AINA; 2018.
60. Muhammad, M.N.; Salcic, Z.; Wang, K.I.K. Indoor Pedestrian Tracking Using Consumer-Grade Inertial Sensors with PZTD Heading Correction. IEEE Sensors Journal 2018, doi:10.1109/JSEN.2018.2833118.
61. Harle, R. A Survey of Indoor Inertial Positioning Systems for Pedestrians. IEEE Communications Surveys and Tutorials 2013.
62. Wu, Y.; Zhu, H.B.; Du, Q.X.; Tang, S.M. A Survey of the Research Status of Pedestrian Dead Reckoning Systems Based on Inertial Sensors. International Journal of Automation and Computing 2019, 16, 65–83, doi:10.1007/s11633-018-1150-y.
63. Fischer, C.; Sukumar, P.T.; Hazas, M. Tutorial: Implementing a Pedestrian Tracker Using Inertial Sensors. IEEE Pervasive Computing 2013, doi:10.1109/MPRV.2012.16.
64. Martindale, C.F.; Sprager, S.; Eskofier, B.M. Hidden Markov Model-Based Smart Annotation for Benchmark Cyclic Activity Recognition Database Using Wearables. Sensors 2019, 19, 1820, doi:10.3390/s19081820.
65. Li, Y.; Wang, J.J. A Robust Pedestrian Navigation Algorithm with Low Cost IMU. In Proceedings of the 2012 International Conference on Indoor Positioning and Indoor Navigation, IPIN 2012 - Conference Proceedings; 2012.
66. Li, Y.; Jack Wang, J. A Pedestrian Navigation System Based on Low Cost IMU. Journal of Navigation 2014, doi:10.1017/S0373463314000344.
67. Ren, M.; Pan, K.; Liu, Y.; Guo, H.; Zhang, X.; Wang, P. A Novel Pedestrian Navigation Algorithm for a Foot-Mounted Inertial-Sensor-Based System. Sensors (Switzerland) 2016, doi:10.3390/s16010139.
68. Wagstaff, B.; Peretroukjin, V.; Kelly, J. Improving Foot-Mounted Inertial Navigation through Real-Time Motion Classification. In Proceedings of the 2017 International Conference on Indoor Positioning and Indoor Navigation, IPIN 2017; 2017.
69. Wagstaff, B.; Kelly, J. LSTM-Based Zero-Velocity Detection for Robust Inertial Navigation. In Proceedings of the IPIN 2018 - 9th International Conference on Indoor Positioning and Indoor Navigation; 2018.
70. Hannink, J.; Ollenschläger, M.; Kluge, F.; Roth, N.; Klucken, J.; Eskofier, B.M. Benchmarking Foot Trajectory Estimation Methods for Mobile Gait Analysis. Sensors (Switzerland) 2017, doi:10.3390/s17091940.

71. Skog, I.; Nilsson, J.O.; Händel, P. Evaluation of Zero-Velocity Detectors for Foot-Mounted Inertial Navigation Systems. In Proceedings of the 2010 International Conference on Indoor Positioning and Indoor Navigation, IPIN 2010 - Conference Proceedings; 2010.
72. Mannini, A.; Sabatini, A.M. Gait Phase Detection and Discrimination between Walking-Jogging Activities Using Hidden Markov Models Applied to Foot Motion Data from a Gyroscope. Gait and Posture 2012, doi:10.1016/j.gaitpost.2012.06.017.
73. Barth, J.; Oberndorfer, C.; Kugler, P.; Schuldhaus, D.; Winkler, J.; Klucken, J.; Eskofier, B. Subsequence Dynamic Time Warping as a Method for Robust Step Segmentation Using Gyroscope Signals of Daily Life Activities. In Proceedings of the Proceedings of the Annual International Conference of the IEEE Engineering in Medicine and Biology Society, EMBS; 2013.
74. Barth, J.; Oberndorfer, C.; Pasluosta, C.; Schülein, S.; Gassner, H.; Reinfelder, S.; Kugler, P.; Schuldhaus, D.; Winkler, J.; Klucken, J.; et al. Stride Segmentation during Free Walk Movements Using Multi-Dimensional Subsequence Dynamic Time Warping on Inertial Sensor Data. Sensors (Switzerland) 2015, 15, 6419–6440, doi:10.3390/s150306419.
75. Leutheuser, H.; Doelfel, S.; Schuldhaus, D.; Reinfelder, S.; Eskofier, B.M. Performance Comparison of Two Step Segmentation Algorithms Using Different Step Activities. In Proceedings of the Proceedings - 11th International Conference on Wearable and Implantable Body Sensor Networks, BSN 2014; 2014.
76. Hannink, J. Mobile Gait Analysis : From Prototype towards Clinical Grade Wearable, 2019.
77. Martindale, C.F.; Roth, N.; Hannink, J.; Sprager, S.; Eskofier, B.M. Smart Annotation Tool for Multi-Sensor Gait-Based Daily Activity Data. In Proceedings of the 2018 IEEE International Conference on Pervasive Computing and Communications Workshops, PerCom Workshops 2018; 2018.
78. Ceron, J.; Lopez, D.M. Human Activity Recognition Supported on Indoor Localization: A Systematic Review. In Proceedings of the Studies in Health Technology and Informatics; 2018.
79. Mainetti, L.; Patrono, L.; Sergi, I. A Survey on Indoor Positioning Systems. In Proceedings of the 2014 22nd International Conference on Software, Telecommunications and Computer Networks, SoftCOM 2014; 2014.
80. Mendoza-Silva, G.M.; Torres-Sospedra, J.; Huerta, J. A Meta-Review of Indoor Positioning Systems. Sensors (Switzerland) 2019.
81. Durrant-Whyte, H.; Bailey, T. Simultaneous Localization and Mapping (SLAM): Part I The Essential Algorithms. Robotics & Automation Magazine 2006, doi:10.1109/MRA.2006.1638022.
82. Gu, Y.; Song, Q.; Li, Y.; Ma, M.; Zhou, Z. An Anchor-Based Pedestrian Navigation Approach Using Only Inertial Sensors. Sensors (Switzerland) 2016, doi:10.3390/s16030334.
83. Robertson, P.; Angermann, M.; Khider, M. Improving Simultaneous Localization and Mapping for Pedestrian Navigation and Automatic Mapping of Buildings by Using Online Human-Based Feature Labeling. In Proceedings of the Record - IEEE PLANS, Position Location and Navigation Symposium; 2010.
84. Huang, J.; Millman, D.; Quigley, M.; Stavens, D.; Thrun, S.; Aggarwal, A. Efficient, Generalized Indoor WiFi GraphSLAM. In Proceedings of the Proceedings - IEEE International Conference on Robotics and Automation; 2011.
85. Zuo, Z.; Liu, L.; Zhang, L.; Fang, Y. Indoor Positioning Based on Bluetooth Low-Energy Beacons Adopting Graph Optimization. Sensors (Switzerland) 2018, doi:10.3390/s18113736.
86. Hardegger, M.; Roggen, D.; Mazilu, S.; Troster, G. ActionSLAM: Using Location-Related Actions as Landmarks in Pedestrian SLAM. In Proceedings of the 2012 International Conference on Indoor Positioning and Indoor Navigation, IPIN 2012 - Conference Proceedings; 2012.
87. Ceron, J.D.; Martindale, C.F.; López, D.M.; Kluge, F.; Eskofier, B.M. Indoor Trajectory Reconstruction of Walking, Jogging, and Running Activities Based on a Foot-Mounted Inertial Pedestrian Dead-Reckoning System. Sensors (Switzerland) 2020, doi:10.3390/s20030651.
88. Faragher, R.; Harle, R. Location Fingerprinting with Bluetooth Low Energy Beacons. IEEE Journal on Selected Areas in Communications 2015, doi:10.1109/JSAC.2015.2430281.
89. Carpenter, J.; Clifford, P. Improved Particle Filter for Nonlinear Problems. IEE Proceedings: Radar, Sonar and Navigation 1999, doi:10.1049/ip-rsn:19990255.
90. Labbe, R.R. Kalman and Bayesian Filters in Python. GitHub repository 2018.

91. Michael Montemerlo; Sebastian Thrun; Yuta, S.; Asama, H.; Thrun, S.; Prassler, E.; Tsubouchi, T.; Andrade-; Cetto, J.; Sanfeliu, A.; et al. FastSLAM - A Scalable Method for the Simultaneous Localization and Mapping Problem in Robotics; 2007; ISBN 9783540334545.
92. Menegatti, E.; Zanella, A.; Zilli, S.; Zorzi, F.; Pagello, E. Range-Only Slam with a Mobile Robot and a Wireless Sensor Networks. In Proceedings of the Proceedings - IEEE International Conference on Robotics and Automation; 2009.
93. Castillo-Cara, M.; Lovón-Melgarejo, J.; Bravo-Rocca, G.; Orozco-Barbosa, L.; García-Varea, I. An Analysis of Multiple Criteria and Setups for Bluetooth Smartphone-Based Indoor Localization Mechanism. Journal of Sensors 2017, doi:10.1155/2017/1928578.
94. Dimitrova, D.C.; Alyafawi, I.; Braun, T. Experimental Comparison of Bluetooth and Wifi Signal Propagation for Indoor Localisation. In Proceedings of the Lecture Notes in Computer Science (including subseries Lecture Notes in Artificial Intelligence and Lecture Notes in Bioinformatics); 2012; Vol. 7277 LNCS.
95. Bifet, A.; Holmes, G.; Kirkby, R.; Pfahringer, B. MOA: Massive Online Analysis. Journal of Machine Learning Research 2010, 11.
96. Khannouz, M.; Glatard, T. A Benchmark of Data Stream Classification for Human Activity Recognition on Connected Objects. Sensors (Switzerland) 2020, 20, doi:10.3390/s20226486.
97. Morris, D.; Saponas, T.S.; Guillory, A.; Kelner, I. RecoFit: Using a Wearable Sensor to Find, Recognize, and Count Repetitive Exercises. In Proceedings of the Conference on Human Factors in Computing Systems - Proceedings; 2014.
98. Banos, O.; Galvez, J.M.; Damas, M.; Pomares, H.; Rojas, I. Window Size Impact in Human Activity Recognition. Sensors (Switzerland) 2014, 14, doi:10.3390/s140406474.
99. Bifet, A.; Zhang, J.; Fan, W.; He, C.; Zhang, J.; Qian, J.; Holmes, G.; Pfahringer, B. Extremely Fast Decision Tree Mining for Evolving Data Streams. In Proceedings of the Proceedings of the ACM SIGKDD International Conference on Knowledge Discovery and Data Mining; 2017; Vol. Part F129685.
100. Khannouz, M.; Li, B.; Glatard, T. OrpailleCC: A Library for Data Stream Analysis on Embedded Systems. Journal of Open Source Software 2019, 4, doi:10.21105/joss.01485.
101. Cadena, C.; Carlone, L.; Carrillo, H.; Latif, Y.; Scaramuzza, D.; Neira, J.; Reid, I.; Leonard, J.J. Past, Present, and Future of Simultaneous Localization and Mapping: Toward the Robust-Perception Age. IEEE Transactions on Robotics 2016, 32, doi:10.1109/TRO.2016.2624754.
102. Ceron, J.D.; Kluge, F.; Küderle, A.; Eskofier, B.M.; López, D.M. Simultaneous Indoor Pedestrian Localization and House Mapping Based on Inertial Measurement Unit and Bluetooth Low-Energy Beacon Data. Sensors (Switzerland) 2020, 20, doi:10.3390/s20174742.
103. Hall, M.; Smith, L. a Feature Selection for Machine Learning : Comparing a Correlation-Based Filter Approach to the Wrapper CFS : Correlation-Based Feature. International FLAIRS Conference 1999.
104. Son, Y.; Oh, S. A Barometer-IMU Fusion Method for Vertical Velocity and Height Estimation. In Proceedings of the 2015 IEEE SENSORS - Proceedings; 2015.
105. Zhang, J.; Edwan, E.; Zhou, J.; Chai, W.; Loffeld, O. Performance Investigation of Barometer Aided GPS/MEMS-IMU Integration. In Proceedings of the Record - IEEE PLANS, Position Location and Navigation Symposium; 2012.
106. Cossy-Gantner, A.; Germann, S.; Schwalbe, N.R.; Wahl, B. Artificial Intelligence (AI) and Global Health: How Can AI Contribute to Health in Resource-Poor Settings? BMJ Global Health 2018, 3, doi:10.1136/bmjgh-2018-000798.
107. Lopéz, D.M.; Blobel, B. MHealth in Low- and Middle-Income Countries: Status, Requirements and Strategies. In Proceedings of the Studies in Health Technology and Informatics; 2015; Vol. 211.